FACULDADE DE ENGENHARIA DA UNIVERSIDADE DO PORTO

Implementing Dynamic System Reconfiguration with Renewables Considering Future Grid Technologies: A Real Case Study

José Filipe Soares Pogeira

Dissertação realizada no âmbito do
Mestrado Integrado em Engenharia Eletrotécnica e de Computadores
Major Energia

Orientador: Prof. Doutor João Paulo da Silva Catalão

Co-orientador: Doutor Sérgio Fonseca Santos

Janeiro de 2018

Resumo

O sistema de energia elétrica encontra-se em evolução, não só devido a questões ambientais, como integração de mais fontes de energia renováveis distribuídas (FERD), mas também devido ao aumento do consumo e à integração de novas tecnologias. A integração múltipla de elementos visa a criação das futuras redes elétricas inteligentes, *Smart Grids*. Assim sendo, é necessário criar técnicas de otimização de forma a melhorar o sistema de energia elétrica atual, sendo o sistema de distribuição uma das componentes deste que mais necessita de ser otimizado. A reconfiguração dinâmica do sistema na distribuição consiste no processo de alteração da topologia da rede durante os períodos operacionais do sistema.

Este processo, em conjunto com a implementação das DRES e outras tecnologias, tais como os sistemas de armazenamento de energia, irá possibilitar uma maior otimização do sistema, quer em termos económicos, quer em técnicos, e também uma maior integração das FERD. A natureza estocástica, incerteza e variabilidade nomeadamente, das FERD é tida em consideração neste processo.

Nesta dissertação, um modelo melhorado da reconfiguração dinâmica do sistema é apresentado, com o objetivo de minimizar os custos totais do sistema, principalmente aos níveis da operação, manutenção, emissão e energia não utilizada. A otimização do sistema é feita, tendo em consideração as suas várias restrições técnicas, operando o sistema de forma estável e fiável.

O modelo computacional foi testado em dois sistemas, o IEEE 119-bus system e num sistema real, o sistema da Lagoa (Ilha de São Miguel, Açores), de forma a validar a eficácia do método proposto.

Palavras-chave - Geração distribuída; reconfiguração dinâmica; fontes de energia renováveis; programação estocástica linear inteira-mista.

Abstract

The electric power systems are in an evolutionary process to respond to environmental concerns, by integrating more distributed renewable energy sources (DRES), and facilitate the integration of new technologies. The aim of such integration of elements is the creation of the future electricity grids, the Smart Grids. In this sense, it is necessary to create optimization techniques to improve the current electrical power system, being the distribution system one part of the electrical power system that needs to be optimized.

Dynamic distribution system reconfiguration is the process of changing the network topology during the system operational periods. This process together with the integration of DRES and other technologies, namely energy storage systems, will allow a greater system optimization in technical and economic terms, but also a greater integration of DRES. In this optimization process the stochastic nature of DRES (its variability and uncertainty) are taken into consideration.

In this dissertation, an improved dynamic system reconfiguration model is presented where the goal is to minimize the total costs of the system, namely costs of operation, maintenance, emissions and energy not supplied. The system optimization is made considering the various technical system constraints, operating the system in a reliable and stable way.

The computational tool is tested in two test systems, the IEEE 119-bus system and in a real system, the system of Lagoa, (in São Miguel Island, Azores) to validate the effectiveness of the proposed method.

Key Words - Distributed generation; dynamic reconfiguration; renewable energy sources; stochastic mixed integer linear programming.

Acknowledgments

First, I would like to express my deepest gratitude to my supervisor, Professor João Catalão, for the opportunity given to work under his supervision and for providing me with such an interesting and challenging subject with such an amazing support structure.

I would also like to say a special thank you to Doctor Sérgio Santos, my co-supervisor, for always being available to answer all questions that emerged throughout this dissertation as well as all the advices that helped me to reach the end of this journey and that will, for sure, help me in my future professional life.

To my parents and my sister, for all the support and efforts they made in order to make this journey come to an end. I know how hard it has been and I am aware that I can be a big challenge from time to time. Thank you for everything and, hopefully, I will be able to repay everything and more in the future.

To my girlfriend, which is also my best friend, Ana Sousa, for all the patience and all the encouragement. Life took a hell of a turn in the last couple of years, mainly because of you. It has been great to share all of this together and I would change nothing. Thank you, from the bottom of my heart, for always being besides me, in bad times and good times.

A special thank you to my partner in crime during this dissertation, Diogo Freitas. True friendships are formed in the most peculiar ways and times, and this is the case. Thank you for all the talks, for the encouragement, the stupid jokes and coffees shared. You are a great individual, best of luck in the future brother.

Finally, a big thank you to all my friends and colleagues. You guys know who you are and the impact you had and still have in my life.

It has been a ride, no doubt about it. Thank you all.

José Filipe Soares Pogeira

Contents

List of Figures

List of Tables

Abbreviation and Symbols

List of Abbreviations

DAC	Distribution Automation Control
DER	Distributed Energy Resources
DG	Distributed Generation
DN	Distribution Network
DNR	Dynamic Network Reconfiguration
DR	Demand Response
DRES	Distributed Renewable Energy Sources
DSO	Distribution System Operator
ESS	Energy Storage System
MICP	Mixed-Integer Cone Programming
MILP	Mixed-Integer Linear Programming
MIP	Mixed-Integer Programming
OPF	Optimal Power Flow
PV	Photovoltaic
RES	Renewable Energy Sources
SCADA	Supervisory Control And Data Acquisition
V2G	Vehicle to Grid

List of Symbols

Sets/Indices

es/Ω^{es}	Index/set of energy storage
g/Ω^{g}	Index/set of generators
h/Ω^{h}	Index/set of hours
l/Ω^{l}	Index/set of lines
$n,m/\Omega^{n}$	Index/set of buses
s/Ω^{s}	Index/set of scenarios
ss/Ω^{ss}	Index/set of energy purchased
$\varsigma/\Omega^{\varsigma}$	Index/set of substations
Ω^{1}/Ω^{0}	Set of normally closed/opened lines
Ω^{D}	Set of demand buses

Parameters

$d_{n,h}$	Fictitious nodal ddemand
$E^{min}_{es,n,s,h}, E^{max}_{es,n,s,h}$	Energy storage limits (MWh)
$ER^{DG}_{g}, ER^{SS}_{\varsigma}$	Emission rates of DGs and energy purchased, respectively (tCO_2e/MWh)
g_l, b_l, S^{max}_l	Conductance, susceptance and flow limit of line l, respectively (Ω^{-1}, Ω^{-1}, MVA)
n_{DG}	Number of candidate nodes for installation of distributed generation
OC_g	Cost of unit energy production (€/MWh)
pf_g, pf_{ss}	Power factor of DGs and substation
$P^{DG,min}_{g,n}, P^{DG,max}_{g,n}$	Power generation limits (MW)
$P^{ch,max}_{es,n}, P^{dch,max}_{es,n}$	Charging/discharging upper limit (MW)
$PD^{n}_{s,h}, QD^{n}_{s,n}$	Demand at node n (MW, MVAr)
R_l, X_l	Resistance and reactance of line l (Ω, Ω)
SW_l	Cost of line switching €/switch
V_{nom}	Nominal voltage (kV)
η^{ch}_{es}, η^{dch}_{es}	Charging/discharging efficiency
λ^{CO_2}	Cost of emissions (tCO_2e)
λ^{es}	Variable cost of storage system (€/MWh)
μ_{es}	Scaling factor (%)
$v^{P}_{s,h}, v^{Q}_{s,h}$	Unserved power penalty (€/MW, €/MVAr)
ρ_s	Probability of scenarios

Variables

$E_{es,n,s,h}$	Reservoir level of ESS (MWh)
$f_{l,h}$	Fictitious current flows through line l
$g^{SS}_{n,h}$	Fictitious current injections at substation nodes
$I^{ch}_{es,n,s,h}$, $I^{dch}_{es,n,s,h}$	Charging/discharging binary variables
$P^{DG}_{g,n,s,h}$, $Q^{DG}_{g,n,s,h}$	DG power (MW, MVAr)
$P^{ch}_{es,n,s,h}$, $P^{dch}_{es,n,s,h}$	Charged/discharged power (MW)
$P^{SS}_{\varsigma,s,h}$, $Q_{\varsigma,s,h}$	Imported power from grid (MW, MVAr)
$P^{SS}_{n,s,h}$, $Q^{NS}_{n,s,h}$	Unserved power (MW, MVAr)
$P_{l,s,h}$, $Q_{l,s,h}$	Power flow through a line l (MW, MVAr)
$PL_{l,s,h}$, $QL_{l,s,h}$	Power losses in each feeder (MW, MVAr)
$\chi_{l,h}$	Binary switching variable of line l
$\Delta V_{n,s,h}, \Delta V_{m,s,h}$	Voltage deviation magnitude (kV)
$\theta_{l,s,h}$	Voltage angles between two nodes line l

Functions

$EC^{DG}, EC^{ES}, EC^{SS}$	Expected cost of energy produced by DGs, supplied by ESSs and imported (€)
$EmiC^{DG}, EmiC^{SS}$	Expected emission costs of power produced by DGs and imported from the grid (€)
ENSC	Expected cost for unserved energy (€)
SWC	Cost of line switching (€)

Chapter 1

Introduction

This chapter provides the dissertation background followed by the problem definition, the main objectives and the methodology used. It presents, as well, the structural organization used in this dissertation.

1.1 Background

Renewable energy sources (RESs) are essential to reduce the energy consumption based in fossil fuels and consequently the green house emissions, changing the world current paradigm. In this respect there are global goals established in order to increase the share of renewable energy in the energy mix. One of the European Union's major efforts resides on implementing policies to encourage such changes, with its efforts resulting on a significant increase of capacity installed as well as the share of renewables[1], as can be seen in Figure 1.1.

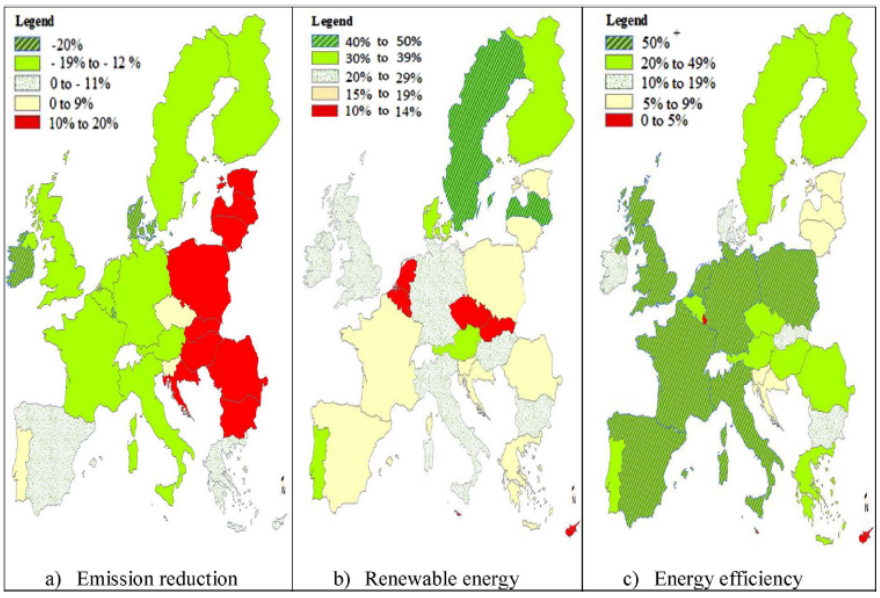

Figure 1.1: Present status of EU H2020 targets based on EU 2014 data [2]

Although RES, especially wind and solar, presents an amazing alternative and, mostly, a solution, also presents a vast amount of challenges, mainly regarding uncertainty and variability. In

addition to the variability and uncertainty of RES, there are other problems, such as technical problems, namely voltage rise, bi-directional power flow, reliability issues, among other. Therefore, there is a need to reshape the distribution grid to solve the challenges presented [3].

One way to alleviate these challenges is through the integration of smart grid enabling technologies, like energy storage systems (ESSs), that helps to offset the renewable stochastic nature, by storing energy in hours of high production and low demand, helping to compensate the system in hours of great demand and low renewable production [4].

Another enabling technology is the dynamic reconfiguration, which through network topology changes, helps to integrate more renewable, deal with bi-directional power flow, minimize energy losses, etc. This technology is one of the keys to the electric system automation.

Therefore, to implement those technologies, there is a need to transform the static distribution grid to an automated grid, which allows to increase the quality and reliability of the service provided to the customers at all times at the lowest operational cost.

1.2 Problem Definition

Nowadays, the concerns with environmental issues are growing, bringing several challenges to the typical power system, which is a centralized system. To overcome such challenges, the grid must be subject to a number of updates in order to make the distribution system operate in a satisfactory way, while ensuring a secure, stable and reliable operation, causing no major interruptions to the final consumer. A large portion of these challenges comes from RES integration, especially due to uncertainty and variability of renewables that makes the operation much more complex. The way to solve such a problem resides in the simultaneous implementation of smart grids enabling technologies such as ESSs and dynamic reconfiguration, therefore reducing the impact of uncertainty. Another point that makes RES integration more difficult is the fact that power flow becomes bi-directional, not having the traditional system the necessary structure to deal with such problems.

This dissertation continues the work done in [5] where the placement and sizing of ESSs and DGs is made considering the IEEE 119 bus system, within a 3-year planning horizon. In mentioned work, the technologies viability was assessed in terms of implementation and maintenance costs. The present dissertation focuses not on the planning but on the operation of the system, concentrating on the system dynamic reconfiguration, through an improved model. This model manages several technologies in order to operate optimally the system, maintaining the reliability and stability in standard levels, at the lowest possible cost. To prove the versatility of the new computational tool, it is then applied to a real system considering the same problem.

1.3 Research Objectives

The main objectives that this dissertations aims are:

- To carry out an extensive and comprehensive literature review on the area of dynamic reconfiguration featuring the integration of distributed generation (DGs) and ESSs;
- To develop a stochastic mixed-integer linear programming (MILP) operation model considering the presence of DGs and ESSs and their impact;
- To perform several case studies with different operation considerations;
- To perform and extensive analysis on dynamic reconfiguration implementation and smart grids enabling technologies at the level of increased renewable energy accommodation and improve network reliability and stability.

1.4 Research Methodology

The work developed throughout this dissertation aims to analyse the performance impact on distribution system that dynamic reconfiguration and the integration of DGs and ESSs cause. To reach the proposed objectives for this work, a mathematical model is developed, which has in consideration RES and demand uncertainty. The proposed model is a stochastic mixed integer linear programming (MILP), aiming to optimize the operation of distribution network systems. The problem is programmed in GAMS 24.0, and solved using the CPLEX 12.0 solver. All simulations are conducted in a HP Z820 workstation with two E5-2687W processors, each clocking at 3.1 GHz frequency.

1.5 Dissertation Structure

The contents presented in the dissertation are essentially divided into six chapters. In Chapter 2 a brief historical evolution of the electrical system is presented, followed by the definition of the prime concepts used and considered in this dissertation. A literature review of relevant works within the subject area is also presented. Chapter 3 presents the mathematical formulation of model where the main equations were explained in detail. Chapter 4 presents the system's main considerations and assumptions, as well as the scenarios considered and the methodology used. Chapter 5 presents an extensive analysis of the results obtained, considering the numerous cases tested for the two test systems. Finally, in Chapter 6 all the conclusions resulting from this dissertation are presented, as well as possible future works and works resulting from this dissertation.

Chapter 2

State-of-the-art

This chapter presents a state-of-the-art in distribution systems network reconfiguration, and it is divided into three major sections. In the first section is presented an introduction focused on the conventional electrical power systems, followed by the electricity grid evolutionary perspective. The renewable integration challenges and the smart grid enabling technologies are also presented. In the second section it is presented the essential concepts on the systems reconfiguration, namely, their definition, necessity and integration, followed by smart grid concept. Finally, in the third section is presented a review in the area of reconfiguration, with special focus on the most current works.

2.1 Introduction

The electric power system is one of the most complex systems that we have daily interaction without even noticing it. This complexity presents innumerous challenges to its management and it just gets harder by the day despite the constant evolution of technology [6]. The purpose of such system is to provide electricity to the customers in the most reliable and economical way possible [7].

This system is composed by generation, transmission and distribution systems. Distribution system makes the bridge between the transmission system and the customers [8]. These systems generally operate in a radial topology due to the fact it provides a simple solution not only in terms of protection, coordination schemes and management but also results in an economical perspective, as it is cheaper to build and to perform maintenance [9], [10]. These systems traditionally followed a hierarchical structure where the generation is based in large power plants, being, posteriorly, transported in the transmission system to the distribution system and then delivered to the customers, as can be seen in Figure 2.1. The relevance of this chain relies in the unidirectional power flow, which translates to efficiency in the power plants, easier management of the entire system and a simple way to perform a really complex and hard task. However, as in any task, not everything is an advantage, as the large need of constant investment in the transmission system due to its isolation of the area it is supposed to feed and the reliability issues created by this factor caused immense concern and discussion [11].

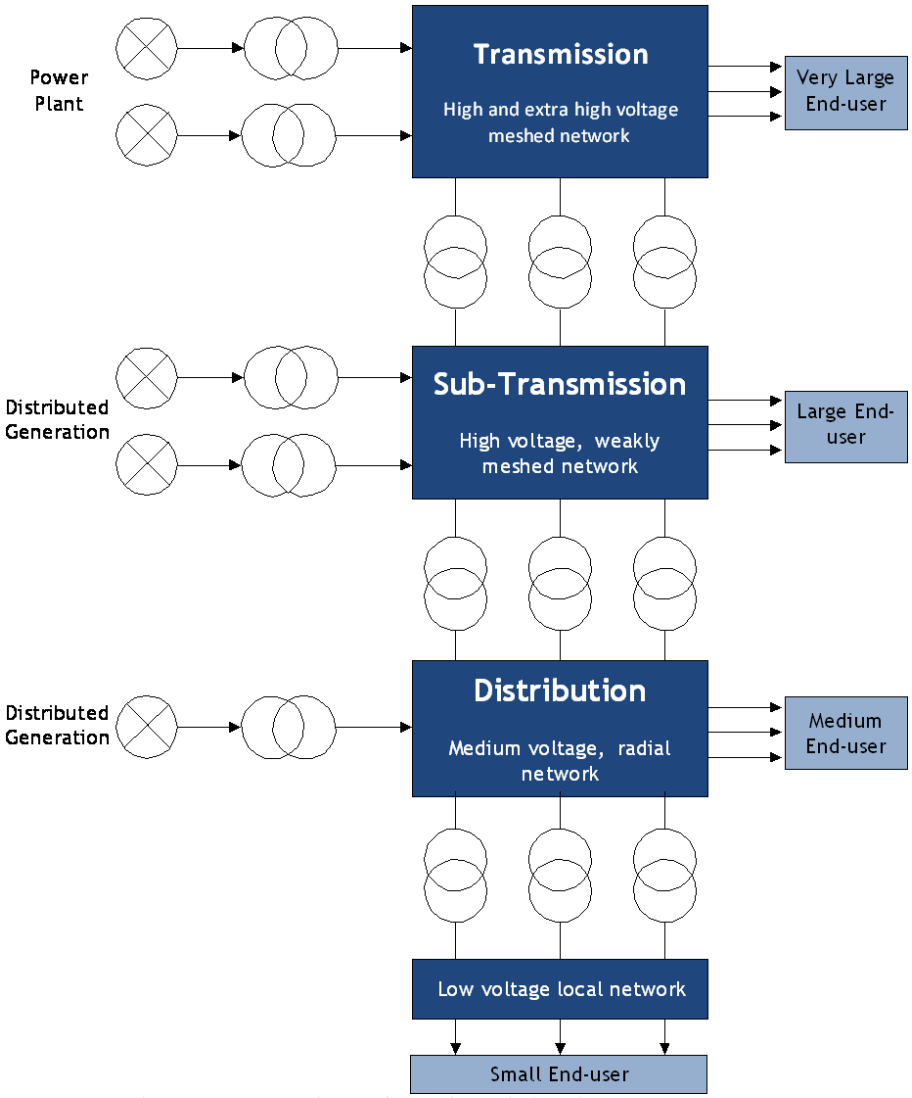

Figure 2.1: Generic configuration of electric power system [8]

All of the concerns with environmental and economic aspects have made it clear that a simple electric power system would not work in the near future [12]. The large power plants should have their importance decreased and should start working not as the main generation source but only as a complement to other sources. It is known that energy supply and consumption are two of the largest sources of air pollution, which translates to one of the major causes of mortality [13]. More than 80% of World energy consumption in 2014 was consumed by burning fossil fuels, with a major part being fossil fuel consumption, meaning a high level of toxic waste going to the atmosphere. In contrast, non-polluting sources such as hydropower production and other renewable sources only amounted to 7% and 2%, respectively [14].

Attempting this with the constant and rapid increase demand of global energy due to an exponential industrial growth as well as a bigger requirement of domestic consumption which has been developing in an unexpected way, a new method of generating energy in a reliable and efficient matter was needed in order to satisfy the demand with the necessary quality [15].

This leads to the appearance of one of the most studied aspects in engineering, Renewable Energy Sources (RES) [16]. The main RES used are wind, biomass and solar energy sources, all of them with its own advantages and concerns. The main concern with any RES is the intermittency of its generation, which arises an uncertainty that makes impossible to put RES as the main generation source of a growing and demanding power system [17], [18], [19]. Besides this, RES also forces the power flow to become bidirectional, which causes severe issues in terms of reliability because the power grid is not prepared to be used in that way [9].

However, the penetration of RES in the system is highly supported by many favorable energy policies, not only because it helps to achieve environmental goals, such as the global decarbonisation but also has less impact in the future of the economy [10]. Allying RES with Energy Storage Systems (ESS), Demand Response Programs (DR) and the traditional power system turns out to be obsolete and needs to be altered in a way that becomes more efficient and reliable with all this new components being introduced [20], [21]. It is important to notice that generation can be centralised, as was typically done with large power plants, or decentralised, mainly using Distributed Generation (DG). As reviewed in [22] ESS can be classified in terms of their functions, response times and suitable storage durations. Taking this into account, it is possible to have mechanical, electrochemical (Conventional rechargeable batteries and flow batteries), electrical (capacitors), thermochemical, chemical and thermal energy storage. One interesting and upcoming ESS application are Vehicle to Grid systems (V2G), which allow energy to flow from the grid and back, being mainly used in order to balance the fluctuation existing between production and consumption, hence their need to be almost equal in every instant in order to guarantee a stable voltage frequency [23], [24] . Electric vehicle batteries can also be considered as small-scale mobile ESS with the ability to function either as a generation and a load to the system. The main cost presented to the user is battery wearing and management costs [14].

DG system is a decentralised power generation system which comprises power generators of smaller capacities, when compared to the larger power plants, directly embedded within distribution network or situated near the points of energy consumption [8].

According with [25] the DGs installed capacity can be classified in four different rates, micro, small, medium and large as can be seen in Figure 2.2.

DGs can be non-renewable, renewable or storage, as ESS. Examples of non-renewable DGs are gas turbines, combustion turbines, micro turbines and reciprocating engines. As per renewable, there are hydro, which can be subdivided by small and micro, wind, solar, which can be divided in solar PV and solar thermal, geo-thermal, biomass and tidal. RES are, as expected, the most popular ones, as they are available worldwide just depending on the geographical area where certain country or area is located [26].

Implementing DG in the electric system presents numerous advantages, such as technical, economical and environmental. Some of the major ones are as follows [7]:

- Reduction of transmission costs due to the allocation of generation closer to the load;
- Decreased construction tie and reduced investment cost of smaller plants;

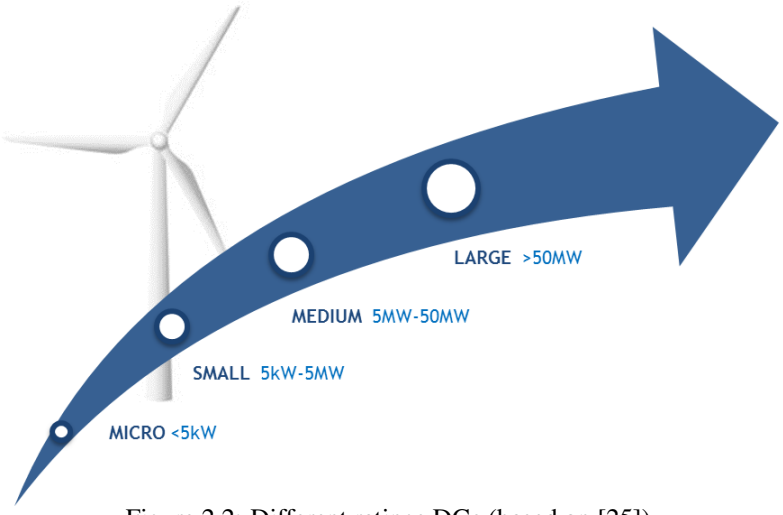

Figure 2.2: Different ratings DGs (based on [25])

- Adequacy to the sector deregulation and competition policy.

Yet, as expected, some major technical challenges are faced, being the most relevant power quality, protection, voltage regulation and stability. The major issue revolves around the bi-directional flow of power that the integration of DGs creates and that traditional DN is not prepared to handle correctly [27]. Some questions are also going to be relevant if the placement of DG is made in a non-optimal location, which results in increased power losses and voltage fluctuations. According to [28] power losses on transmission and sub-transmission line made up 30% of the total power losses, while in a distribution network system accounted for 70%, with the technical possibility of such losses considerably affecting and reducing the voltage profile of a system, especially when dealing with heavily loaded ones. Hence, the integration of DG into the existing distribution network is one of the most common techniques for supplying green energy to the clients [16].

As previously said, the integration of DGs makes the traditional power system outdated, turning it less reliable and efficient. With that appears the necessity of changing the paradigm of such system, always counting on the fact that remaking the total system and making a new one capable of sustaining such changes in an optimal way is not an economic or social possibility. This leads to network reconfiguration in which part of this dissertation relies on, and it is going to be subject of an extended review in.

2.2 Dynamic Reconfiguration

2.2.1 Definition

The increasing global demand for energy and the recently imposed rules and sanctions on carbon emissions have made the traditional large power plants less reliable and have forced the integration of new and different sources of generation like RES and DG, which leads to a necessity of reshaping the distribution system [3], where there needs to have a large amount of smart technologies in

order to present a smooth operation. Network reconfiguration is one of the alternatives possible in distribution automation that provides the necessary conditions to the proper function of the grid [29].

A simple way to define the concept of reconfiguration is that it is a method that intends to change the network construction with the objective of obtaining the optimal operational efficiency [30]. So, network reconfiguration is the way to modify the topology of an electric power system. This can be done, mainly, with two processes, static and dynamic. Static reconfiguration considers all switches, manually or remotely controlled, and looks for an improved fixed topology at the planning stage. On the other hand, dynamic reconfiguration contemplates remotely controlled switches in a centralized active network management scheme to remove grid congestion's in real time [31].

The process of reconfiguration as become increasingly relevant and easier to implement and execute due to the increasing use of the Supervisory Control and Data Acquisition System (SCADA) and Distribution Automation Control (DAC), which are equipped by automated switches and remote monitoring facilities [32].

2.2.2 Necessity

Network reconfiguration has gained a widespread traction and importance in studies due to the increasing integration of RES in the grid. As previously said, the amount of variables that the integration of DG brings to the system makes it of extreme importance to have the ability of changing the system according to the scenario presented at any given instance.

The reconfiguration has innumerous objectives which can be single or multi-objective. Single objective ones can be minimization of the total power losses, reliability indices, total cost of the network, switching costs, voltage deviations, etc. In terms of multi-objectives, they can be done by different techniques and they are decomposed and expressed into a single objective function [29].

Dynamic reconfiguration can also ensure a safe, high-quality and economical operation of distribution network. When compared with static reconfiguration, dynamic is much more in line with the requirements and specifications of the actual operation schedule of a distribution network [31].

It is important to notice that network reconfiguration is subjected to constraints which have to be strictly satisfied in order to have a solution and a proper function of the system. Normally, during the reconfiguration, the following are the constraints that need to be satisfied: all feeder sections are energized, radial network structure must be maintained, feeders and transformers are not overloaded and voltage limitations are not exceeded [29]. Proper methodologies are considered when constructing the algorithm, which can be, mainly, decomposed in three categories such as heuristic, meta-heuristic and mathematical programing [33], [34].

2.2.3 Integration in the grid

Although it is extremely important to rely on reconfiguration, the execution and implementation of such complicated method presents several problems, being some of the most recent the intermittency and uncertainty of RES as well as the integration of ESS [32], making the process subject to innumerous studies and approaches.

In [35] it is pointed out that is not possible to perform a wide number of switches in real distribution systems due to operational and safety aspects which presents a difficult assessment on whether to utilize and take most advantage of reconfiguration, appearing the need to create a system that has enough artificial intelligence in order to account with all the variables that the distribution system presents.

2.2.4 Smart Grids

Just a few decades ago, the idea of having an intelligent electricity grid seemed pure science fiction; however, the evolution of the network in this direction is occurring, being one of the most discussed topics in the area at the moment. This transition brings with it several challenges, whether they are technical, economic, regulatory, etc.

A Smart Grid, functionally, needs to be able to provide abilities like self-healing, high level of reliability, proper energy management and a real-time market pricing [36]. It uses a system of advanced communication and information technologies that should create the necessary base to potentially integrate large or small sources of generation like renewable generation [37], [38], energy storage systems [39] and demand response, as can be seen in the Figure 2.3.

The concept of self-healing in smart grids is, probably, one of the most interesting and challenging aspects to be considered, which would make complicated situations such as a congested feeder, where there would be extreme danger of violation of several constraints, an easier process to solve, as the grid would simply analyse every single component, performing reconfiguration and finding the optimal topology for that case. More than that, the grid would perform such analysis at every moment, making the operational management a lot easier and smoother.

2.3 Review

The energy systems reconfiguration is a topic that has been addressed in the recent decades under different objectives. Some of those objectives are to minimize the network power losses, network balancing, improved voltage profiles, system restoration [35], [41], [42], network reliability [43], among others [32]. However, although one might think that this is a topic that has already been properly studied, the fact is that the evolution from conventional systems to intelligent systems has reinvigorated the importance of the subject, whether by the integration of new technologies such as DGs base renewables [44], the ESSs integration [45] or the need to automate the system (making it "intelligent"). Therefore, in recent years, the automated systems progress, as well as the increase in computational capacity, has also created a new gap at this level, leading to the investigation

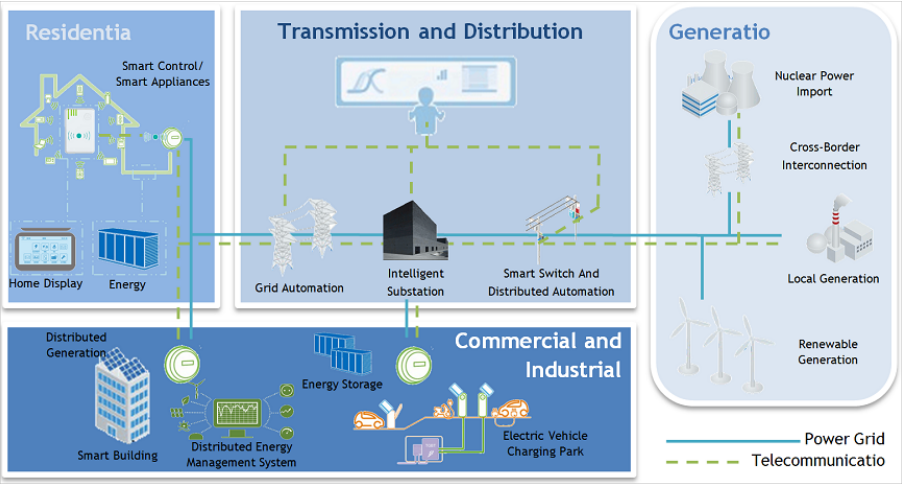

Figure 2.3: Smart Grid representation (adapted from [40])

of new reconfiguration methodologies, either in operation [41], [46] or at the planning level [47], [48]. However, computational time and computing resources remain one of the biggest challenges. This is because network reconfiguration is a complex combinatorial problem that involves many binary variables and operational constraints.

The integration of RES (wind and solar in particular) brings with it, a number of additional problems for the system, mainly from renewables nature (their uncertainty and variability). Consequently, it becomes important to use dynamic reconfiguration in order to obtain the optimum network configuration, that is, different topologies for different operational periods, because, it is extremely unlikely that due to the several network uncertainties (renewable and demand), that a single reconfiguration is good enough over a long period of time.

Considering the creation of the future electricity network [49], the use of dynamic reconfiguration is an indispensable step and on this matter several works in this area have been developed [30], [31], [35], [42], [50], [51], [52], [53]. Namely, Lizhou *et al.* [30] present a network reconfiguration method to obtain the best operation but considering the existence of renewable DGs. In [31] a similar work is presented, but using a different methodology. In [35] Capitanescu *et al.* focus on the use of reconfiguration as a mean to minimize or delay network reinforcement due the integration of renewables in the network, whether at planning or dynamic reconfiguration level. Baie *et al.* [50] focuses on the integration of power electronics and the ability to generate reactive power by DGs together in planning considering a Volt/Var control. Lei *et al.* [42] identifies the critical switches to perform dynamic system reconfiguration, considering the presence of renewable DGs to minimizing curtailment and the number of switches. Kennedy and Marden [52] present a work focused on the reliability of isolated microgrids considering stochastic generation and prioritizing the load. In this work dynamic reconfiguration is used in case of failure. In [53] a two-stage approach is proposed for optimum short-term scheduling of intermittent energy resources in a coordinated schedule system with hourly reconfiguration.

However, in recent years the works performed in reconfiguration have not focused only on dynamic reconfiguration, but on several other methodologies. In general, the different methodolo-

gies coming from the different works in the literature can be classified in heuristics, metaheuristic, numerical, among others. Between the metaheuristic methods there are several advanced artificial intelligence algorithms that have been used in the most recent works, namely, Genetic Algorithms [54], [55], [56], [57], [58], Neural Networks [59], Particle Swarm Algorithm [30], [53], [4], Tabu Search [60]. Some of the works in the area of heuristic methods are Backwards–Forwards Sweep [61], Heuristic Rules [62], Nonlinear Branch-and-Bound [63], Search Based [64]. Some of the more recent work on numerical method are Mixed Integer Nonlinear Programming (MINLP) Some of the more recent work on numerical method are Mixed Integer Nonlinear Programming (MINLP), [65], Mixed Integer Linear Programming (MILP) [17], [18], [23], [25], [33], [34], [51], [66–77], Mixed Integer Programming (MIP) [78], Mixed Integer Cone Programming (MICP) [50], Optimal Power Flow (OPF) [14], [46], [53]. There are also some other works, like hybrid, [31], [79], Analytical Approach [46], [80], among others.

Regarding the numerical works the great majority uses MILP, as can be seen in [17] is addressed the uncertainty management from RES integration in planning. The same authors in [25] do the renewable integration model expansion in the distribution system. Haddadian *et al.* [23] present an optimal coordination model of variable DGs jointly with electric vehicles, from the storage for energy sustainability point of view. The work identifies strategies of variable DGs integration without compromising the safety of the electrical infrastructure. Bizuayehu *et al.* presents in [33] an analysis on distribution systems reconfiguration with great penetration of renewable energy in a 24 hours period, considering the stochastic nature of renewables. In [69] the same authors perform the work expansion of work [33] where an economic dispatch is performed. In [34] Quevedo *et al.* present a work on distribution system contingencies, considering network reconfiguration as well as the presence of wind energy sources and ESSs. The contingency model is based on two-stage stochastic linear programming focusing on reconfiguration to solve the contingency problem. Novoselnik and Baotié [51] present a preliminary work to find the best topology in the presence of DGs and ESSs. In [70] is presented a distribution system multistage expansion work, considering the feeders, transformers, and distributed generators installation, in order to identify the best option, for the location and time to install these elements. The DGs integration uncertainty and the demand uncertainty are also considered. Yang *et al.* [71] focus on the optimal integration of distributed energy sources considering the uncertainties and their influence on the gas turbine performance. In [73] Ho *et al.* focus on the operation of ESSs analysis in the presence of renewable energy. In [76] and [78] two similar works are presented focusing on the planning of ESSs in isolated networks (microgrids), with the last work focusing more on ESSs sizing.

2.4 Chapter Summary

In this chapter was presented a review on the electrical systems evolution, where problems and the possible ways of overcoming these problems, especially with the help of distribution systems reconfiguration. In the review can be seen that the most recent works give relevance to the systems uncertainty and variability (at the level of renewables and demand). However, there are very few

studies that focus on system reconfiguration together with smart-grids enabling technologies, such as the present work, being the presented approach different from all the analysed works.

Chapter 3

Mathematical Formulation

This chapter presents an improved dynamic system reconfiguration model aiming to optimize system operation, allowing greater integration of distributed energy sources in the system. The problem is formulated as a stochastic mixed integer linear programming in order to account the stochastic nature that renewable power outputs presents, other traditional sources of variability and uncertainty such as demand. The objective function is to minimize the sum of all costs, considering the most important technical and economic constraints.

3.1 Objetive Function

The aim of the formulated Dynamic Network Reconfiguration (DNR) problem is to minimize the sum of relevant cost terms, namely, switching costs SWC, expected costs of operation TEC, emissions TEmiC and unserved power TENSC in the system as:

$$MinTC = SWC + TEC + TENSC + TEmiC \tag{3.1}$$

where TC refers to the total cost.

A switching cost is incurred when a change of status in a given line occurs, i.e, it goes from 0(open) to 1(closed) or the other way around. Thus, the first term in the objective function in (3.1), *SWC*, can be expressed as followed, where the function is the sum of new auxiliary variables:

$$SWC = \sum_{l \in \Omega^l} \sum_{h \in \Omega^h} SW_l * (y^+_{l,h} + y^-_{l,h}) \tag{3.2}$$

where

$$\chi_{l,h} - \chi_{l,h-1} = y^+_{l,h} - y^-_{l,h}; y^+_{l,h} \geq 0; y^-_{l,h} \geq 0 \tag{3.3}$$

$$\chi_{l,0} = 1; \forall l \in \Omega^1 \text{ and } \chi_{l,0} = 0; \forall l \in \Omega^0 \tag{3.4}$$

The switching action leads to the absolute value of difference in successive switching variables. Having the need to linearize such module, two non-negative auxiliary variables $y^+_{l,h}$ and $y^-_{l,h}$

are introduced in (3.2). The binary variable $\chi_{l,0}$ represents the two states that the line can assume at any time, 0 and 1, which represent, respectively, open and closed states.

TEC is given by the sum of the cost of power produced by DGs, discharged from energy storage systems and imported from upstream as in (3.5).

$$TEC = EC^{DG} + EC^{ES} + EC^{SS} \tag{3.5}$$

Where each constant in (3.5) is calculated as follows:

$$EC^{DG} = \sum_{s\in\Omega^s} \rho_s \sum_{h\in\Omega^h} \sum_{g\in\Omega^g} OC_g P^{DG}_{g,n,s,h} \tag{3.6}$$

$$EC^{ES} = \sum_{s\in\Omega^s} \rho_s \sum_{h\in\Omega^h} \sum_{es\in\Omega^{es}} \lambda^{es} P^{dch}_{es,n,s,h} \tag{3.7}$$

$$EC^{SS} = \sum_{s\in\Omega^s} \rho_s \sum_{h\in\Omega^h} \sum_{\varsigma\in\Omega^\varsigma} \lambda^{\varsigma}_h P^{SS}_{\varsigma,n,s,h} \tag{3.8}$$

In (3.6) the equation represents the expected cost of energy produced by DGs, given by the sum of scenarios probability product (ρ_s), with the cost produced (OC_g) bounded by the generation limits ($P^{DG}_{g,n,s,h}$). The cost of energy supplied by the ESSs is presented by equation (3.7), which is calculated by the sum of scenarios probability (ρ_s), with the energy storage cost (λ^{es}) limited by the discharge limit of the energy storage system ($P^{dch}_{g,n,s,h}$). Following the same line of thought, (3.8) models the cost of energy imported from the upstream network, again given by the sum of scenarios probability (ρ_s), with the electricity price purchased (λ^{ς}_h) by the energy imported from the network ($P^{SS}_{\varsigma,n,s,h}$).

The cost of load shedding, given by *TENSC*, is formulated as follows:

$$TENSC = \sum_{s\in\Omega^s} \rho_s \sum_{h\in\Omega^h} \sum_{n\in\Omega^n} (v^P_{s,h} P^{NS}_{n,s,h} + v^Q_{s,h} Q^{NS}_{n,s,h}) \tag{3.9}$$

where $v^P_{s,h}$ and $v^Q_{s,h}$ represent penalty terms corresponding to active and reactive power demand curtailment and $P^{NS}_{n,s,h}$ and $Q^{NS}_{n,s,h}$ are the active and reactive unserved power.

The following equation indicates the total cost of emissions that result from power production either using DG or imported power.

$$TEmiC = EmiC^{DG} + EmiC^{SS} \tag{3.10}$$

With each of the terms that compose (3.10) determined as follows:

$$EmiC^{DG} = \sum_{s\in\Omega^s} \rho_s \sum_{h\in\Omega^h} \sum_{g\in\Omega^g} \sum_{n\in\Omega^n} \lambda^{CO_2} ER^{DG}_g P^{DG}_{g,n,s,h} \tag{3.11}$$

$$EmiC^{SS} = \sum_{s\in\Omega^s} \rho_s \sum_{h\in\Omega^h} \sum_{\varsigma\in\Omega^\varsigma} \sum_{n\in\Omega^n} \lambda^{CO_2} ER^{SS}_\varsigma P^{SS}_{\varsigma,s,h} \tag{3.12}$$

The equation (3.11) represents the expected emission costs of power produced by DGs, given by the sum of scenarios probability product (ρ_s), with the sum of emission cost λ^{CO_2}, the emission rate and power of DGs (ER_g^{DG}), ($P_{g,n,s,h}^{DG}$). In (3.12) is represented the (ρ_s), with the sum of the emissions cost λ^{CO_2}, the emission rate of energy purchased and energy imported from the grid.

3.2 Constraints

3.2.1 Kirchhoff's Current Law

The sum of all incoming flows to a node should be equal to the sum of all outgoing flows, which is given by the Kirchhoff's Law. This is applied to both active and reactive power flow and must be respected at all time. In (3.13) and (3.14) both of these constraints are given:

$$\begin{aligned}\sum_{g\in\Omega^g} P_{g,n,s,h}^{DG} + \sum_{es\in\Omega^{es}} (P_{es,n,s,h}^{dch} - P_{es,n,s,h}^{ch}) + P_{\varsigma,s,h}^{SS} + P_{n,s,h}^{NS} + \sum_{in,l\in\Omega^l} P_{l,s,h} - \sum_{out,l\in\Omega^l} P_{l,s,h} \\ = PD_{s,h}^{n} + \sum_{in,l\in\Omega^l} \frac{1}{2} PL_{l,s,h} + \sum_{out,l\in\Omega^l} \frac{1}{2} PL_{l,s,h}; \forall\varsigma\in\Omega^{\varsigma}; \forall\varsigma\in n; l\in n\end{aligned} \tag{3.13}$$

$$\begin{aligned}\sum_{g\in\Omega^g} Q_{g,n,s,h}^{DG} + Q_{c,n,s,h}^{c} + Q_{\varsigma,s,h}^{SS} + Q_{n,s,h}^{NS} + \sum_{in,l\in\Omega^l} Q_{l,s,h} - \sum_{out,l\in\Omega^l} Q_{l,s,h} \\ = QD_{s,h}^{n} + \sum_{in,l\in\Omega^l} \frac{1}{2} QL_{l,s,h} + \sum_{out,l\in\Omega^l} \frac{1}{2} QL_{l,s,h}; \forall\varsigma\in\Omega^{\varsigma}; \forall\varsigma\in n; l\in n\end{aligned} \tag{3.14}$$

3.2.2 Kirchhoff's Voltage Law

The AC power flow equations, with a natural complex nonlinear and non-convex functions of voltage magnitude and angles are as follows:

$$P_{l,s,h} = V_{n,s,h}^2 g_k - V_{n,s,h} V_{m,s,h} (g_k \cos\theta_{l,s,h} + b_k \sin\theta_{l,s,h}) \tag{3.15}$$

$$Q_{l,s,h} = -V_{n,s,h}^2 b_k + V_{n,s,h} V_{m,s,h} (b_k \cos\theta_{l,s,h} - g_k \sin\theta_{l,s,h}) \tag{3.16}$$

Due to the non-linearity, the equations above are linearized according to [67] making few assumptions. The linearized active and reactive flows are given by the disjunctive inequalities.

$$|P_{l,s,h} - (V_{nom}(\Delta V_{n,s,h} - \Delta V_{m,s,h}) g_k - V_{nom}^2 b_k \theta_{l,s,h})| \leq M P_l (1 - \chi_{l,h}) \tag{3.17}$$

$$|Q_{l,s,h} - (-V_{nom}(\Delta V_{n,s,h} - \Delta V_{m,s,h}) b_k - V_{nom}^2 g_k \theta_{l,s,h})| \leq M Q_l (1 - \chi_{l,h}) \tag{3.18}$$

It is relevant to note that, due to reconfiguration, equations (3.17) and (3.18) have binary variables to make sure the flow through a given line is equal to zero when its switching binary

variable is zero, meaning that the line is disconnected. The results of introducing such variables can result in bilinear products, which can result in non-linearity. That is the reason why the big-M formulation is used, setting to the maximum transfer capacity, avoiding non-linearity. Lastly, it should be noted that in inequalities (3.15), (3.16), (3.17) and (3.18), the angle difference $\theta_{l,s,h}$ is defined as $\theta_{l,s,h} = \theta_{n,s,h} - \theta_{m,s,h}$ where n and m indices correspond to the same line l.

3.2.3 Power Flow Limits and Losses

Power flow in each line shoud not exceed the maximum value of transfer capacity, which is enforced by (3.19):

$$P_{l,s,h}^2 + Q_{l,s,h}^2 \leq \chi_{l,h}(S_l^{max})^2 \tag{3.19}$$

The constraints below are related to active and reactive power losses in a given line l, respectively (3.20) and (3.21).

$$PL_{l,s,h} = R_l(P_{l,s,h}^2 + Q_{l,s,h}^2)/V_{nom}^2 \tag{3.20}$$

$$QL_{l,s,h} = X_l(P_{l,s,h}^2 + Q_{l,s,h}^2)/V_{nom}^2 \tag{3.21}$$

The quadratic flows in (3.19), (3.20) and (3.21) are linearized using as SOS2 approach, presented in [81] and can be seen in Appendix A.

3.2.4 Energy Storage Model

The constraints given from (3.22) to (3.27) represent the energy storage model employed. (3.22) and (3.23) give the limit amount of power charged and discharged. (3.24) guarantees that the process of charging and discharging must not occur at the same time. The constraint that represents the stage of charge for a given ESS is modelled in (3.25). Constraint (3.26) restrains the storage level to always be within the permissible range. Finally, (3.27) sets the initial state of storage level, making sure that the storage level at the end of the operation time is exactly the same as in the begining of the operation. η_{es}^{dch} and η_{es}^{ch} are often set as equal, with their efficiencies expressed in percentage of energy at the nodes where the respective ESS are connected.

$$0 \leq P_{es,n,s,h}^{ch} \leq I_{es,n,s,h}^{ch} P_{es,n,h}^{ch,max} \tag{3.22}$$

$$0 \leq P_{es,n,s,h}^{dch} \leq I_{es,n,s,h}^{dch} P_{es,n,h}^{ch,max} \tag{3.23}$$

$$I_{es,n,s,h}^{ch} + I_{es,n,s,h}^{dch} \leq 1 \tag{3.24}$$

$$E_{es,n,s,h} = E_{es,n,s,h-1} + \eta_{es}^{ch} P_{es,n,s,h}^{ch} - P_{es,n,s,h}^{dch} / \eta_{es}^{dch} \tag{3.25}$$

$$E_{es,n}^{min} \leq E_{es,n,s,h} \leq E_{es,n}^{max} \tag{3.26}$$

$$E_{es,n,s,h0} = \mu_{es} E_{es,n}^{max}; E_{es,n,s,h24} = \mu_{es} E_{es,n}^{max} \tag{3.27}$$

3.2.5 Active and Reactive Power Limits of DGs

In this section, inequations (3.28) and (3.29) serve to impose active and reactive power limits for DGs, at the nodes where the respective ESS are connected. The actual production level of the specific unit should equal the upper bound of (3.28), with the lower bound always being equal to zero.

$$P_{g,n,s,h}^{DG,min} \leq P_{g,n,s,h}^{DG} \leq P_{g,n,s,h}^{DG,max} \tag{3.28}$$

$$Q_{g,n,s,h}^{DG,min} \leq Q_{g,n,s,h}^{DG} \leq Q_{g,n,s,h}^{DG,max} \tag{3.29}$$

Inequation (3.29) can only be used for DGs that do not possess reactive power support capabilities. For DGs that have reactive power support capabilities, modifications must be done due to their distinguished operation modes. Inequation (3.30) considers both lower and upper limits, which intend to present an expression that should be able to feature double fed induction generators, for example, that possess the ability to inject of consume reactive power in the grid.

$$-\tan(\cos^{-1}(pf_g)) P_{g,n,s,h}^{DG} \leq Q_{g,n,s,h}^{DG} \leq \tan(\cos^{-1}(pf_g)) P_{g,n,s,h}^{DG} \tag{3.30}$$

3.2.6 Reactive Power Limits of Substations

Because of stability reasons, the power from the substation can have bouding limits, as follows:

$$P_{\varsigma,s,h}^{SS,min} \leq P_{\varsigma,s,h}^{SS} \leq P_{\varsigma,s,h}^{SS,max} \tag{3.31}$$

$$Q_{\varsigma,s,h}^{SS,min} \leq Q_{\varsigma,s,h}^{SS} \leq Q_{\varsigma,s,h}^{SS,max} \tag{3.32}$$

The reactive power from the transmission grid is subjected to bounds as presented below in the inequality:

$$-\tan(\cos^{-1}(pf_{ss})) P_{\varsigma,s,h}^{SS} \leq Q_{\varsigma,s,h}^{SS} \leq \tan(\cos^{-1}(pf_{ss})) P_{\varsigma,s,h}^{SS} \tag{3.33}$$

where pf_{ss} represents the power factor at the substation, with its value assumed equal to 0.9 through the entirety of this dissertation.

3.2.7 Radiality Constraints

Distribution networks are usually operated in a radial configuration. This means that a few more constraints need to be used:

$$\sum_{l\in\Omega^l} \chi_{l,h} = 1, \quad \forall m \in \Omega^D; l \in n \tag{3.34}$$

$$\sum_{in,l\in\Omega^l} \chi_{l,h} - \sum_{out,l\in\Omega^l} \chi_{l,h} \leq 1 \quad \forall m \notin \Omega^D; l \in n \tag{3.35}$$

Equation (3.34) imposes that it is mandatory for nodes with demand at a given hour h to be connected and must have a single input flow through a given line l. In (3.35), a inequality is presented, where it is set a maximum of one input flow for each of the terminal nodes.

Having the inclusion of DGs in this dissertation, the equations above do not satisfy every single case, with the possibility of having particular nodes that could be supplied by DGs and, because of that, are not connected to the remainder of the grid. The following constraints intend to avoid islanding, modeling a ficticious system with a given number of fictitious loads. These ficticious loads can only be supplied by fictitious sources of energy through the actual feeders.

$$\sum_{in,l\in\Omega^l} f_{l,h} - \sum_{out,l\in\Omega^l} f_{l,h} = g^{SS}_{n,h} - d_{n,h}, \quad \forall n \in \Omega^\varsigma; l \in n \tag{3.36}$$

$$\sum_{in,l\in\Omega^l} f_{l,h} - \sum_{out,l\in\Omega^l} f_{l,h} = -1, \quad \forall n \in \Omega^g; \forall n \in \Omega^D \tag{3.37}$$

$$\sum_{in,l\in\Omega^l} f_{l,h} - \sum_{out,l\in\Omega^l} f_{l,h} = 0, \quad \forall n \notin \Omega^g; \forall n \notin \Omega^D; \forall n \notin \Omega^\varsigma \tag{3.38}$$

$$0 \leq \sum_{in,l\in\Omega^l} f_{l,h} + \sum_{out,l\in\Omega^l} f_{l,h} \leq n_{DG}; l \in n \tag{3.39}$$

$$0 \leq g^{SS}_{n,h} \leq n_{DG}, \quad \forall n \in \Omega^\varsigma; l \in n \tag{3.40}$$

Limits of fictitious flows through the feeders are imposed by constraints (3.37) and (3.38), with (3.36) representing the fictitious current balance equations for the nodes. (3.39) intends to limit the fictitious flow present in a line to the number of nodes that could have fictitious sources of energy. Lastly, (3.40) limits the fictitious currents injected by fictitious substations.

3.3 Chapter Summary

This chapter presented the operational model developed where the equations (objetives and constraints) are described. This particular model was developed in order to perform the operational analysis of a given distribution network system that features dynamic reconfiguration alonside with DERs. The mathematical model is solved using a stochastic mixed integer linear programming

optimization, minimizing the expected cost of the entire operation, while minimizing switching costs, emission costs and energy not served, respecting all the techinal constraints referenced in the chapter. The following chapter presents the assumptions and considerations of the systems used to test this model, IEEE 119-bus network system, a theoretical case study, and the system of Lagoa, in São Miguel Island, Azores, which represents a real case study.

Chapter 4

System Data and Assumptions

In this chapter the system data, assumptions, and grid framework are presented, as well as the scenarios, considered in the optimization model.

4.1 IEEE 119-bus test system

A standard IEEE 119-bus test system is applied in order to test the proposed operational model and perform an extensive analysis of technical and economic aspects of the DNR performed. The total active and reactive loads of this system are, respectively, 22.71MW and 17.04MVar. The wind and solar DGs, as well as the ESSs, which capacities can be found in Appendix B, are assumed as optimally placed as can be seen in Figure 4.1. Other data and assumptions had to be made throughout the course of this work and are described as follows:

- A period of 24 hours is considered;
- The possibility of an hourly configuration is projected;
- Nominal voltage value is 12.66kV;
- The range of permissible voltage deviation at each node is $\pm 5\%$ of the nominal voltage value;
- The reference node considered is the substation, having its voltage magnitude and angle values set to the voltage nominal value and 0, respectively;
- Rate of charge and discharge considered is the same for both cases, 90%;
- The substation has a power factor set as constant, with the value being 0.8;
- All DGs considered have the power factor set to 0.95;
- Electricity prices follow the same trend as the demand, with values ranging from 42€/MWh to 107€/MWh, with the lower values being during shallow hours while the higher values occur during peak hours;

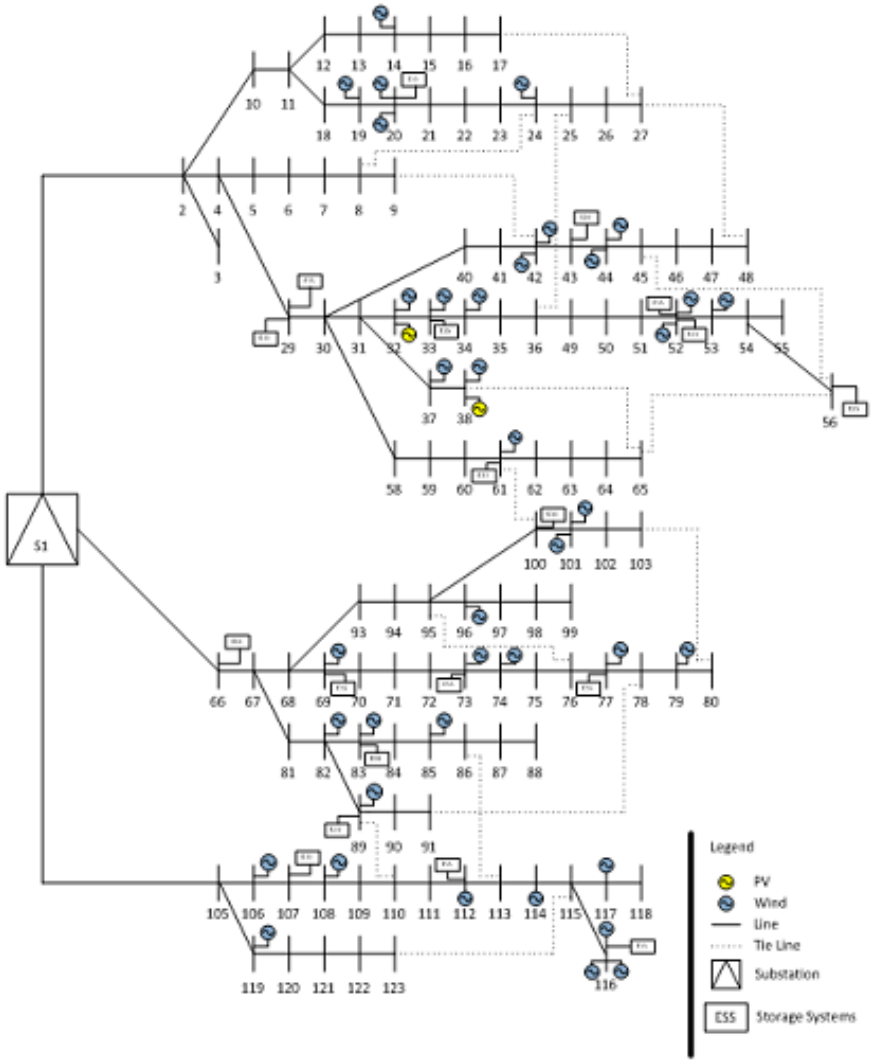

Figure 4.1: 119-bus test system with all technologies considered

- The variable cost considered in ESS is 5€/MWh;
- The price of emissions in the substation is set to 7€/tCO_2e with an assumed rate of 0.4/tCO_2e/MWh;
- Tariffs of solar and wind power generation are also set, being equal to 40€/MWh for solar and 20€/MWh for wind;
- Finally, the switching cost of each line as a cost of 5€/switch.

4.2 Lagoa test system

On December 31st of 2016, the electrical system of the island of São Miguel Island included eleven power plants and eleven substations. The São Miguel system, in Figure 4.2, has three levels of power, the high voltage at 60kV (transmission), the medium voltage at 30kV and 10kV (distribution) and the low voltage at 0,4kV(distribution).

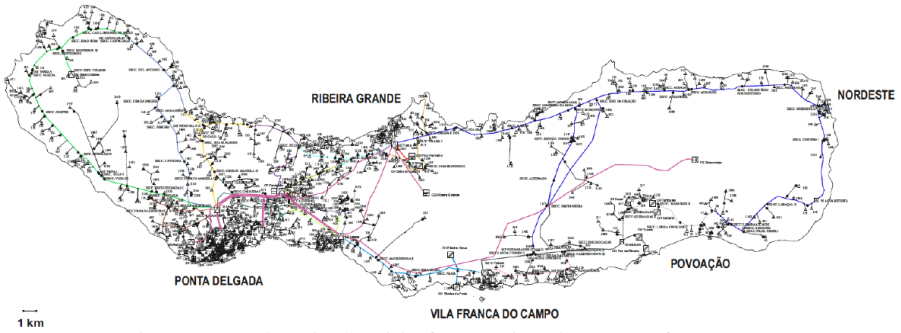

Figure 4.2: Electrical Grid of São Miguel,Azores (from [82])

4.2.1 Island's electric production system characterization

The electric production system of São Miguel is constituted by the Thermoelectrical Plant of Caldeirão (CTCL), the Geothermal Plants of Ribeira Grande (CGRG) and Pico Vermelho (CGPV), the Wind Farm of Graminhais (PEGR) and the Hydroelectric Plants of Túneis (CHTN), Tambores (CHTB), Fábrica Nova (CHFN), Canário (CHCN), Foz da Ribeira (CHFR),Ribeira da Praia (CHRP) and Salto do Cabrito (CHSC), which data can be seen in table 4.1.

Table 4.1: Electric production system of São Miguel Island : Adapted from [82]

				Grupos Geradores			Transformadores de Acoplamento		
Nome	Sigla	Entrada em Serviço	Fonte Primária	Tensão de Geração [kV]	Unidades	Potência Instalada [kW]	Relação Transformação	Unidades	Potência Instalada [kW]
Caldeirão	CTCL	1987	Térmica - Fuel	11	4	67.280	11/60 kV	4	92,00
				6,3	4	30.784	6,3/60 kV	4	40
Ribeira Grande	CGRG	1994	Geotérmica	10	4	16.600	–	–	–
Pico Vermelho	CGPV	2006	Geotérmica	11	1	13.000	11/30 kV	1	17,00
Graminhais	PEGR	2012	Eólica	0,4	10	9.000	0,4/30 kV	10	10,00
Túneis	CHTN	1951	Hídrica	6	1	1.658	6/30 kV	1	2,00
Tambores	CHTB	1909	Hídrica	0,4	1	94	0,4/30 kV	1	0,16
Fábrica Nova	CHFN	1927	Hídrica	3	1	608	3/30 kV	1	0,50
Canário	CHCN	1991	Hídrica	0,4	1	400	0,4/30 kV	1	0,50
Foz da Ribeira	CHFR	1990	Hídrica	0,4	1	800	0,4/30 kV	1	1,00
Ribeira da Praia	CHRP	1991	Hídrica	0,4	1	800	0,4/30 kV	1	1,00
Salto do Cabrito	CHSC	2006	Hídrica	0,4	1	670	0,4/30 kV	1	1,00
			Totais São Miguel	–	30	141694	–	26	165,16

4.2.1.1 Transmission System

This network transmission system in high voltage has nine high voltage/medium voltage substations: Caldeirão (SECL 60/30kV), Milhafres (SEMF 60/30kV), Lagoa (SELG 60/30-10kV), Foros (SEFO 60/30-10kV), Ponta Delgada(SEPD 60/10kV), Aeroporto (SEAE 60/10kV), São Roque (SESR 60/10kV) and the two associated with the Geothermical Plant of Ribeira Grande (SERG 10/60kV) and the Wind Farm of Graminhais (SEGR 30/60kV). The distribution system in medium voltage possesses two medium voltage/low voltage substations, Vila Franca (SEVF 30/10kV) and Sete Cidades (SESC 30/10kV). Table 4.2 presents the general data of the eleven substations. Figures 4.3 and 4.4 present the transmission network and the area of influence of each substation.

Table 4.2: Substation data of São Miguel: Adapted from [82]

Nome	Sigla	Entrada em Serviço	Concelho	Relação de Transformação	Número de Transformadores	Potência Instalada [MVA]
Caldeirão	SECL	2006	Ribeira Grande	60/30 kV	1	12,50
Milhafres	SEMF	1992	Ponta Delgada	60/30 kV	2	25,00
Lagoa	SELG	1992	Lagoa	60/30 kV	1	12,50
				60/10 kV	2	16,25
Foros	SEFO	1992	Ribeira Grande	60/30 kV	1	12,50
				60/10 kV	3	20,00
Vila Franca	SECF	2000	Vila Franca	30/10 kV	2	10,00
Ponta Delgada	SEPD	1960	Ponta Delgada	60/10 kV	2	40,00
Aeroporto	SEAE	2006	Ponta Delgada	60/10 kV	1	20,00
São Roque	SESR	2002	Ponta Delgada	60/10 kV	2	22,50
Sete Cidades	SESC	1992	Ponta Delgada	30/10 kV	1	0,50
Graminhais	SEGR	2012	Nordeste	30/60 kV	1	10,00
Ribeira Grande	SERG	1994	Ribeira Grande	10/60 kV	2	16,00
				Totais São Miguel	21	217,75

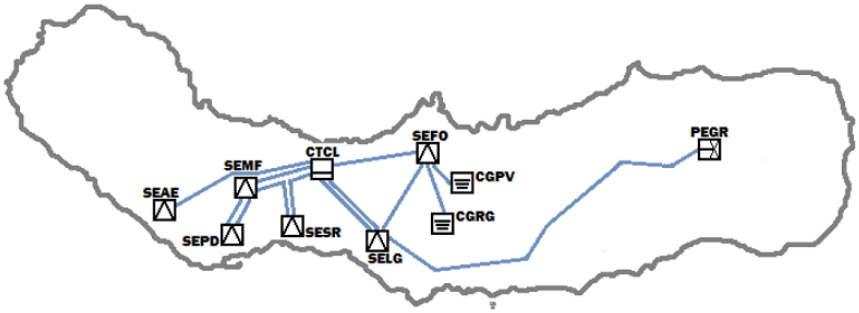

Figure 4.3: Transmission network of São Miguel (from [82])

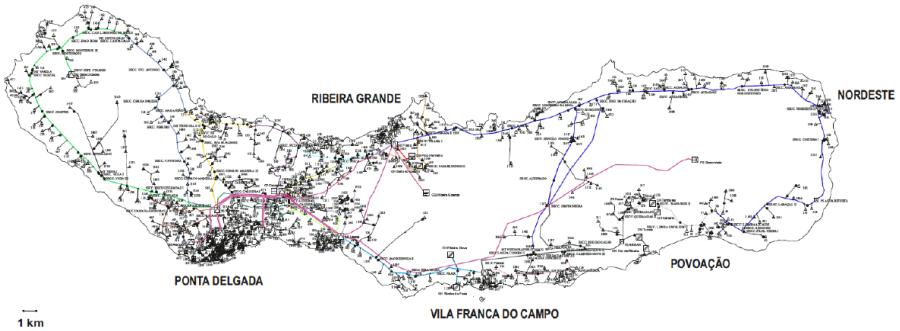

Figure 4.4: Area of influence of each substation (from [82])

4.2.1.2 Distribution system

The distribution system in medium voltage is established at 10kV in the cities of Ponta Delgada, Ribeira Grande and Lagoa, in the village of Vila Franca do Campo and Sete Cidades. The remaining locations are supplied by a distribution system set to 30kV. Table 4.3 gives the data for both types of distribution.

Table 4.3: Substation data of São Miguel: Adapted from [82]

Nível de Tensão [kV]	Extensão da Rede [km]			Postos de Transformação					
	Aérea	Subterrânea	Total	PTD		PTC		Número Total	Potência Instalada Total [kVA]
				Número	S [kVA]	Número	S [kVA]		
10	0,00	173,45	173,45	181	95.130	147	81.170	328	176.300
30	436,72	87,52	524,24	332	99.205	218	60.060	550	159.265
Totais São Miguel	436,72	260,97	697,69	513	194.335	365	141.230	878	335.565

4.2.2 Production

Figure 4.5 presents two graphics that represent the monthly evolution of emission per primary energy source and the total values for the year.

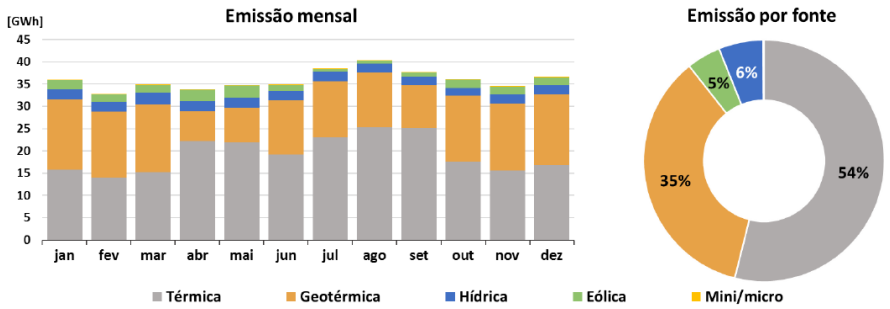

Figure 4.5: Substation data of São Miguel (from [82])

The diagrams that represent the demand in days corresponding to the 4 season of the year are presented in Figure 4.6, which include the type of energy used to fulfill the demand. The graphics have the purpose to describe the variations in the demand and the differences in the impact that renewable resources present depending heavily on the season of the year.

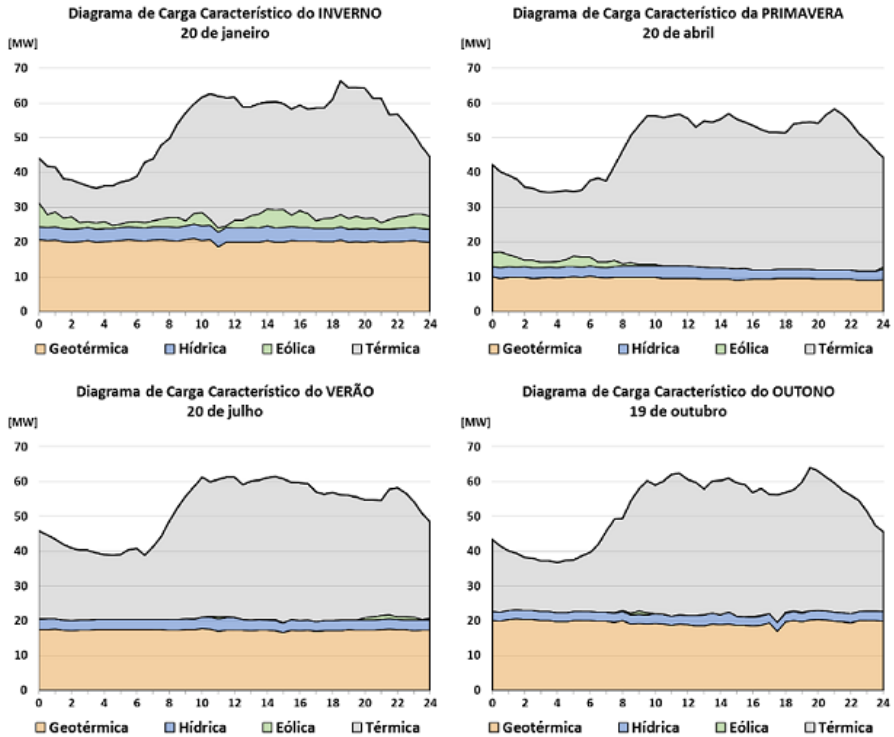

Figure 4.6: Production diagrams (from [82])

The following diagrams, presented in Figure 4.7, refer to different days of the week: week days, saturdays, sundays/holidays. The week days are always from a wednesday. Sundays are considered equal to holidays.

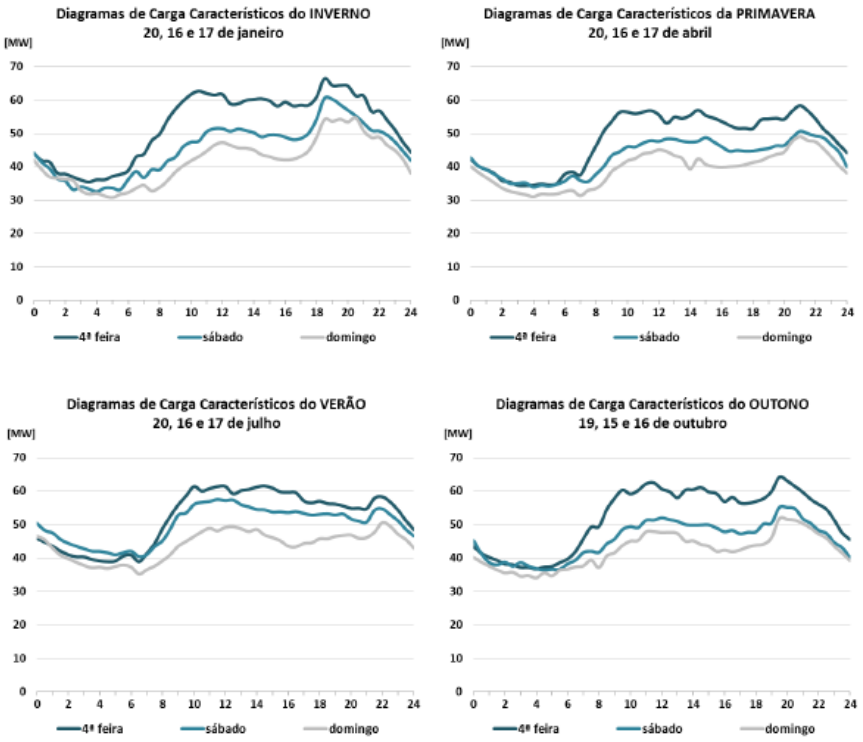

Figure 4.7: Load diagrams for diffrent days of the week (from [82])

4.2.3 Real Case Study: Lagoa System (10kV)

Tables 4.4 to 4.6 show, respectively, the area of action of the Lagoa System, grid extension and the transformer stations and finally two typical days for two different seasons of the year (Winter and Spring).

Table 4.4: Area of action of the Lagoa System: Adapted from [82]

Instalação	Concelhos	Freguesias				
SELG	Lagoa	Nossa Sª do Rosário	Santa Cruz	Água de Pau	Cabouco	Ribeira Chã
	Vila Franca do Campo	Água d'Alto				
	Ribeira Grande	Santa Bárbara				
	Ponta Delgada	Livramento				

Table 4.5: Grid Characterization: Adapted from [82]

Instalação	Nível Tensão [kV]	Saída MT	Extensão da Rede			Postos de Transformação					
			Aérea	Subterrânea	Total	PTD		PTC		Número Total	Potência Instalada Total [kVA]
						Número	S [kVA]	Número	S [kVA]		
		Total	0,00	34,87	34,87	37	15.895	15	7.510	52	23.405
SELG	10	Lagoa 1	–	10,68	10,68	15	6.775	5	1.890	20	8.665
		Lagoa 2	–	4,03	4,03	5	2.220	–	–	5	2.220
		Lagoa 3	–	6,92	6,92	5	2.940	4	3.315	9	6.255
		Sub-Total 10 kV	0,00	21,62	21,62	25	11.935	9	5.205	34	17.140

Table 4.6: Typical days in two different seasons of the year: Adapted from [82]

Instalação	Saída MT	Nível Tensão [kV]	Inverno 20 de Janeiro						Primavera 20 de Abril					
			Máximo			Mínimo			Máximo			Mínimo		
			P [kW]	Q [kVAr]	S [kVA]	P [kW]	Q [kVAr]	S [kVA]	P [kW]	Q [kVAr]	S [kVA]	P [kW]	Q [kVAr]	S [kVA]
SELG	Lagoa - Livramento	30	286	-25	287	152	-56	162	190	-36	193	115	-60	130
	Lagoa - Vila Franca	30	6.413	1.843	6.673	3.914	1.224	4.101	4.782	1.063	4.898	3.584	741	3.660
	Lagoa - Cabouco	30	1.367	110	1.371	754	-120	764	917	-25	917	420	-51	423
	Lagoa 1	10	1.575	455	1.639	879	227	908	1.303	411	1.366	731	181	753
	Lagoa 2	10	482	160	507	202	42	207	379	138	404	169	38	173
	Lagoa 3	10	2.101	770	2.237	254	26	255	2.006	705	2.126	221	26	223

Figure 4.8 shows the Lagoa System grid with 3 different colors that represent the 3 different exits from the medium voltage substation and Figure 4.9 shows a simplified grid with the different locations of the substations and its considerations like lines out of service.

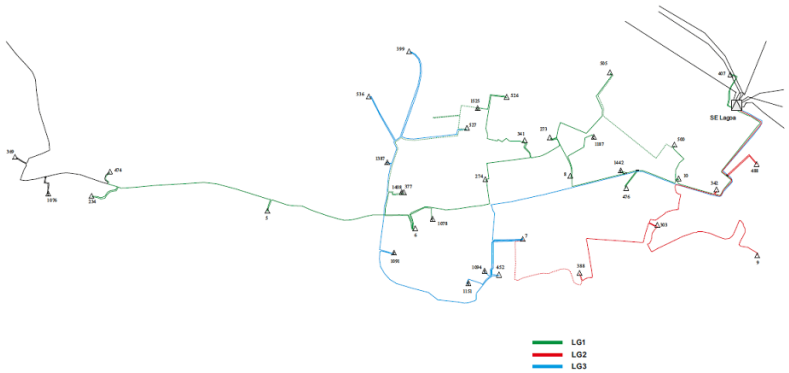

Figure 4.8: Grid Representation (from [82])

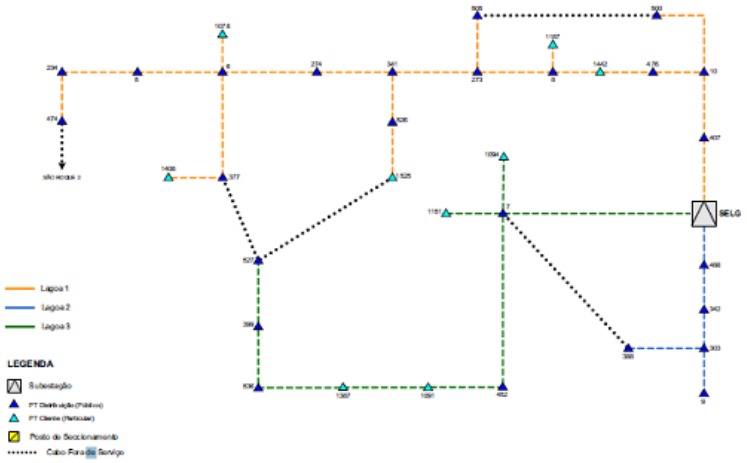

Figure 4.9: Grid Representation (from [82])

4.3 Scenario Description

There are innumerous sources of variability and uncertainty on energy systems operation, so they have, to be considered in the problem solution. The introduction of these uncertainties and variability creates a problem in optimization terms because of the excessive amount of constraints and variables, turning the problem into an exhausting computationally problem, that takes too long to solve and which additional conditions do not make that much of a difference. In this work were considered ten different scenarios of solar, wind and demand from São Miguel Island, Azores. Since the combination of all scenarios (10x10x10), a thousand in total, creates problems in terms of computational effort, the scenarios were reduced using a clustering technique, the k-means. Using the clustering technique the ten scenarios were reduced to three of solar, wind and demand

(3x3x3). With the combination of these scenarios, twenty-seven different scenarios are obtained and are the ones used in this dissertation analysis.

4.3.1 Solar Power Scenarios

Figure 4.10 shows the solar power output scenarios, obtained by the cluster of 10 different demand profiles. The reduction in the solar power output as well as in wind power output and electricity demand is done in order to ensure that the problem can be tracked.

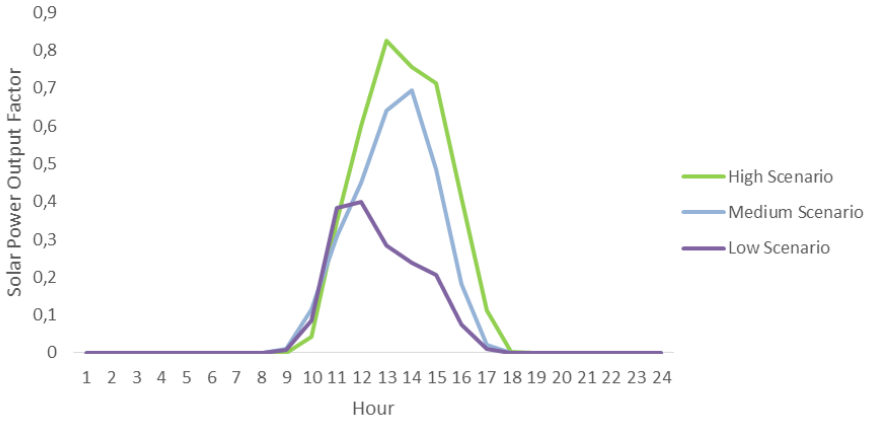

Figure 4.10: Solar Scenarios

4.3.2 Wind Power Scenarios

Figure 4.11 shows the solar power output scenarios, obtained by the cluster of 10 different demand profiles.

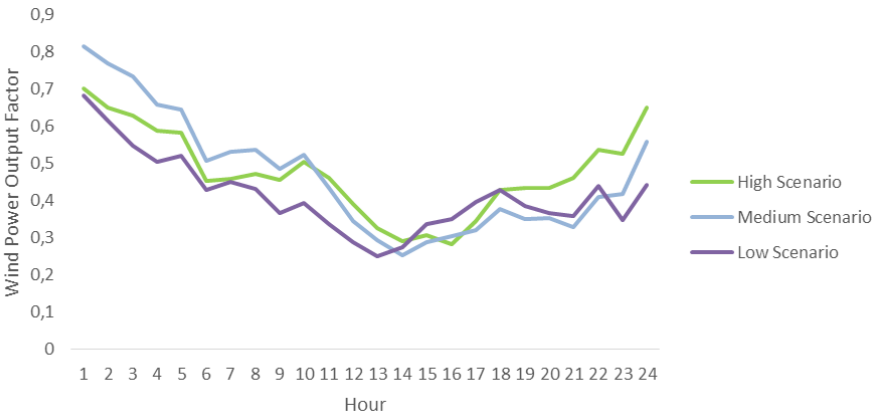

Figure 4.11: Wind Scenarios

4.3.3 Demand Scenarios

Figure 4.12 refers to the demand scenarios, obtained by the cluster of 10 different demand profiles.

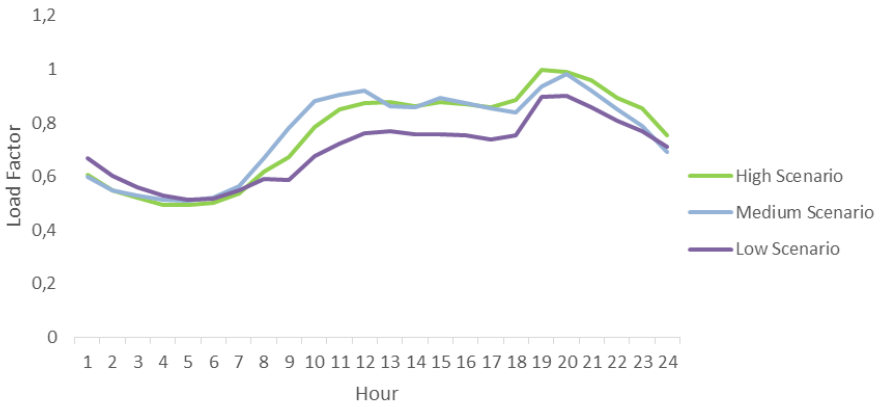

Figure 4.12: Demand Scenarios

4.4 Chapter Summary

This chapter has presented the considerations and assumptions used in order to perform the optimization process and consequent results analysis, in the next chapter, Chapter 5. The system data details of DGs and ESSs capacity placement, for both cases, can be seen in Appendix B.

Chapter 5

Results and Discussion

This chapter presents two different test systems, a theoretical and a real test system, to assess the mathematical formulation described in Chapter 3. The results obtained are analysed and discussed in terms of dynamic network reconfiguration, voltage deviation profiles, energy losses, energy matrix and total cost of each solution, considering several case studies for each system.

5.1 Introduction

The results of the test systems presented in the previous chapter will be now shown and discussed. First, the 119 bus test system results will be presented followed by the real system, Lagoa distribution system, from S. Miguel Island, Portugal. For both test systems, four case studies were considered, namely Case A, Case B, Case C and Case D, which are respectively summarized in table 5.1.

Case A represents the original case, where there is no reconfiguration, no DGs of any type and no ESSs devices. Case B is the same as Case A, but in this case reconfiguration was added. In Case C, different types of DGs are considered (namely PV and wind) together with reconfiguration. Finally in Case D, all the tools considered are used, specifically ESSs, DGs (PV and Wind) and reconfiguration.

Table 5.1: Case Studies

Case	Reconfiguration	DGs	ESSs
A	–	–	–
B	✓	–	–
C	✓	✓	–
D	✓	✓	✓

5.2 119 Bus Test System

5.2.1 Case A - Base Case

As stated before, Case A refers to the original case, where reconfiguration is not considered and DER is not implemented as part of the daily system operation. In this particular case, no bound for voltage deviation was considered, because otherwise the problem would not converge for some of the hours under analysis, making the simulation impossible. The voltage deviation for this Case can be seen in Figure 5.1, where the limit of $\pm 5\%$ was integrated in order to show where the case would be unable to converge. It is important to notice that the voltage deviation values are given by the average voltage deviation in each node. All the values are negative due to the fact that power flow goes from upstream to downstream. In this case there is only one source of power, the substation, and since the substation provides both active and reactive power for the entire system, the voltage deviation limits are not considered as previously stated, leading to limits violations. As further way the node is from the substation, higher is the voltage deviation value obtained, which is one of the issues that reconfiguration and DERs integration intends to solve.

Regarding the system losses, they are higher than they should be, as a consequence of the high voltage deviation, which lead to obtaining in this particular case, a total of 30.17 MW of active losses. Figure5.2 shows the losses in each hour and its trend.

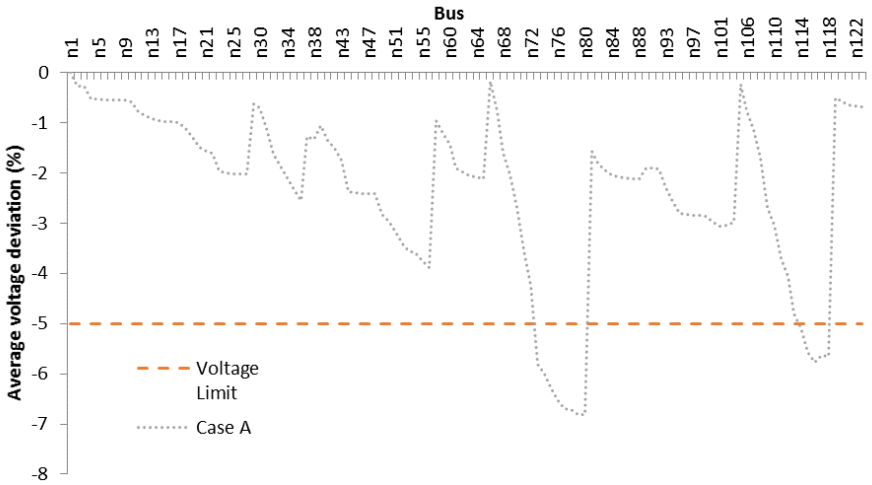

Figure 5.1: Average voltage deviation in Case A

5.2.2 Case B – Base Case together with Reconfiguration

Case B is the same as Case A, but in this case reconfiguration was added in order to perform dynamic reconfiguration on the systems operation. As mentioned in Chapter 2, the distribution systems reconfiguration can be used for different purposes, always aiming to improve the system performance. In this particular case, the use of reconfiguration will improve the system losses.

Comparing Case A with Case B it is possible to verify the active power losses decrease from 30.17 MW to 20.38 MW, respectively, representing a decrease of 32%. This variation happens

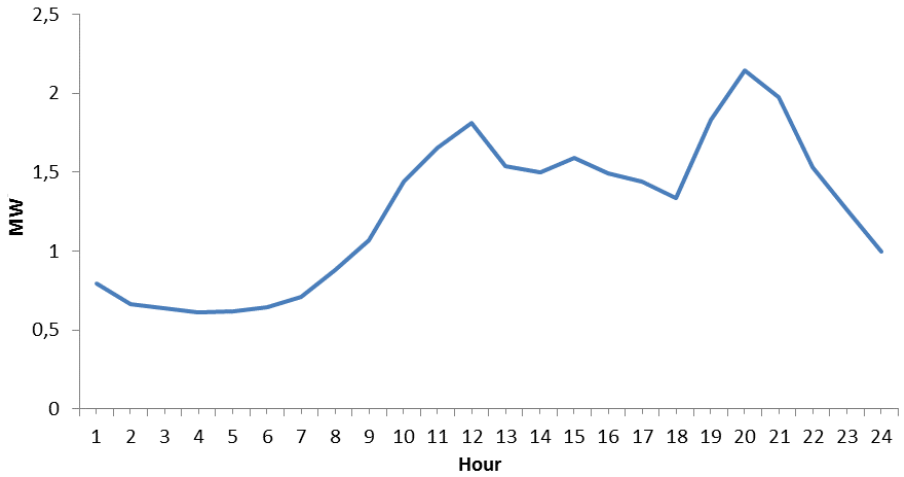

Figure 5.2: Base Case losses

due to the constant grid need to fulfill the demand, aiming to give at each hour, the most efficient possible network. Figure 5.3 shows the hourly losses values and its tendencies. As previously stated, the losses in Case A are higher in peak hours, however, the variation between peak and shallow hours decreases largely due to the application of dynamic reconfiguration. The period that has the greater amount of losses in Case B does not go much more above 1 MWh, while in Case A that values goes over 2MWh, which is relevant in terms of cost. Although grid reconfiguration at each hour has an aggregated cost, the total cost of operation has a big reduction, something that will be shown and analysed later in this chapter.

The distribution system reconfiguration for each hour is presented in Figures 5.4 to 5.27. In these figures is possible to see that all nodes are fed, and the network topologies at all times, for the different configurations are radial. The reconfiguration is done in order to feed the demand in all nodes, considering the scenarios, in every hour, through the less congested path and with the lower R / X.

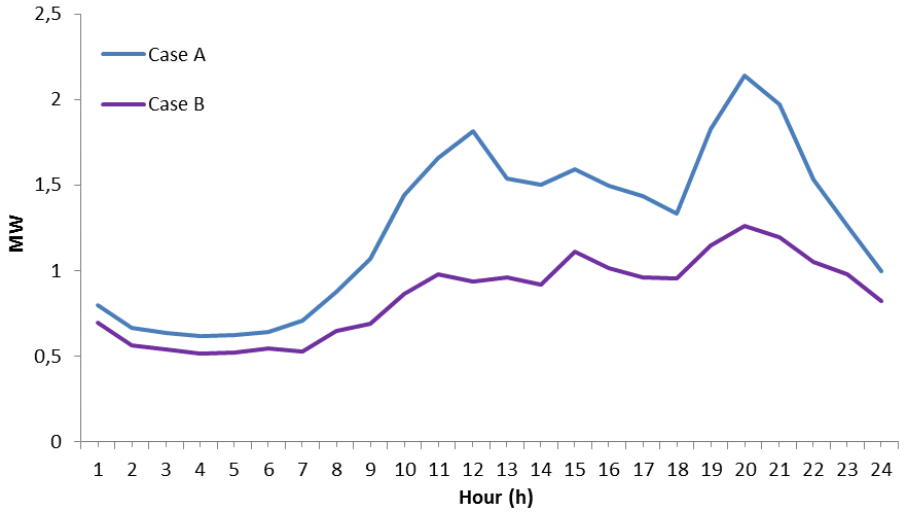

Figure 5.3: Case A and Case B system losses

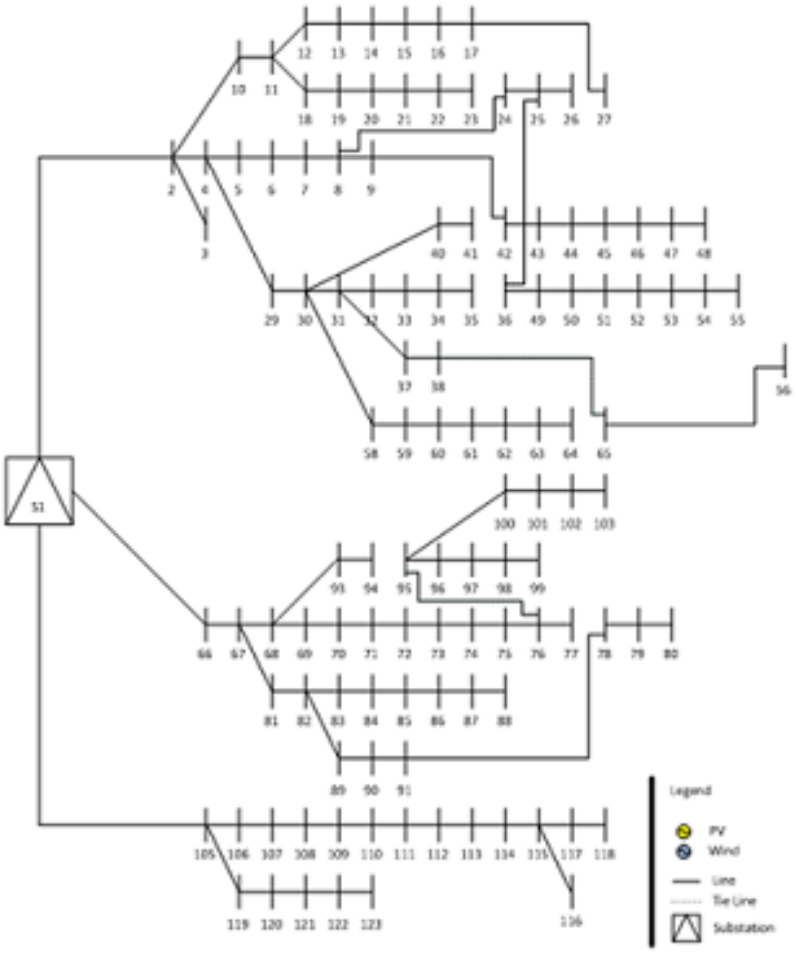

Figure 5.4: 119 Bus test system reconfiguration for h=1

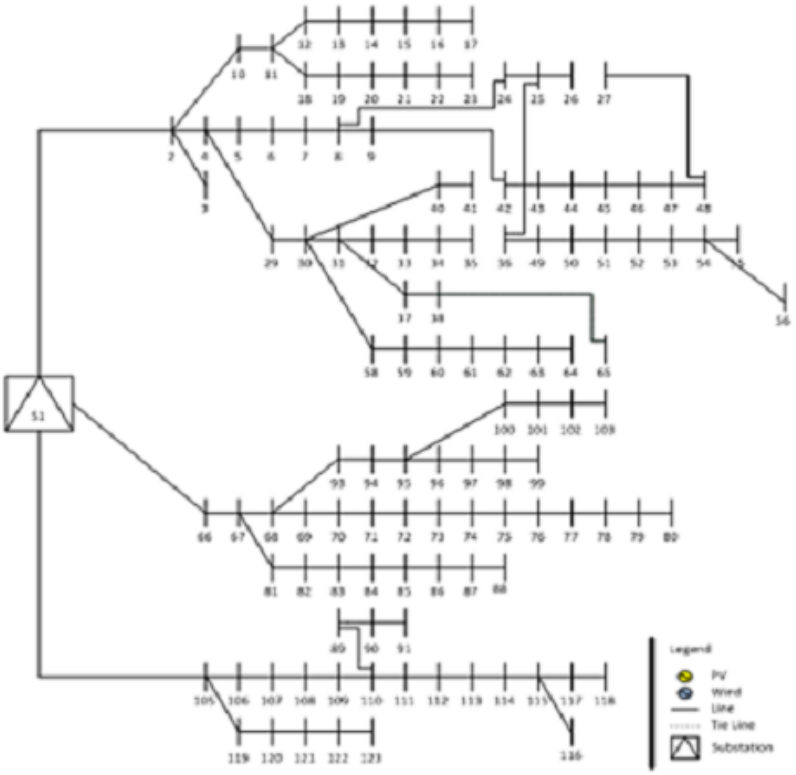

Figure 5.5: 119 Bus test system reconfiguration for h=2

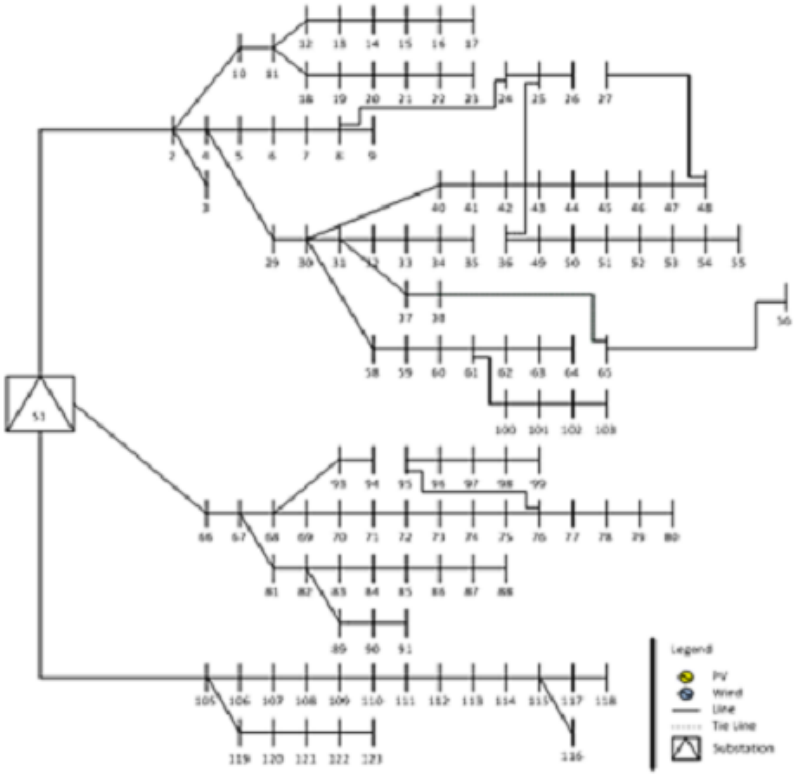

Figure 5.6: 119 Bus test system reconfiguration for h=3

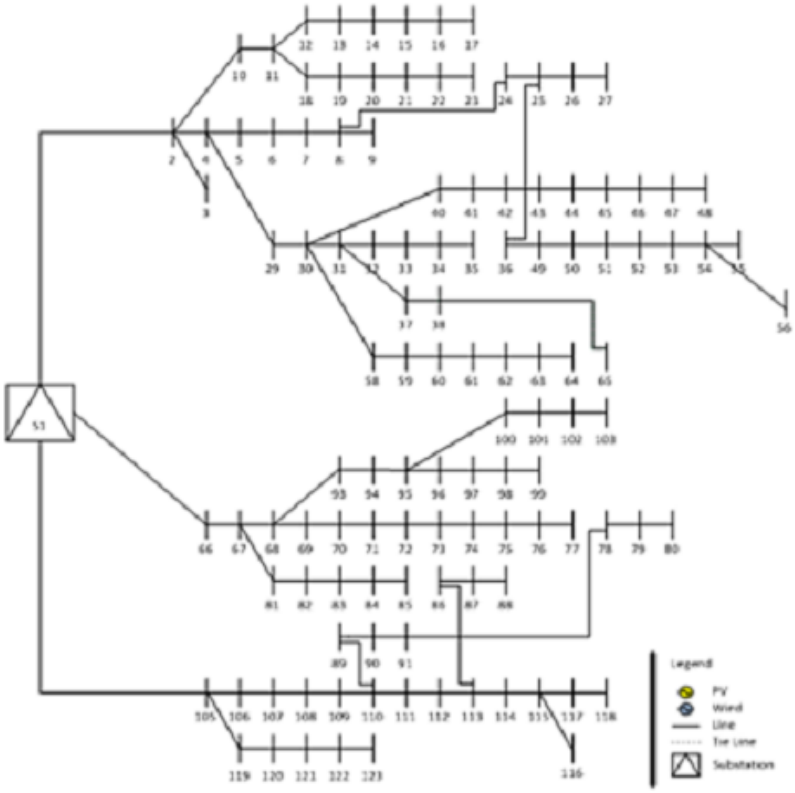

Figure 5.7: 119 Bus test system reconfiguration for h=4

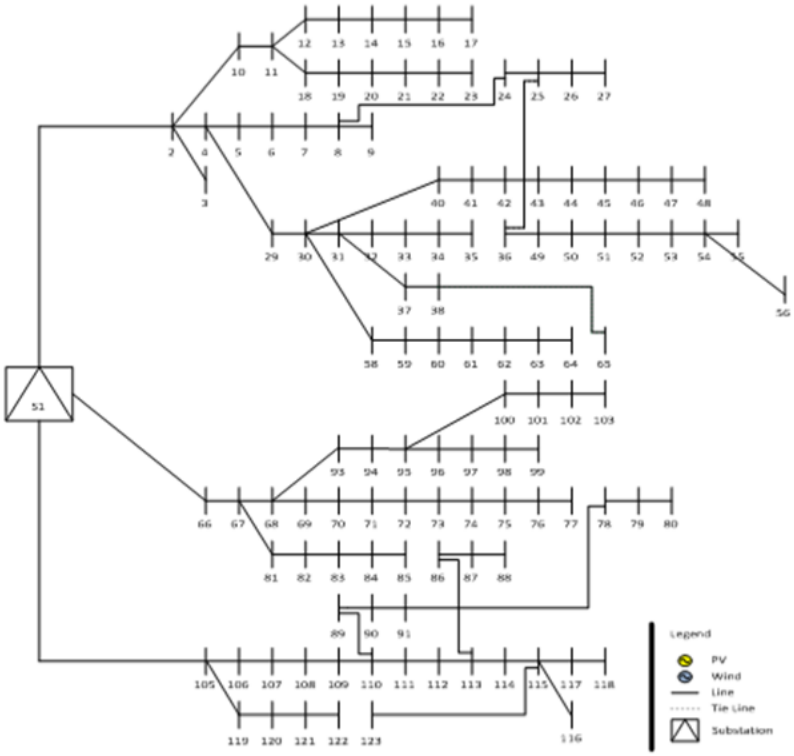

Figure 5.8: 119 Bus test system reconfiguration for h=5

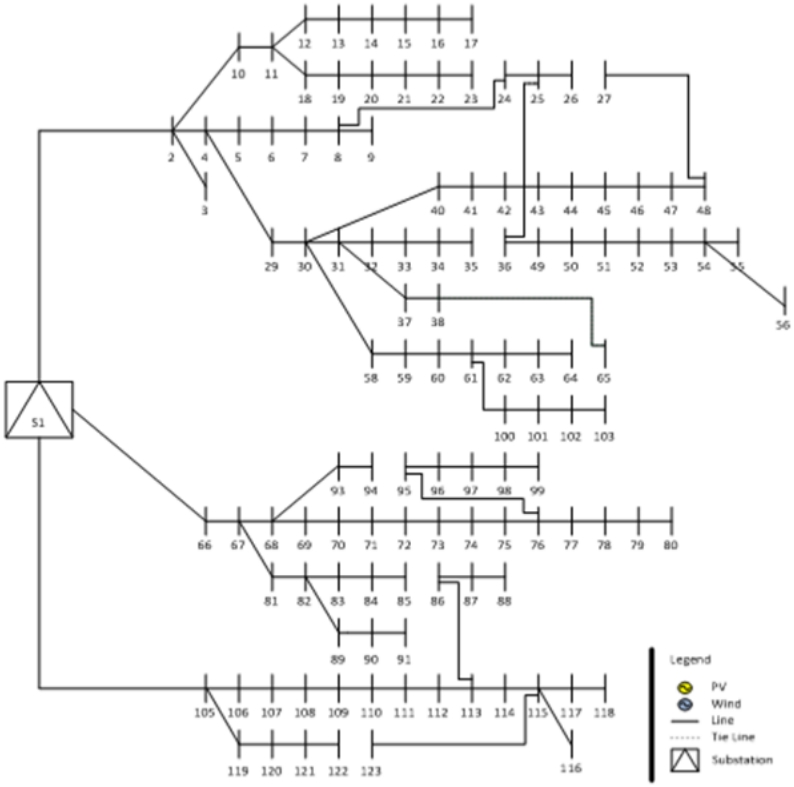

Figure 5.9: 119 Bus test system reconfiguration for h=6

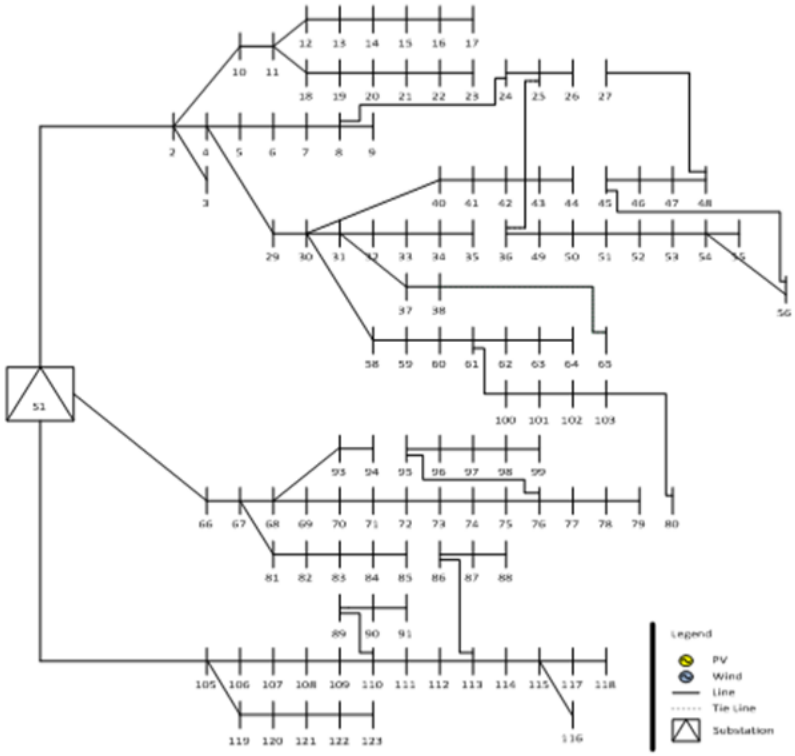

Figure 5.10: 119 Bus test system reconfiguration for h=7

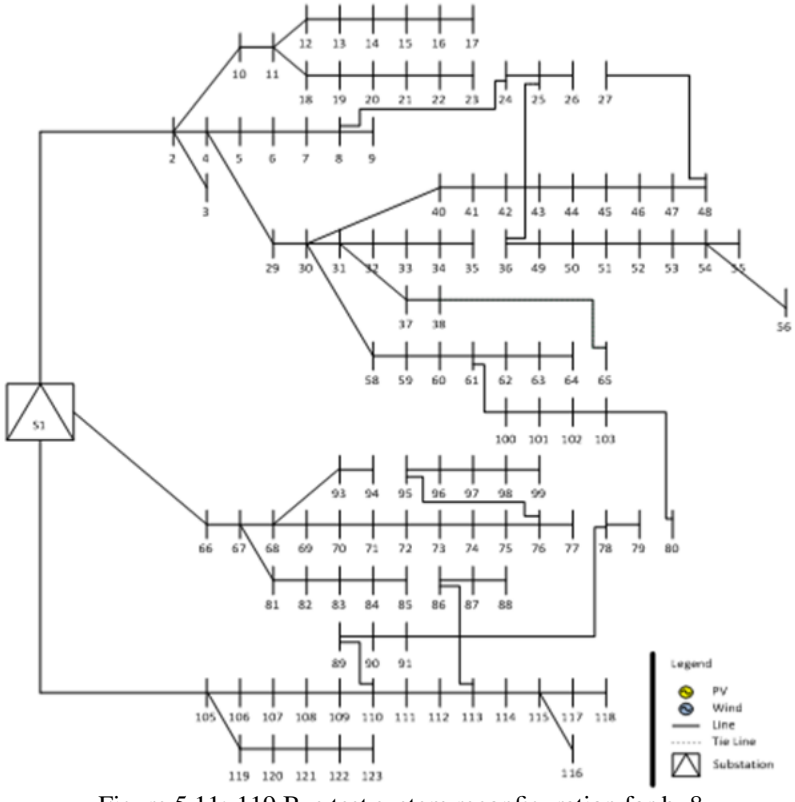

Figure 5.11: 119 Bus test system reconfiguration for h=8

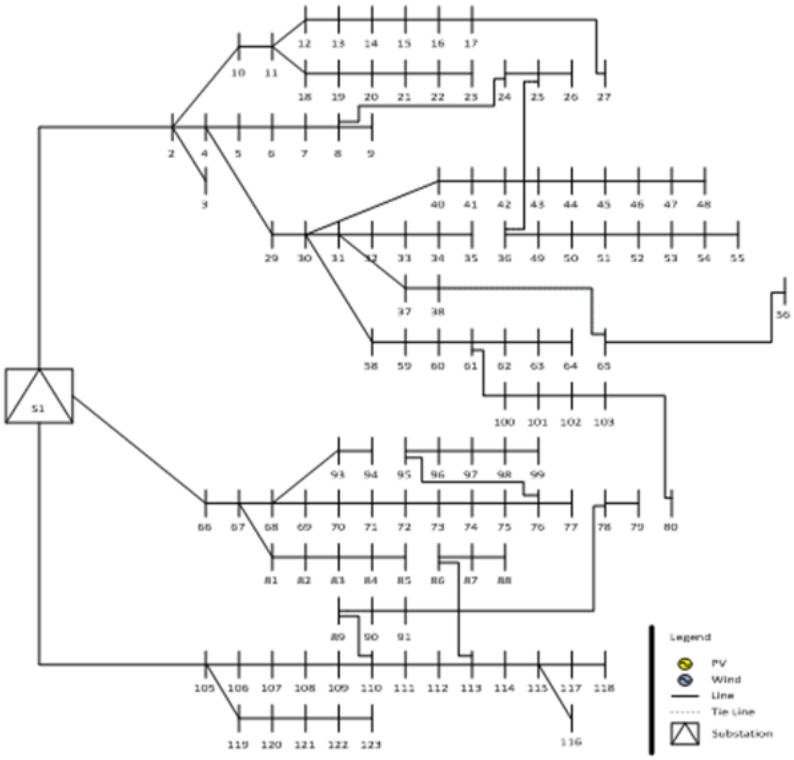

Figure 5.12: 119 Bus test system reconfiguration for h=9

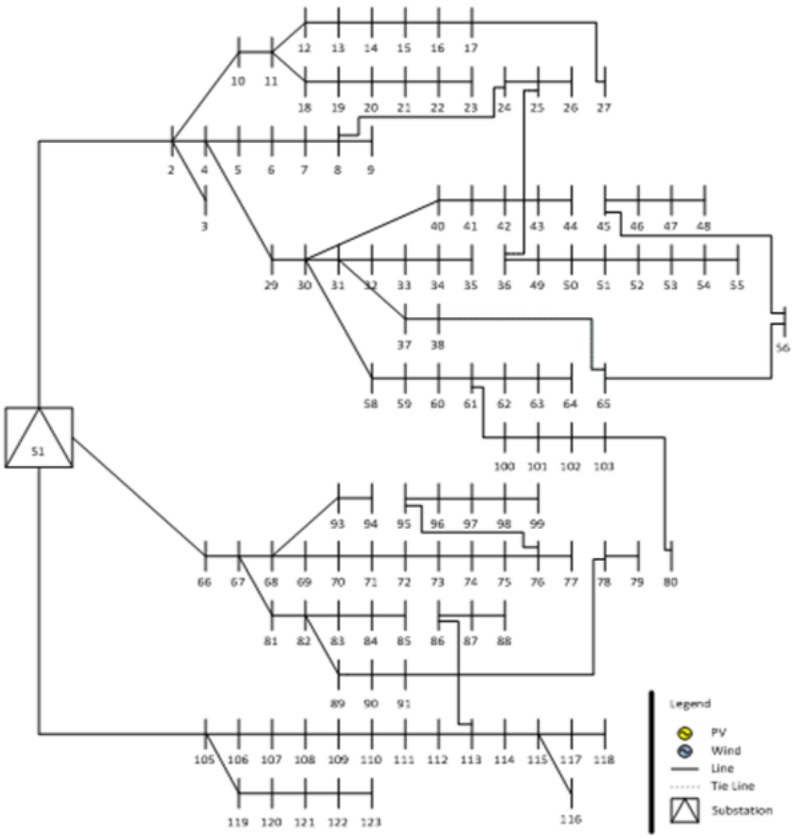

Figure 5.13: 119 Bus test system reconfiguration for h=10

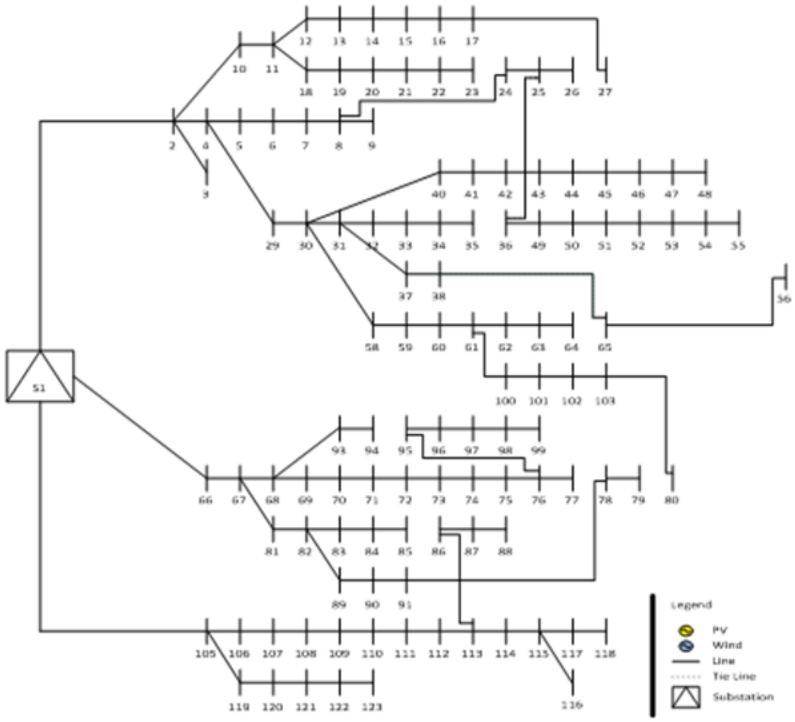

Figure 5.14: 119 Bus test system reconfiguration for h=11

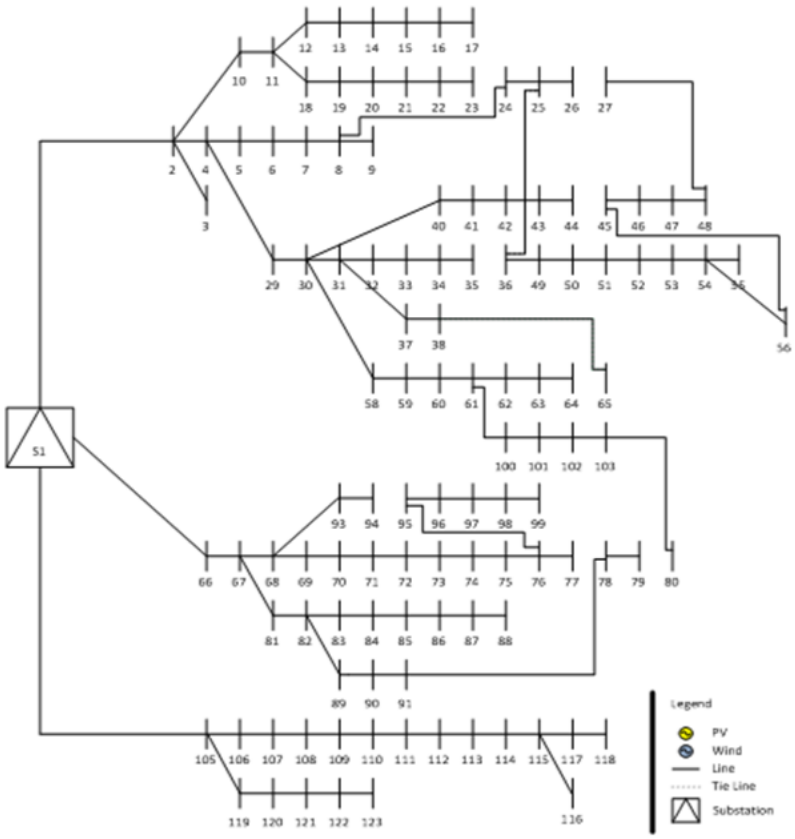

Figure 5.15: 119 Bus test system reconfiguration for h=12

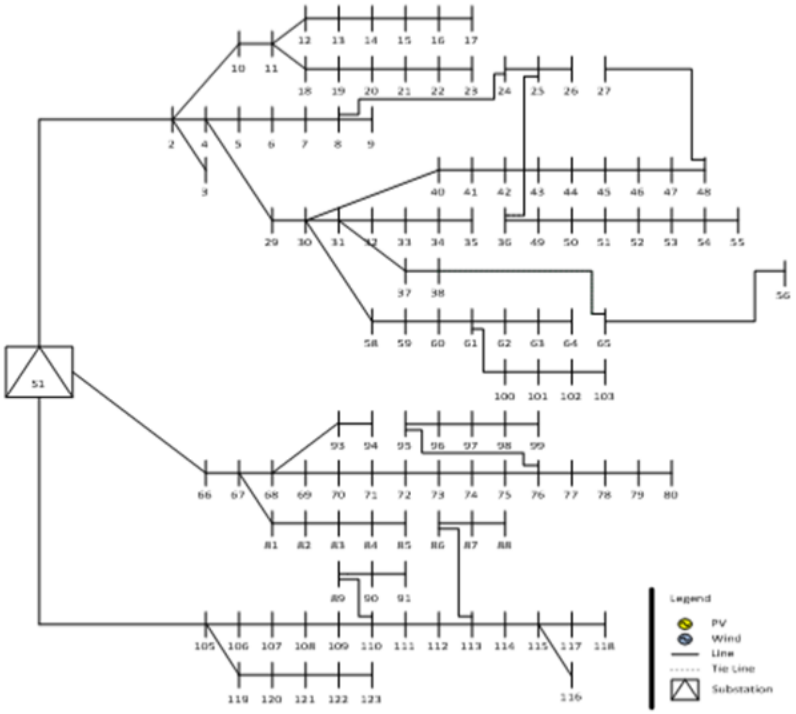

Figure 5.16: 119 Bus test system reconfiguration for h=13

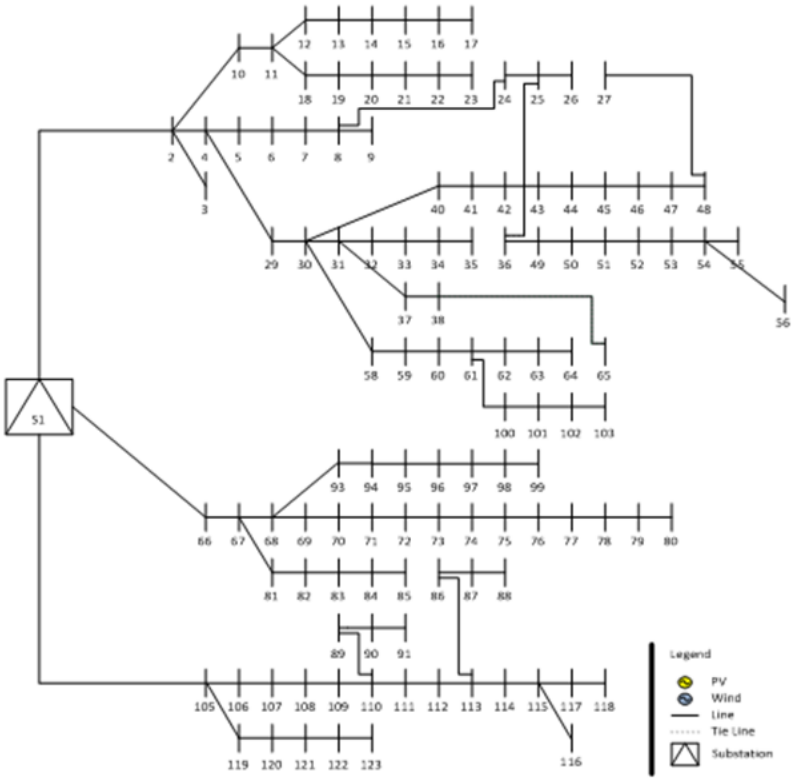

Figure 5.17: 119 Bus test system reconfiguration for h=14

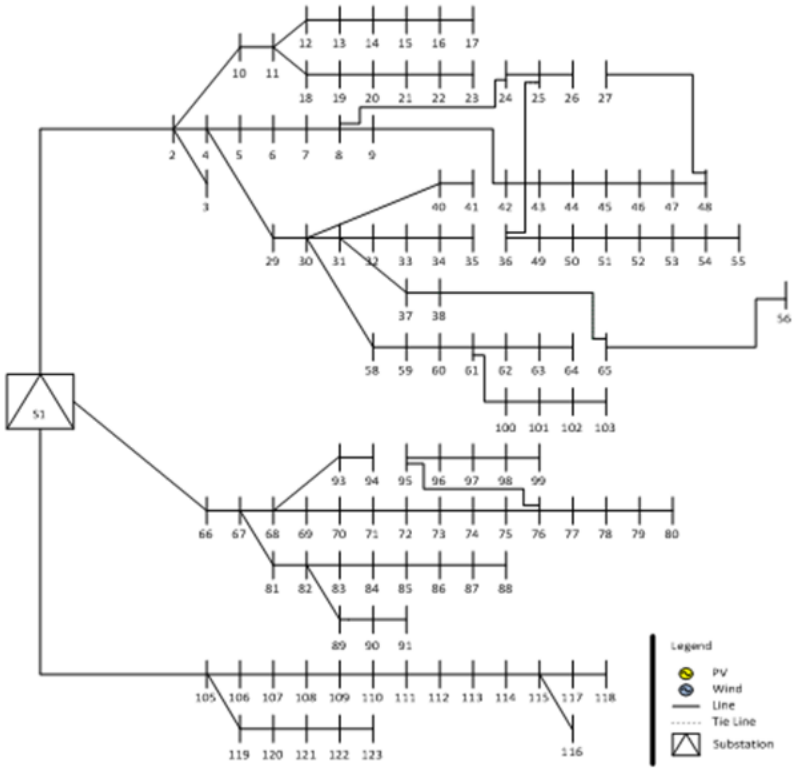

Figure 5.18: 119 Bus test system reconfiguration for h=15

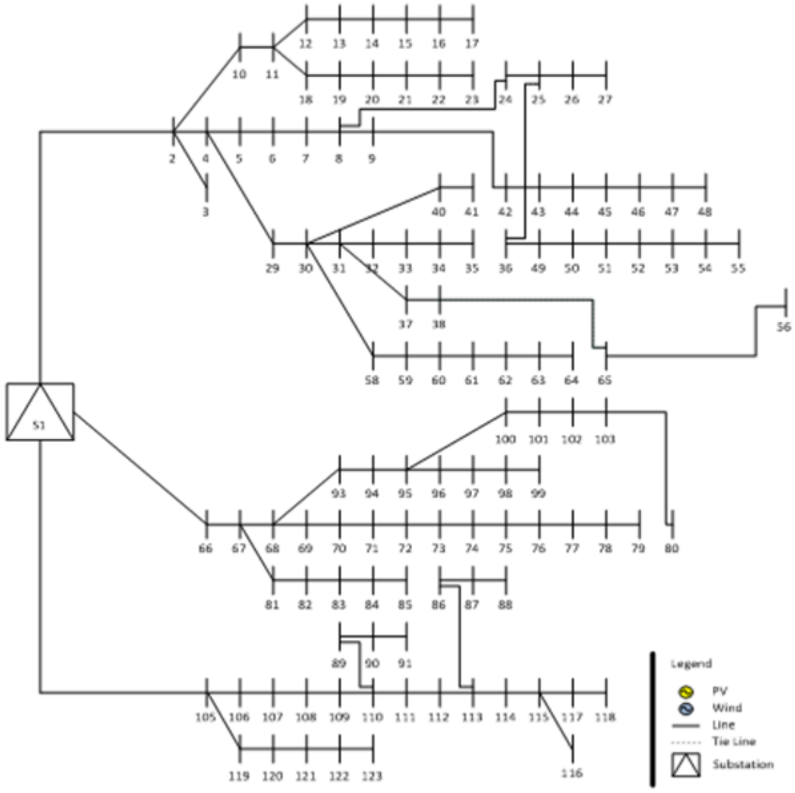

Figure 5.19: 119 Bus test system reconfiguration for h=16

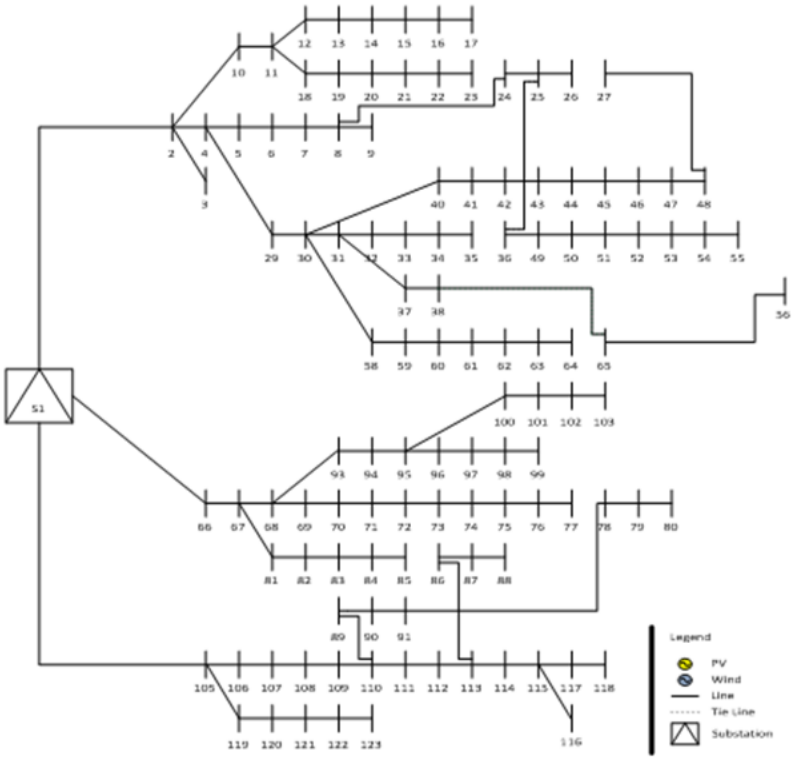

Figure 5.20: 119 Bus test system reconfiguration for h=17

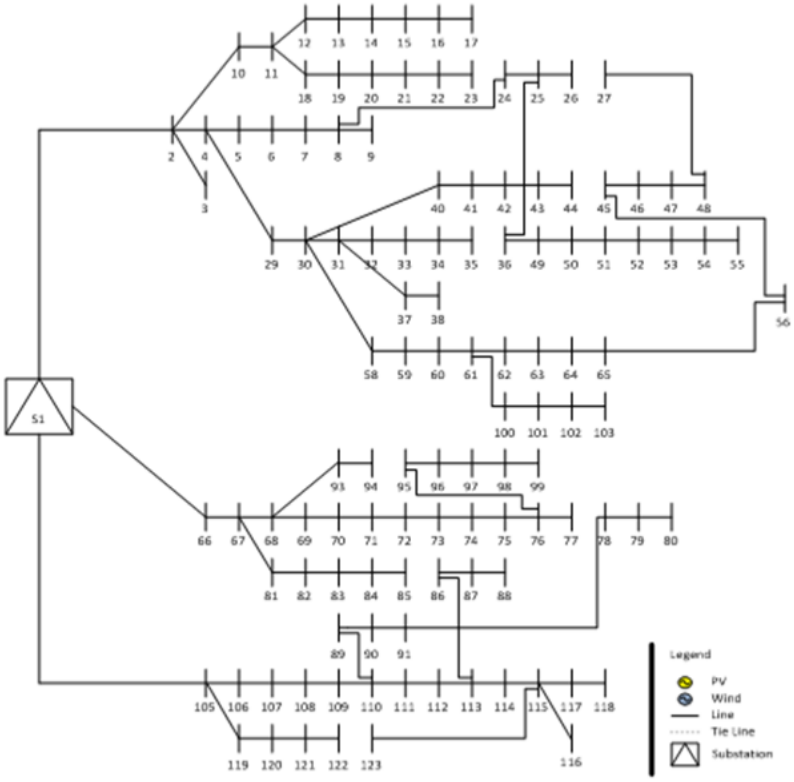

Figure 5.21: 119 Bus test system reconfiguration for h=18

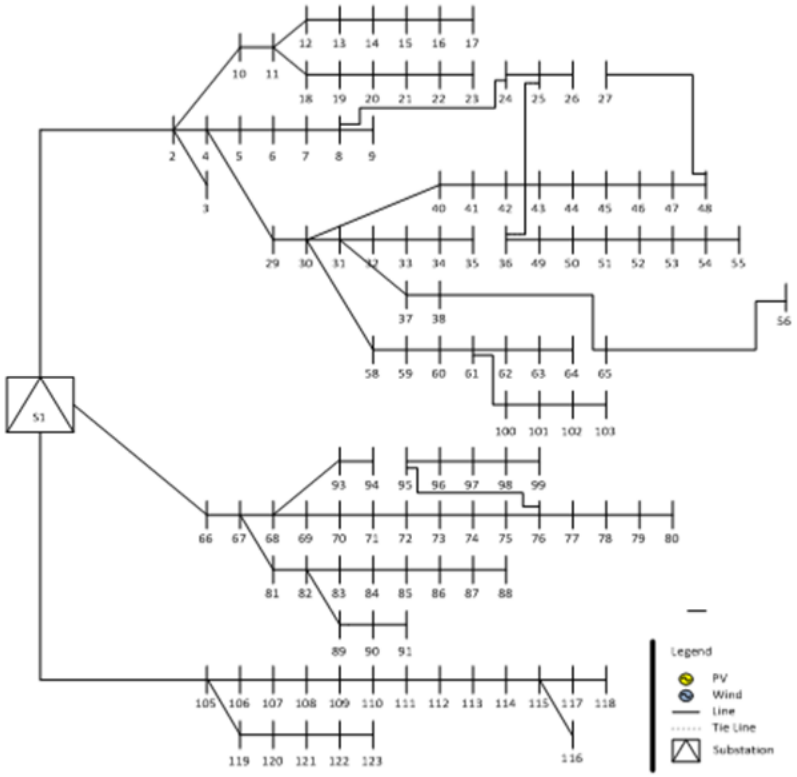

Figure 5.22: 119 Bus test system reconfiguration for h=19

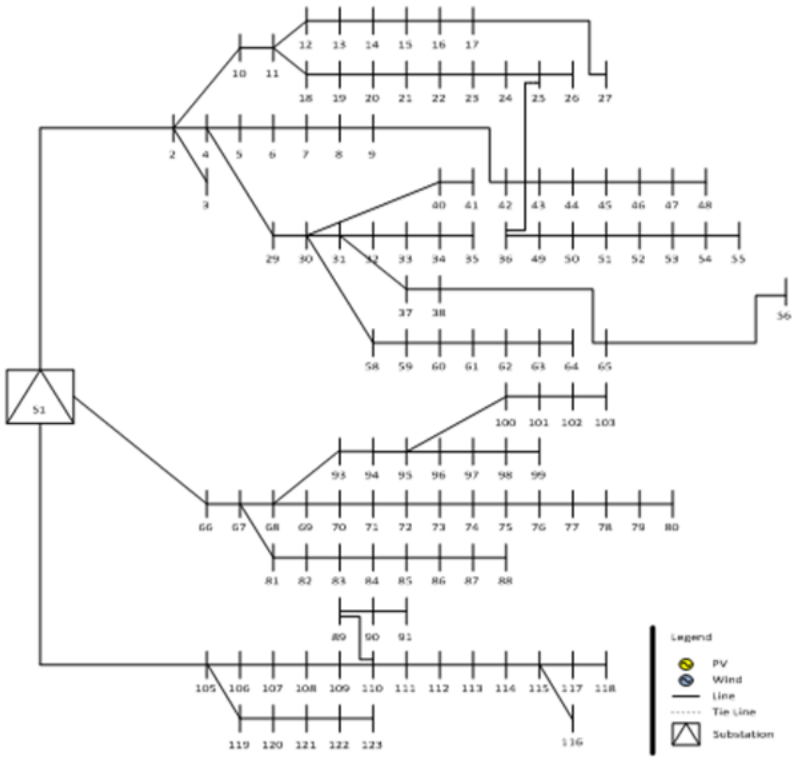

Figure 5.23: 119 Bus test system reconfiguration for h=20

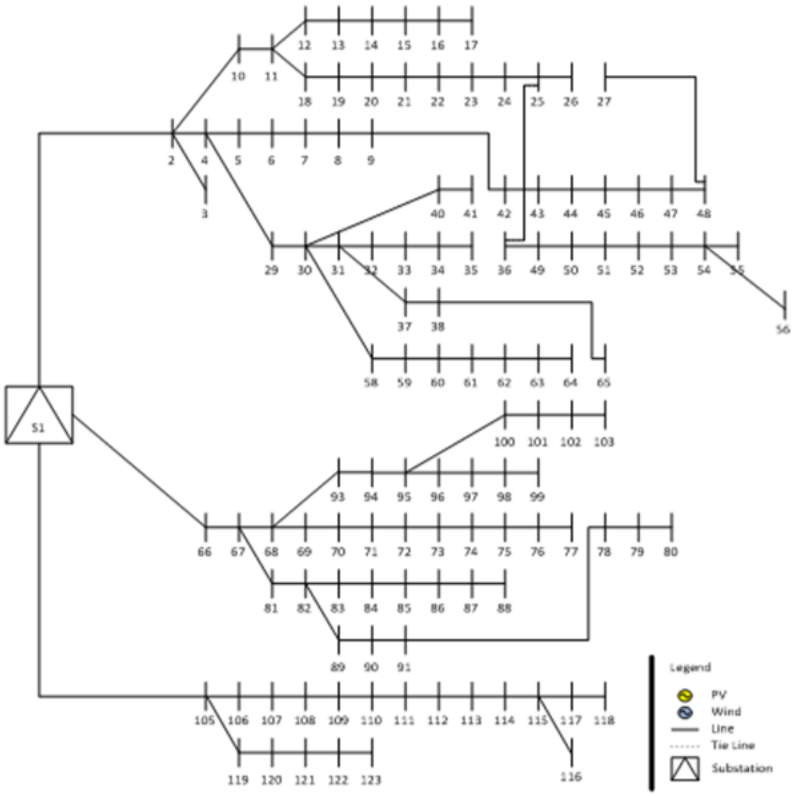

Figure 5.24: 119 Bus test system reconfiguration for h=21

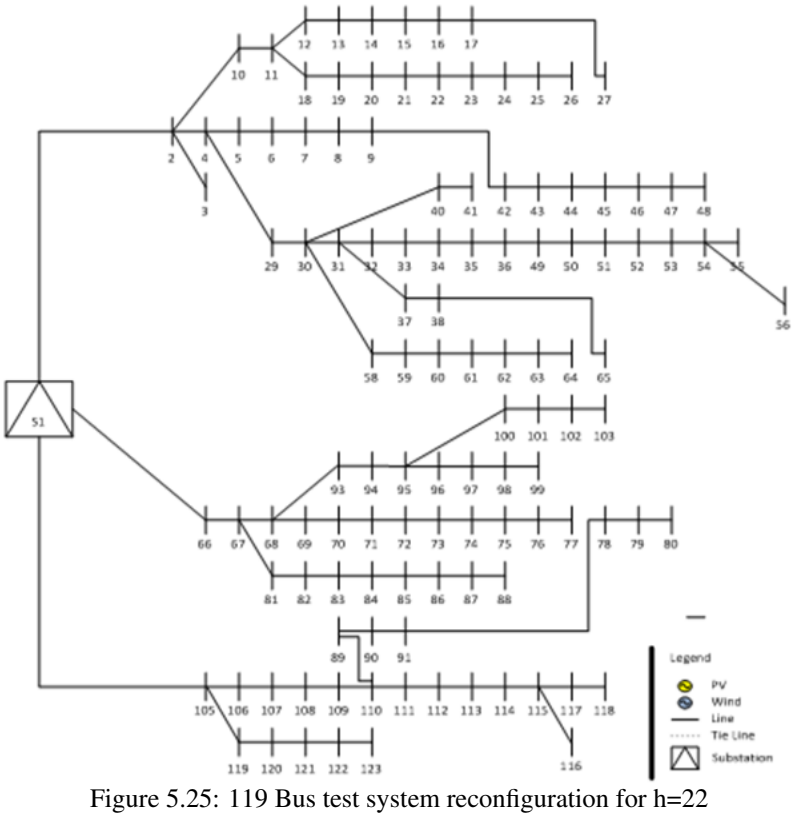

Figure 5.25: 119 Bus test system reconfiguration for h=22

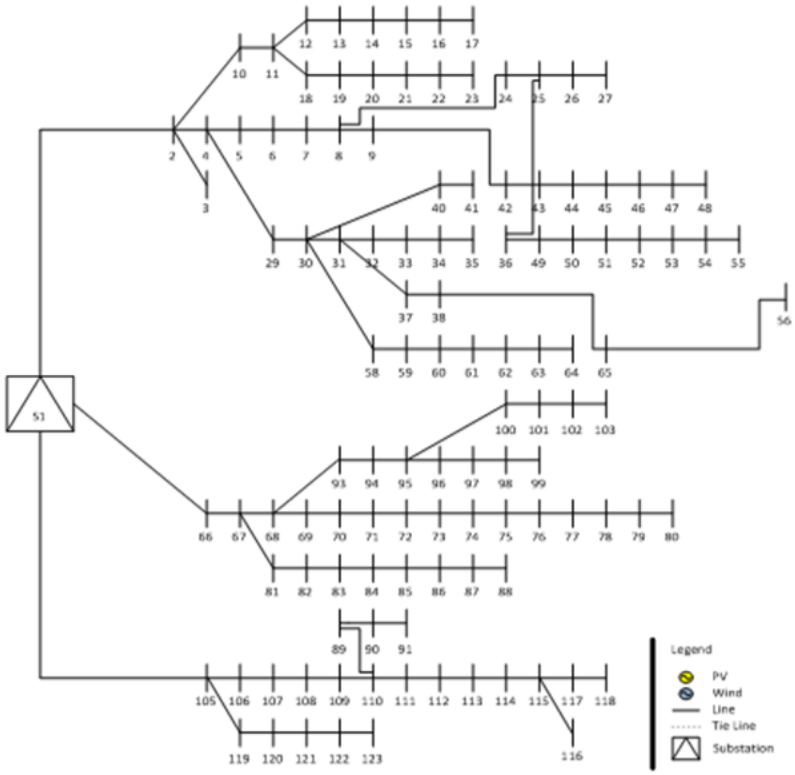

Figure 5.26: 119 Bus test system reconfiguration for h=23

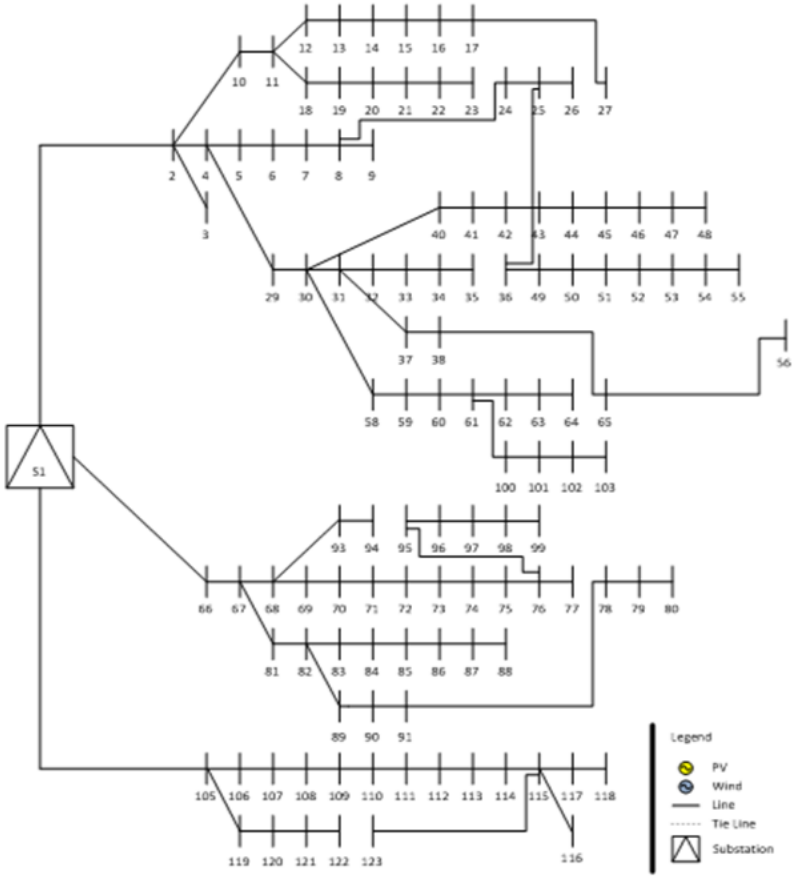

Figure 5.27: 119 Bus test system reconfiguration for h=24

5.2.3 Case C – Considering Dynamic Reconfiguration and Distributed Energy Resources

The third case study, Case C, is the case where different types of DGs are considered (namely PV and wind) together with dynamic reconfiguration. In this case it is relevant to analyse the influence of these two technologies combined in terms of voltage deviation. Contrarily to Case A, the voltage deviation limits are considered, and the substation is not now the only source of power in the network. The system dynamic reconfiguration for this case study, for every hour can be seen in Figure C.1 to Figure C.24 in the Appendix C (in order to make the present document more fluid). Similarly to the previous case, all nodes are fed, and the network topologies at all times, for the different configurations are radial. The reconfiguration is done in order to feed the demand in all nodes, considering the scenarios, in every hour, through the less congested path and with the lower R / X.

Figure 5.28 shows the case study average voltage deviation, where it is easily seen that the voltage deviation for Case C is not even near to the pre-defined limit. It is also important to notice that, the values are much lower for the nodes that are further way from the main source of power (the substation), when comparing this case with Case A. Besides, there are a large deviation decrease in Case C, close to 2% in the nodes 117 and 118. However, the voltage deviation still follows the same pattern as Case A, where the further nodes are still more affected in voltage deviation terms. Nerveless, the integration of DGs into the network considerably alleviates the nodes voltage deviation (decreases) in relation to the voltage limits.

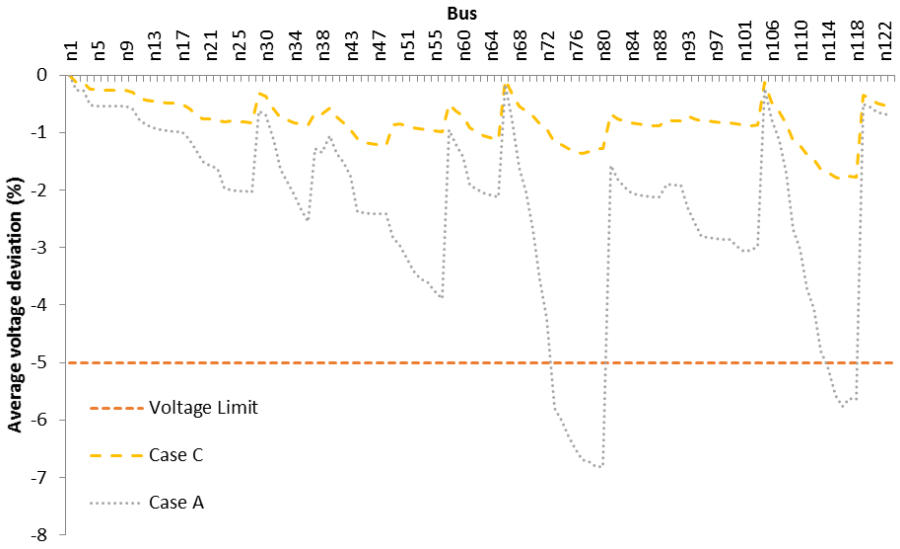

Figure 5.28: Average voltage deviation in Case C

Regarding the losses, they are much lower when compared to Case A and Case B, as can be seen in Figure 5.29. The inclusion of DGs in the system makes the power system requirements lower when compared with Case A. This power decrease need happens because the DGs are partially supplying the demand of the vicinity nodes. Consequently these nodes are partially fed by the substation, therefore the energy losses are reduced, since most of the power needed to

supply the nodes needs is produced locally. Comparing Case C to Case B, it is possible to note that as expected losses decrease, having a fluctuation around 0.5 MWh on average, with a peak in the evening, around hour 19 and 21 in both cases. The total active power losses in Case C are 14.42 MW, representing a decrease of 29.27% e 52.22% in cooperation with Case B and Case A, respectively.

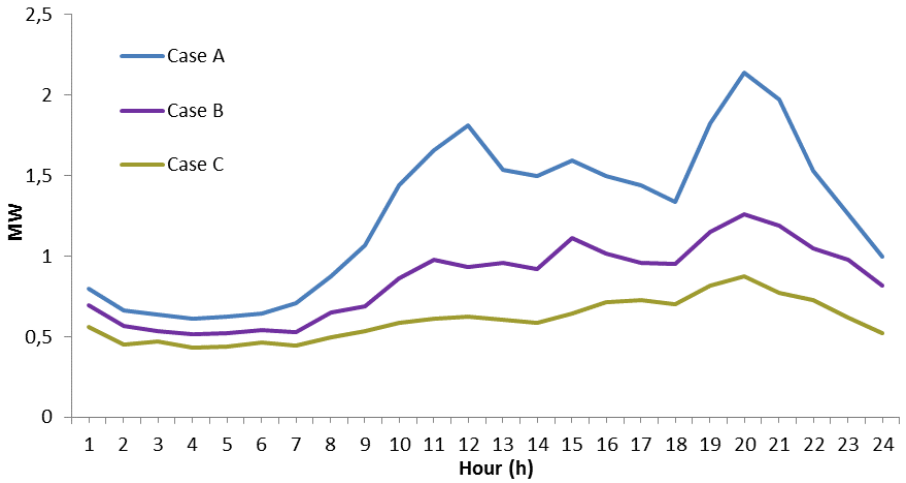

Figure 5.29: Case A, Case B and Case C system losses

The integration of DGs in the system considerably affects the energy matrix and this effect can be seen in the comparison analysis of Case A and Case C. This analysis allows not only comparing the variation of the power supplied by the original source but also the real impact of DGs in the system. Observing Figure 5.30 (Case A), has a simple correlation between the demand and the PSS (power purchased from the upstream grid), which is easily explained with the fact that the substation is the only source.

In Figure 5.31 can be seen the Case C energy matrix. In this case a vast part of the demand is supplied by the substation (proximally 70.50%) and the remaining demand is fulfilled by DGs (proximally 29.50%). This means that a good part of the energy supplied to the customer is from a renewable source. The biggest renewable contribution comes from the wind type DGs as expected, since they are large minority of renewable DGs present are from wind type. It is also possible to verify that a fraction of the renewable energy produced is not used. The DGs resource brings great advantages to the system in economic and environmental terms, and this analysis is made in subsection 5.2.5.

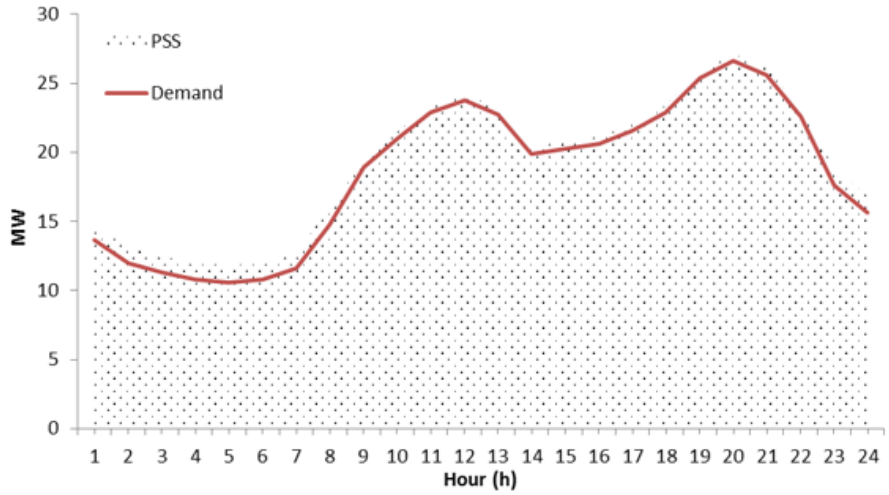

Figure 5.30: Case A energy matrix

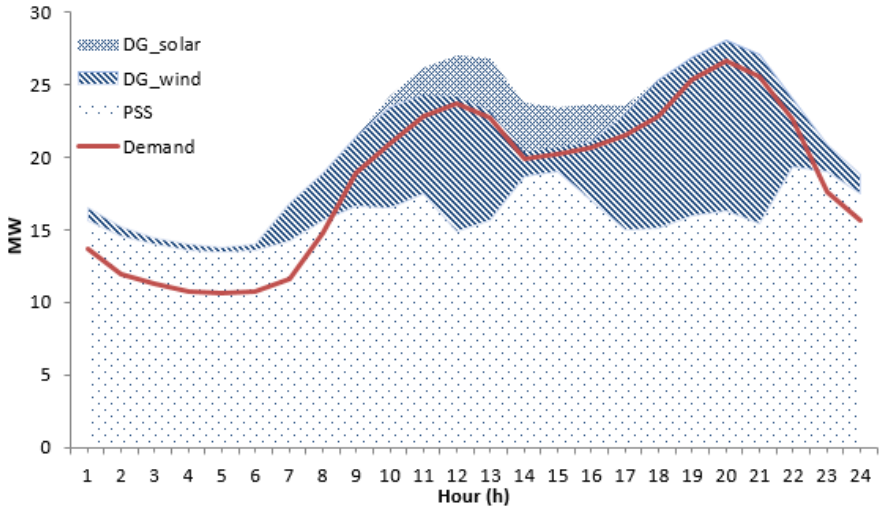

Figure 5.31: Case C energy matrix

5.2.4 Case D – Considering Dynamic Reconfiguration, Distributed Energy Resources and Energy Storage Systems

Finally Case D, which is the most complex case since all technologies considered in this work are used (dynamic reconfiguration, distributed energy resources (wind and PV) and energy storage systems). The system dynamic reconfiguration for this case study, for every hour can be seen in Figure C.25 to Figure C.48 in the Appendix C (similarly to the previous case, in order to make the present document more fluid). From the system reconfiguration analysis can be seen that all nodes are fed, and the network topologies at all times, for the different configurations are radial. Also the hourly topology configuration is always different from the previous hour to the next hour. The reconfiguration is done in order to feed the demand in all nodes, considering the scenarios, in every hour, through the less congested path and with the lower R / X.

In Figure 5.32 is presented the average voltage deviations of the Cases A, C and D. The best voltage deviation profile is presented by Case D which is different from Case C only in one technology type added, the ESSs. The ESSs presence improves the voltage profile proximally 1% as expected, since this will act the same way as the DGs, when they are discharging, supplying the demand locally.

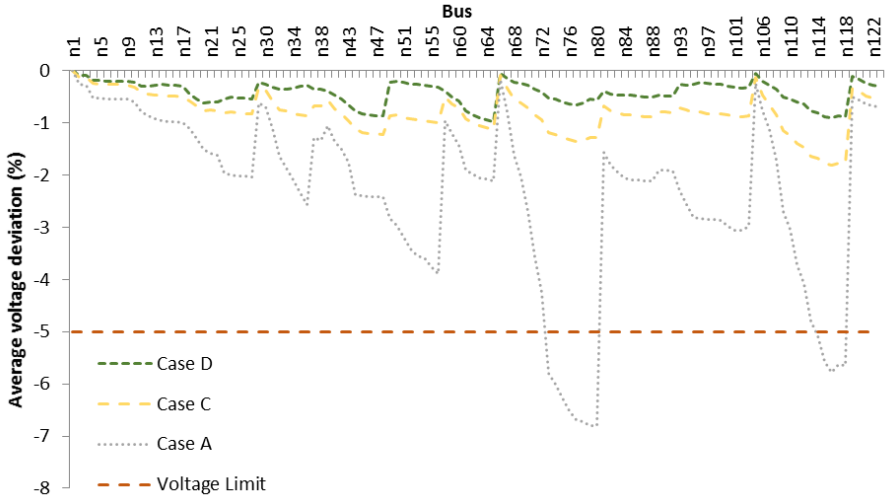

Figure 5.32: Average voltage deviation of the Cases A, C and D

The losses for the different case studies are presented in Figure 5.33. Looking at all the case studies, it can be seen that Case D is the one with the lowest losses, as expected. The losses are lower than in Case C because the introduction of ESSs, since this technology charge some of the power that would otherwise be lost by curtailment. That is, ESSs will charge energy in periods where the energy is cheaper and/or periods when there is an excess of renewable production, and will discharge in the periods where energy prices are higher and/or the renewable production is less in order to satisfy the demand at all time. This reduces the losses since the majority of the system losses occur in the lines between the production and the consumptions. Since the ESSs when they are discharging partially feed the nodes in the vicinities, the energy coming from further generation points will be smaller, therefore reducing the losses. Also, the ESSs integration creates a healthier system operation since the peak hours are reduced transforming the system into one that is closer to its optimal operational point.

The total active losses for Case D is equal to 10MW, representing a decrease of 30.66%, 50.95% and 66.87% from Case C, B and A, respectively. With the implementation of ESSs, the peak hours stop being the hours with the most amounts of losses, which is justified by the fact that the ESSs are discharging to the grid as already stated. The average losses over a 24 hours period are considerably lower when comparing to a system like the one in Case C.

Figure 5.34 shows the energy matrix in this case, where it is important to notice that, despite being installed and available, no solar DG was used by the system due to its price, making the optimal operation state only having wind and the ESSs. The power dependence from the upstream grid is still high, as mentioned earlier, due to the grid size and the DGs installed capacity level in

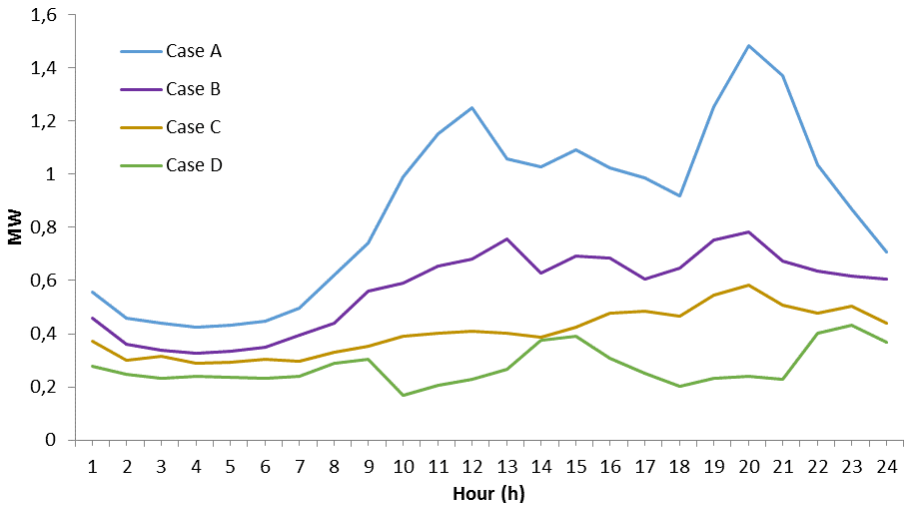

Figure 5.33: System losses for all cases

the grid. In a general way, the energy matrix, as well as the losses and voltage deviation resulting from the grid operation show the increase in the efficiency and quality of the system operation. This improvement comes from the integration of several key technologies in the system, working in a coordinated way.

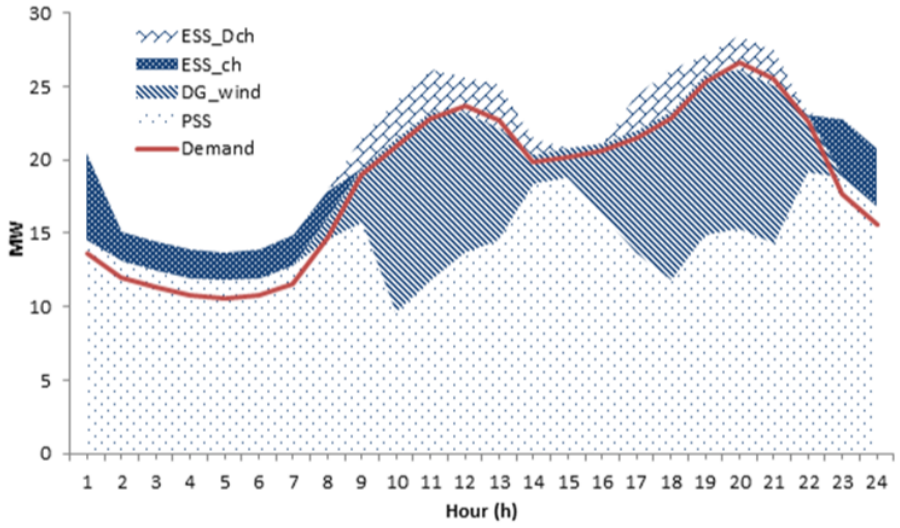

Figure 5.34: Case D energy matrix

5.2.5 Cost Analysis

In Table 5.2 is summarized the 119 Bus Test System Costs for the different case studies (A to D) as well as the losses. From the results presented in this table it is possible to see the significant differences in terms of costs between the different case studies. As expected, the Base Case, Case A, presents not only the highest total cost but also the highest values in terms of energy, emissions and power not served costs, as well as the highest system losses. All of these factors have a huge weight in the total costs, therefore the value being so high. In Case B (where dynamic

reconfiguration is used), the system presents a significant total costs reduction (approximately 12,57%) considering already the switching line costs. Also losses were reduced by 32% in relation to the Base Case.

Table 5.2: 119 Bus Test System: Different Case Studies Costs

	Case A	Case B	Case C	Case D
Total Cost [€]	43217,38	37784,05	33911,80	29912,27
Reconfiguration Cost [€]	0	1050	1120	1010
Energy Cost [€]	40349,82	34452,69	31442,59	27901,72
Emission Cost [€]	2219,56	1743,54	1206,19	1000,55
Power not served [€]	648,00	537,82	143,02	0
P Losses [MW]	30,17	20,38	14,42	10,00
Q Losses [MVAR]	20,83	13,56	9,77	6,60

In Case C (where DGs are integrated in the system together with dynamic reconfiguration), the total cost is reduced on 3872,25€ in comparison with Case B (approximately 10,25%) being the cost term with the most significant decrease, the energy cost. The reduction in terms of emission costs does not have the same relevance but is also easily noticed. Finally, Case D is the case that has the integration of all technologies considered in this dissertation. The total cost reduction remains proximally the same as the previous case (3999,53€), but has a much more relevant situation to analyse, which is the power not served being 0MW. This is explained due to the integration of ESSs, taking advantage of the shallow hours in order to charge itself, with the excess of production that can be observed in the energy matrix shown in Figure 5.34. As expected and explained in the previous subsection 5.2.4, the losses also have a significant reduction. As a result, the introduction of all technologies results in a healthier system operation and also leads to a significant reduction of the total costs.

5.3 Lagoa Test System

5.3.1 Case A – Base Case

As stated in 5.1, the Lagoa Test System follows the same analysis structure as the 119 Bus Test System. Accordingly, in Case A, the original case, reconfiguration is not considered and DER is not implemented as part of the daily system operation. No bound for voltage deviation was considered, as some of the hours under analysis do not respect that value, which would make the problem impossible to converge in this particular case. The voltage deviation for this Case is represented in Figure 5.35, where the limit of $\pm 5\%$ was included, showing where the limit is not respected. Like in the first test system considered, the voltage deviation values are given by the average voltage deviation in each node. The values for this case are negative because the power flow travels from upstream to downstream. The only source of energy in this particular Case is just the substation, which provides both active and reactive power for the system, leading to voltage deviation limits violations, thus being the reason no limit is considered. As further away the node

is from the power source, the greater the voltage deviation, as in the previous test system. The reconfiguration and DGs integration intend to improve this voltage profile.

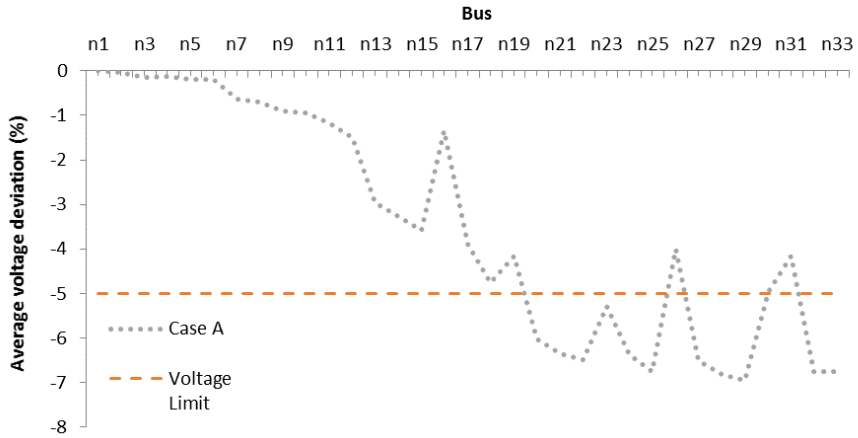

Figure 5.35: Average voltage deviation in Case A

The system losses for this Case account to a total of 9.47 MW (which are higher) being explained by the present high values that voltage deviation. Figure 5.36 shows losses for its hour and its trend.

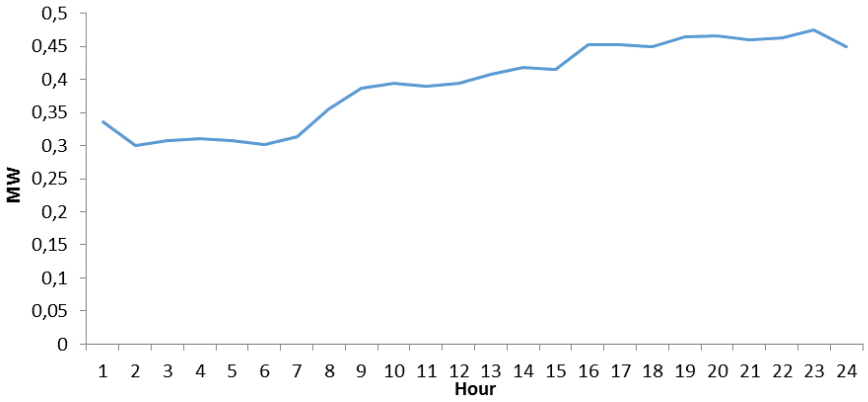

Figure 5.36: Base Case losses

5.3.2 Case B – Base Case together with Reconfiguration

This Case is exactly the same as Case A, but in this Case reconfiguration was added in order to perform dynamic reconfiguration on the systems operation. Although reconfiguration has many utilities, as seen in Chapter 2, the aim for this particular Case is to reduce system losses. Firstly, comparing the active power losses from the two cases a significant difference is verified, having a decrease in total losses from 9.47 MW in Case A to 6.07 MW in case B, which represents a 35.86% reduction. Such a variation is explained because the grid now possesses the ability to adapt itself and provide the most efficient network possible for each given hour. Figure 5.37 shows the hourly losses values and its tendencies.

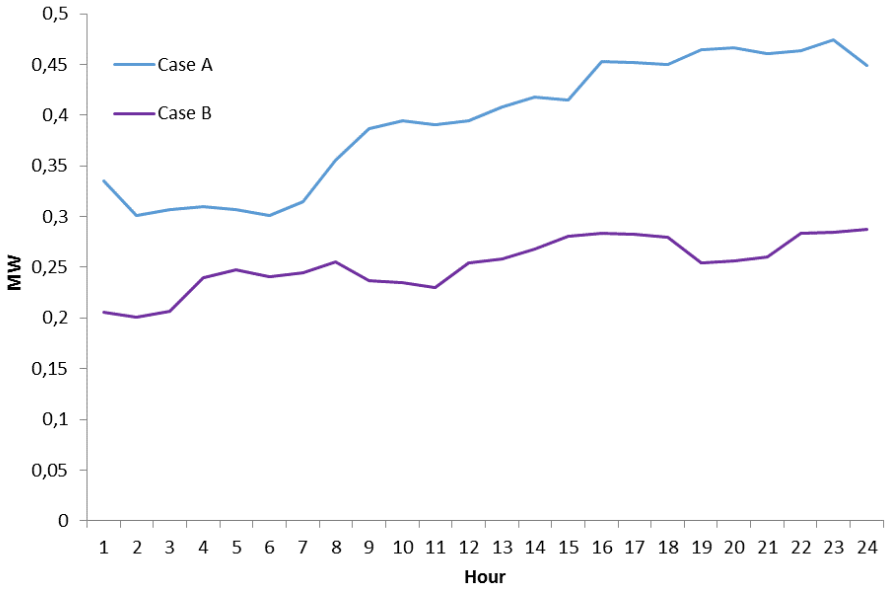

Figure 5.37: Case A and Case B system losses

The application of dynamic reconfiguration causes a considerable decrease in the losses corresponding to peak hours. For example, the higher peak in case B does not go above 0.3MWh, while in Case A that values almost reaches 0.5MWh, which is relevant in the operational cost. Although grid reconfiguration at each hour has an aggregated cost, the total cost of the operation has a big reduction, something that will be shown and analysed later in this chapter.

In Figure 5.38 to 5.61 is shown that all nodes are fed and that network topologies, at all times, maintain its radial configuration. The reconfiguration, as previously done in the 119 bus test system, is done in order to feed the demand in all nodes, at all times, considering all the scenarios, through the less congested path and with the lower R / X.

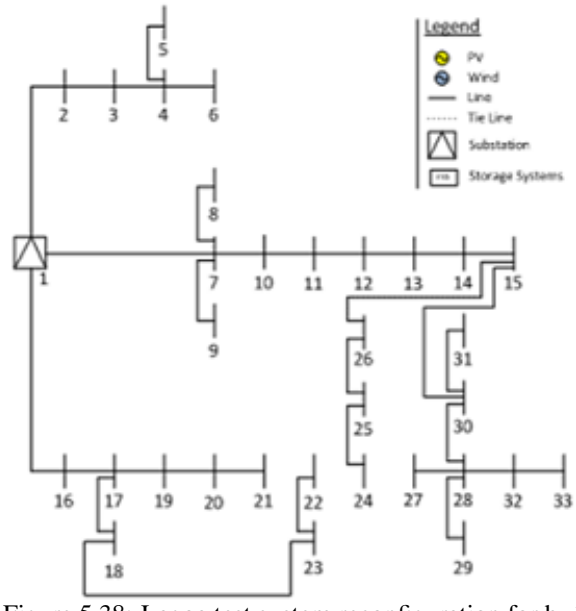

Figure 5.38: Lagoa test system reconfiguration for h=1

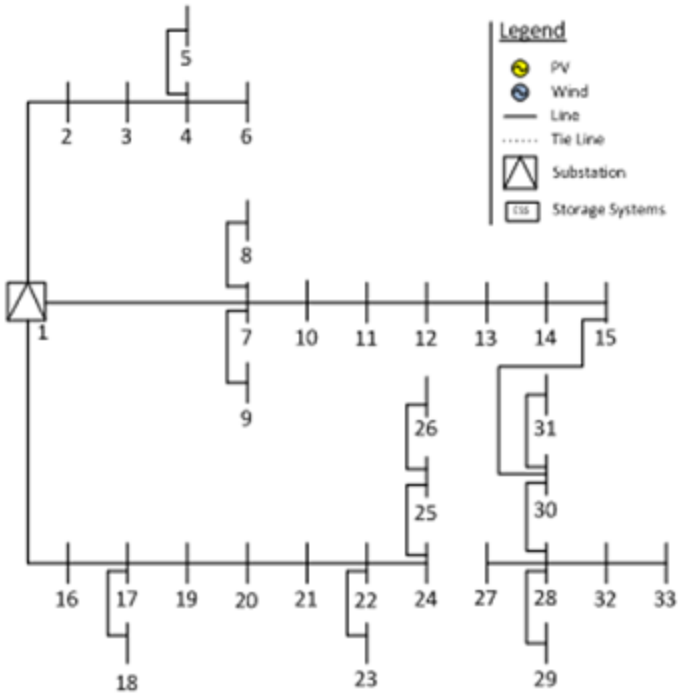

Figure 5.39: Lagoa test system reconfiguration for h=2

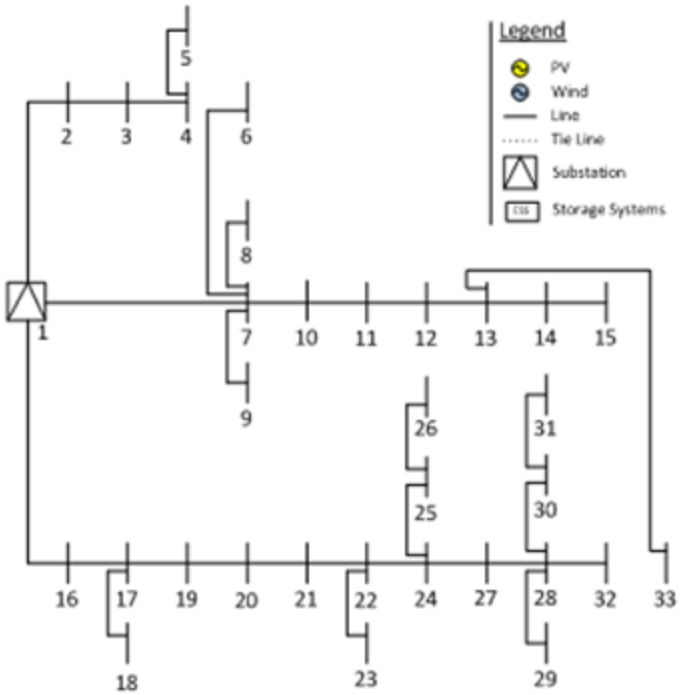

Figure 5.40: Lagoa test system reconfiguration for h=3

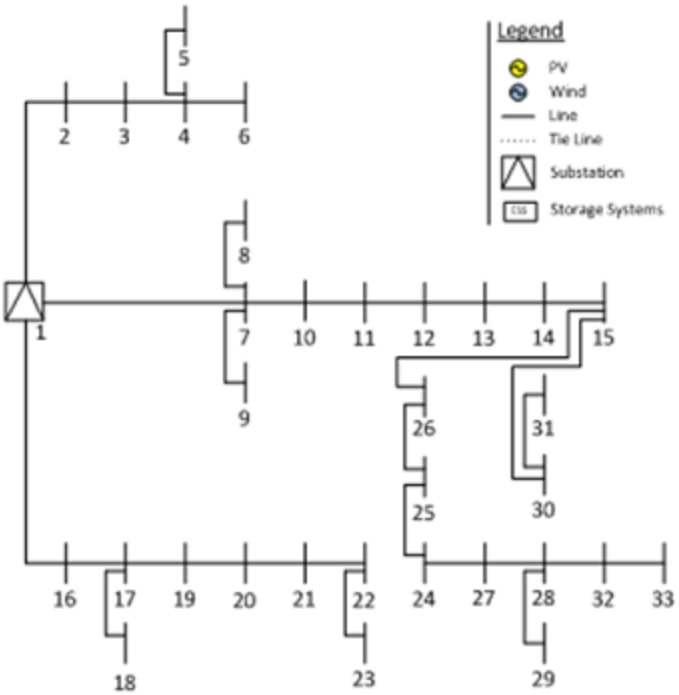

Figure 5.41: Lagoa test system reconfiguration for h=4

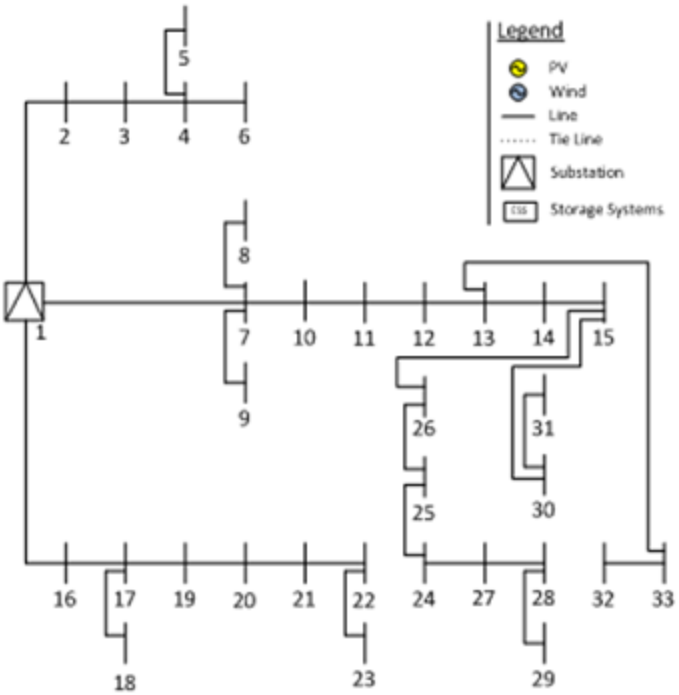

Figure 5.42: Lagoa test system reconfiguration for h=5

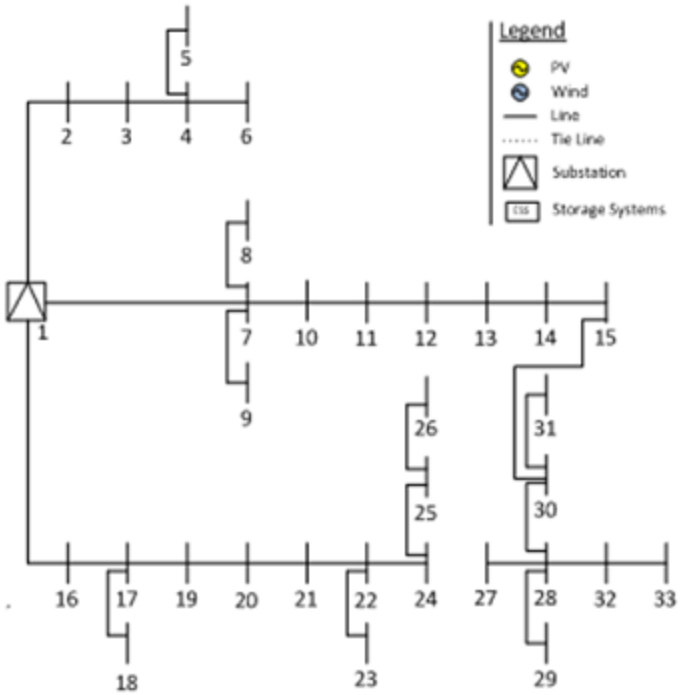

Figure 5.43: Lagoa test system reconfiguration for h=6

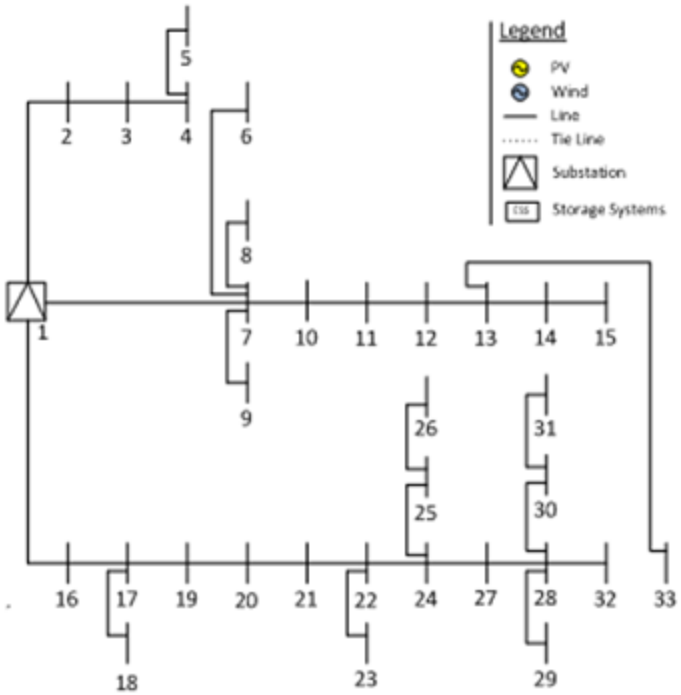

Figure 5.44: Lagoa test system reconfiguration for h=7

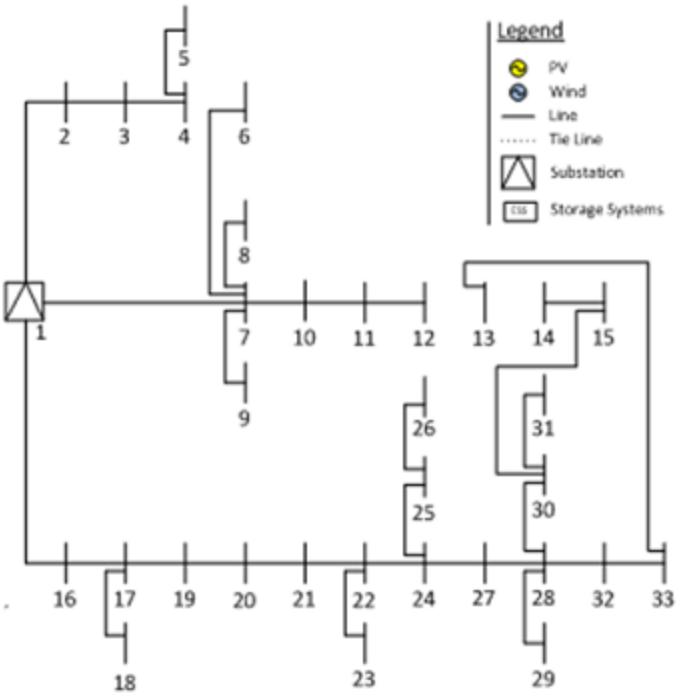

Figure 5.45: Lagoa test system reconfiguration for h=8

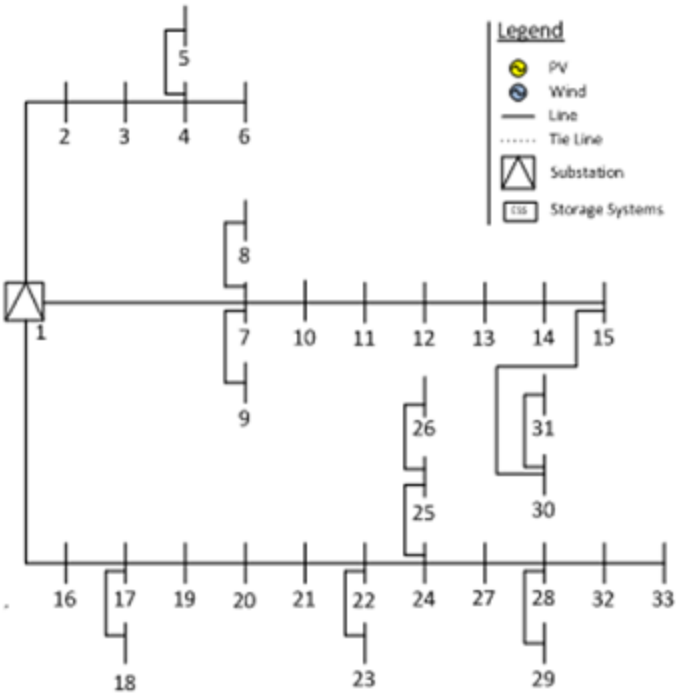

Figure 5.46: Lagoa test system reconfiguration for h=9

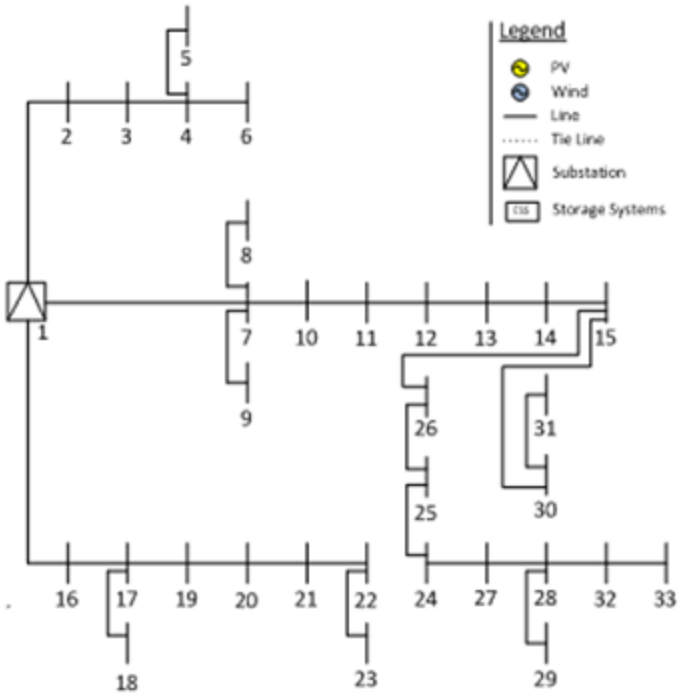

Figure 5.47: Lagoa test system reconfiguration for h=10

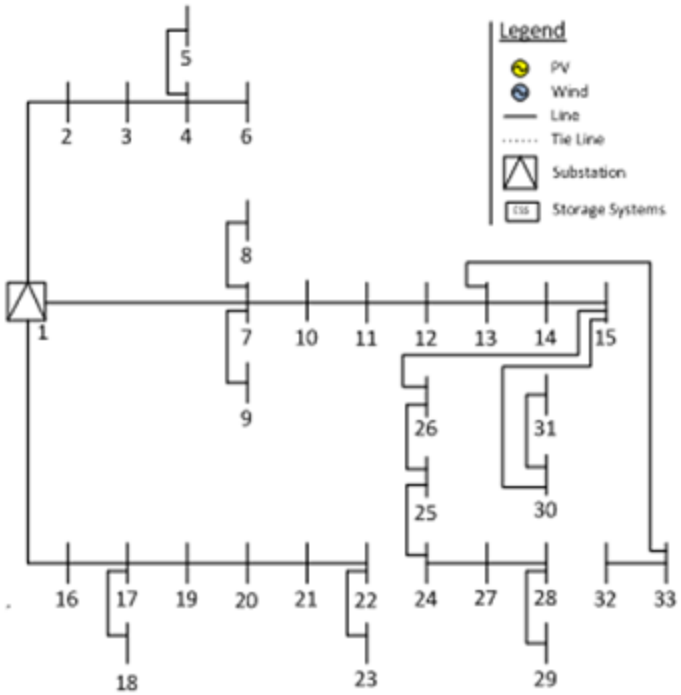

Figure 5.48: Lagoa test system reconfiguration for h=11

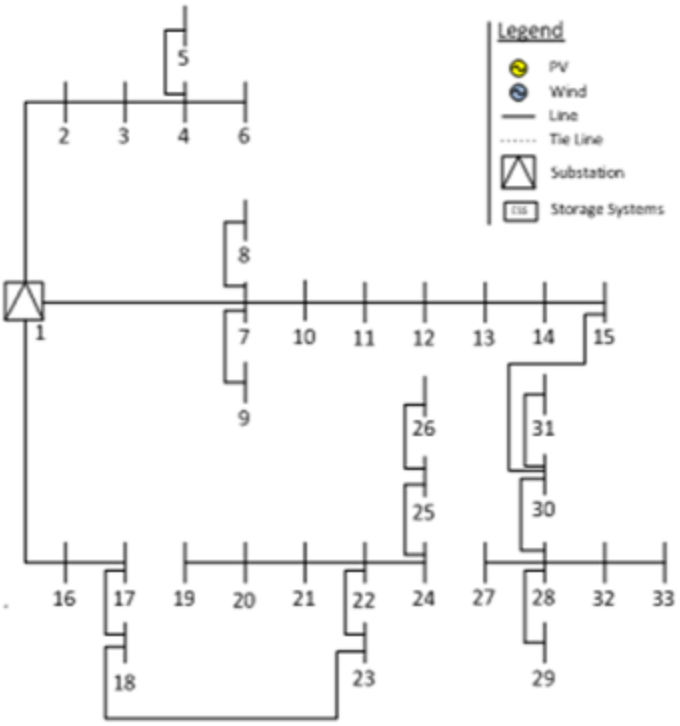

Figure 5.49: Lagoa test system reconfiguration for h=12

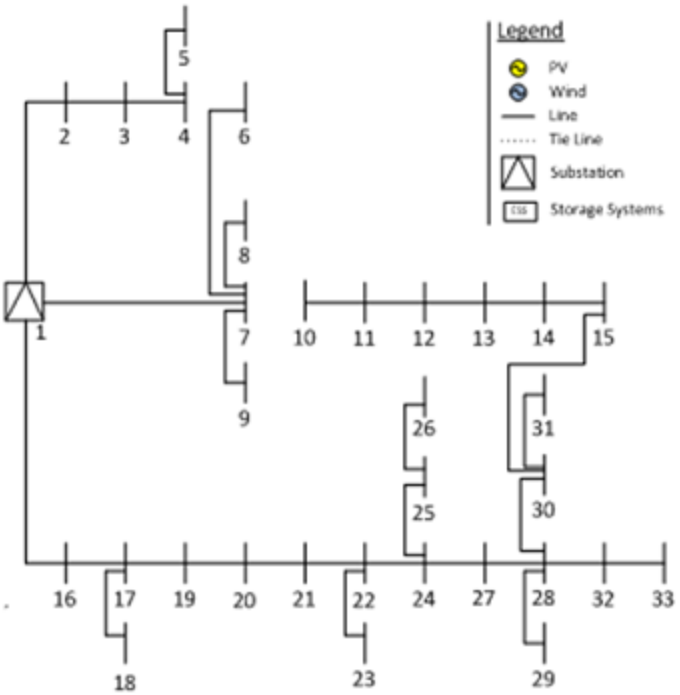

Figure 5.50: Lagoa test system reconfiguration for h=13

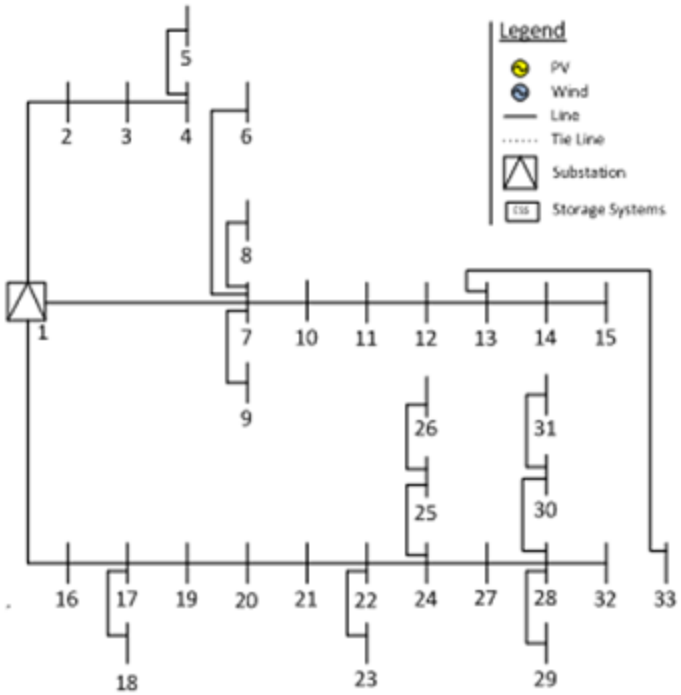

Figure 5.51: Lagoa test system reconfiguration for h=14

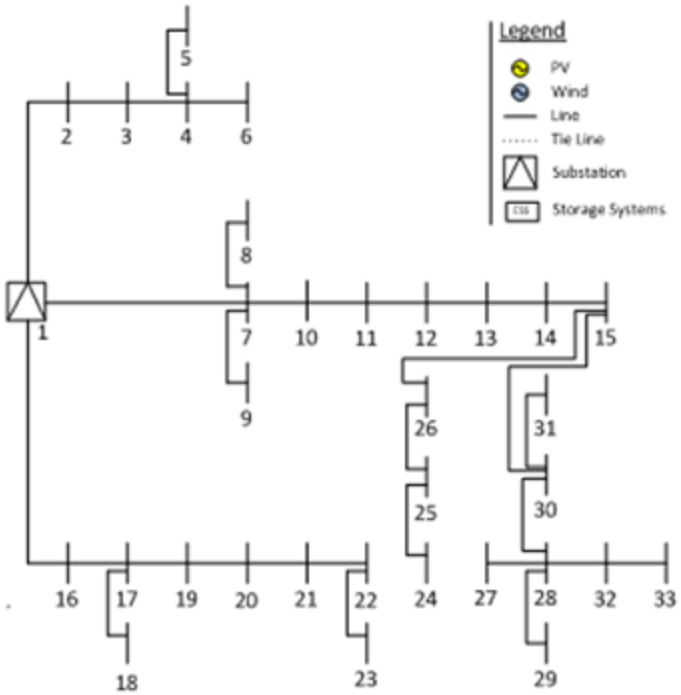

Figure 5.52: Lagoa test system reconfiguration for h=15

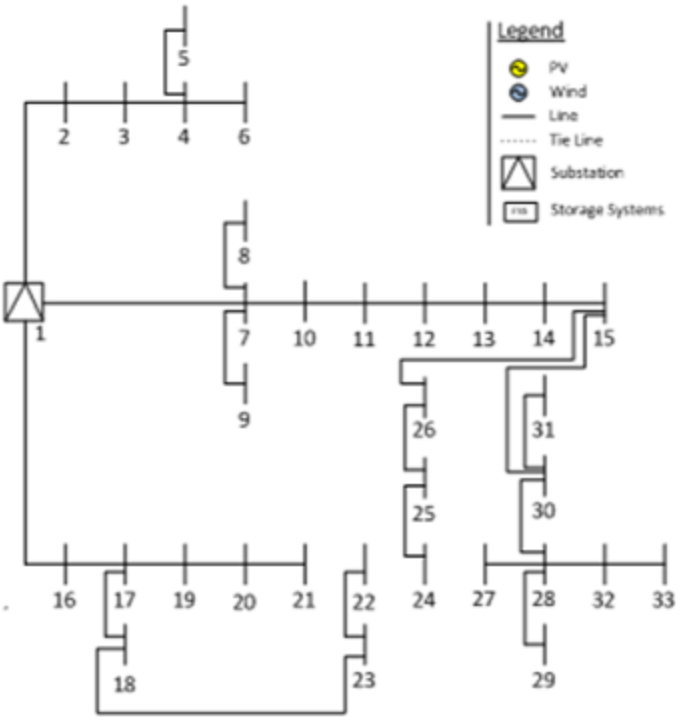

Figure 5.53: Lagoa test system reconfiguration for h=16

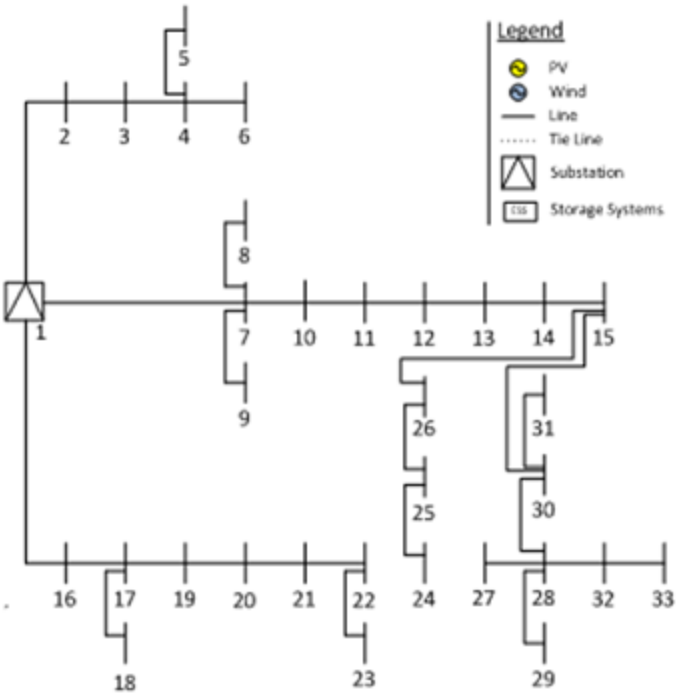

Figure 5.54: Lagoa test system reconfiguration for h=17

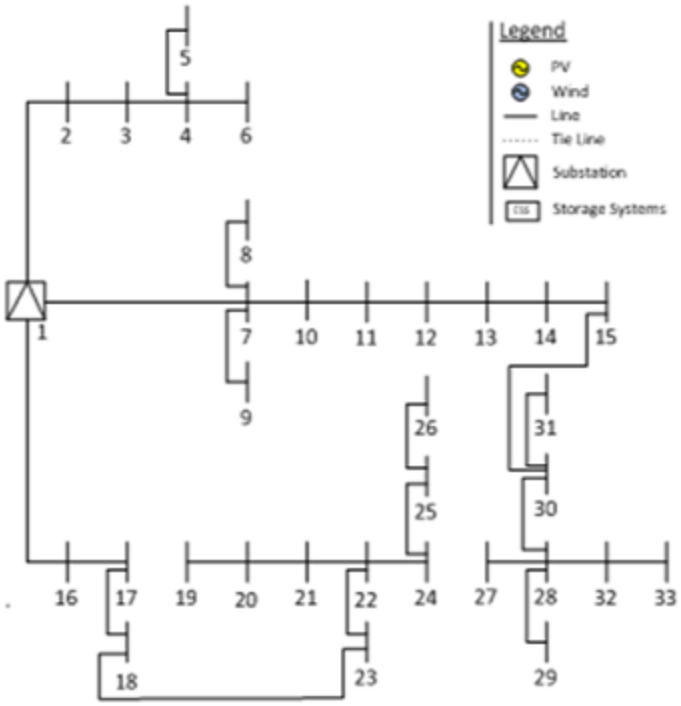

Figure 5.55: Lagoa test system reconfiguration for h=18

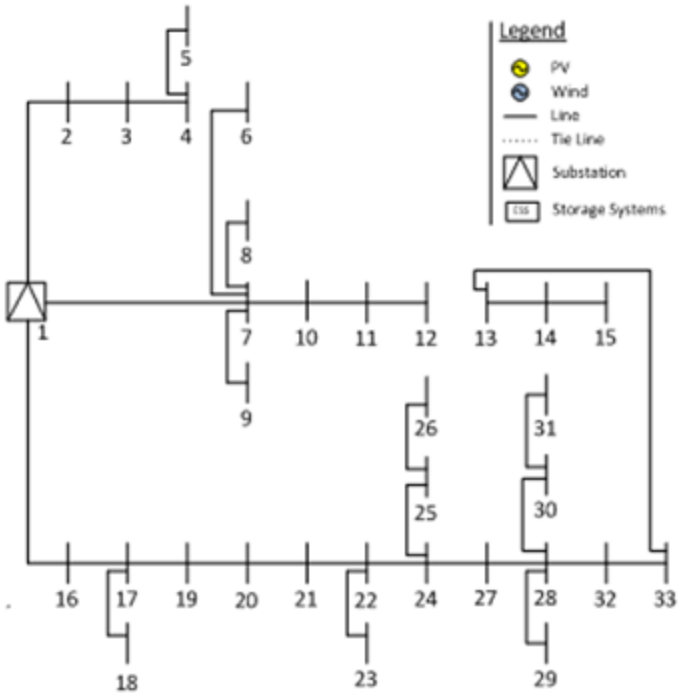

Figure 5.56: Lagoa test system reconfiguration for h=19

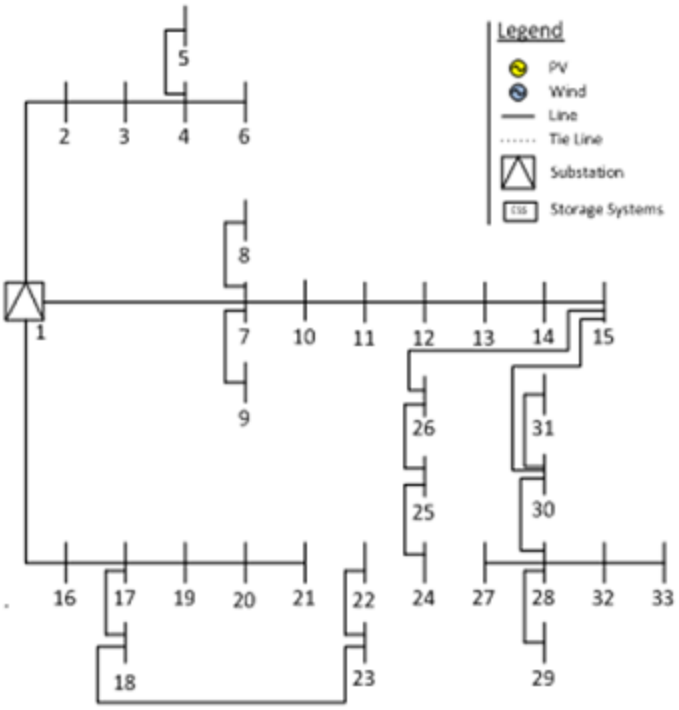

Figure 5.57: Lagoa test system reconfiguration for h=20

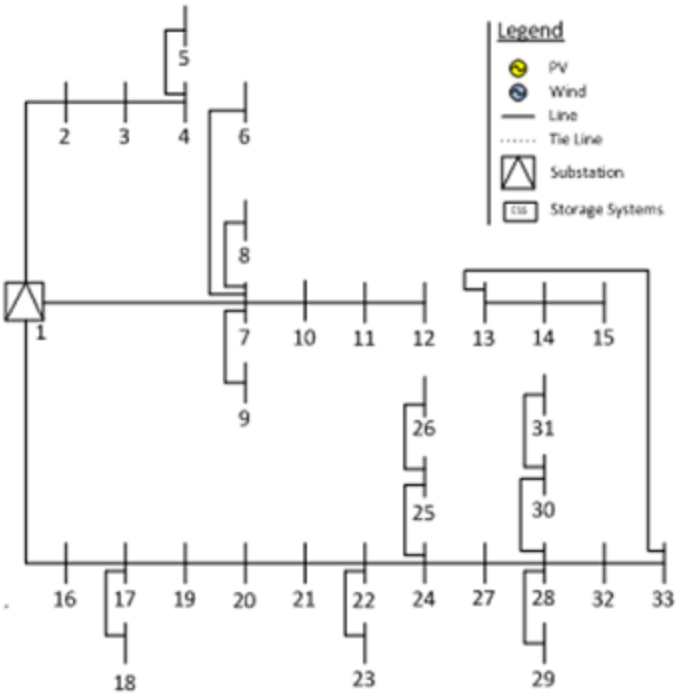

Figure 5.58: Lagoa test system reconfiguration for h=21

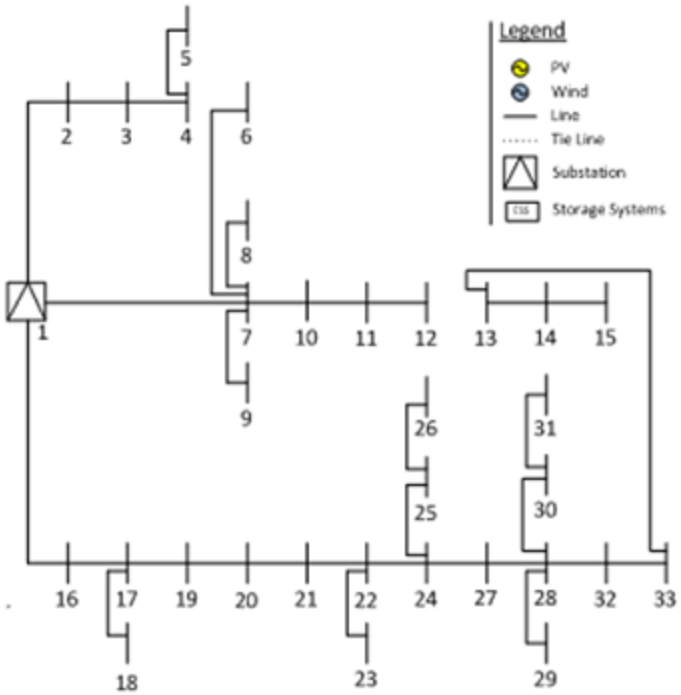

Figure 5.59: Lagoa test system reconfiguration for h=22

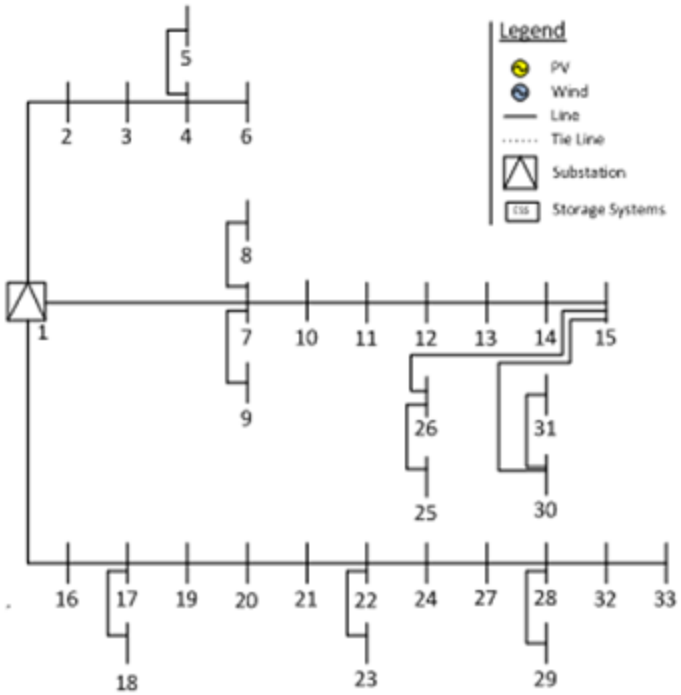

Figure 5.60: Lagoa test system reconfiguration for h=23

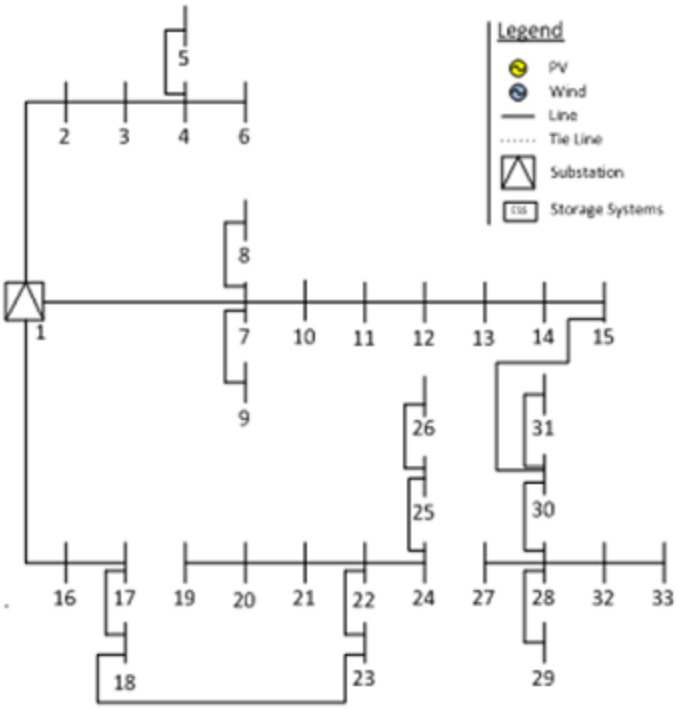

Figure 5.61: Lagoa test system reconfiguration for h=24

5.3.3 Case C – Considering Dynamic Reconfiguration and Distributed Energy Resources

In Case C, wind and PV DGs are considered together with dynamic reconfiguration. It is important to analyse the relevance and the influence of these two technologies combined in terms of voltage deviation, where the voltage deviation limits of $\pm 5\%$ are considered.

The system dynamic reconfiguration for this case study can be seen from Figure C.49 to Figure C.72 in the Appendix C. Similarly to all cases analysed so far when considering reconfiguration, all nodes are fed and the radial configuration is maintained at all times, considering all the scenarios, through the less congested path and with the lower R / X.

Figure 5.62 shows the average voltage deviation for this case study. The reduction is tremendous, with deviation not assuming values superior to 2%, which represents a great improvement to the system. Also, it should be noticed that the values go from negative in Case A to positive in Case C, which means that the power flow can now occur from downstream to upstream. Both this changes are justified by the integration of DGs in the grid and its installed capacity.

When comparing the power losses in Case A, Case B and Case C (Figure 5.63), a considerable decrease is easily noticeable. That is, the total amount of active losses, it reduces from 9.47MW to 6.07MW from Case A to Case B and to 4.20MW in Case C, representing a reduction of 30.78% from Case B to Case C and 55.60% from Case A to Case C, which represents a big portion of the system total operation costs. The use of reconfiguration and DGs together, in a coordinated way, cause a large system transformation, leading it closer to the optimal operational

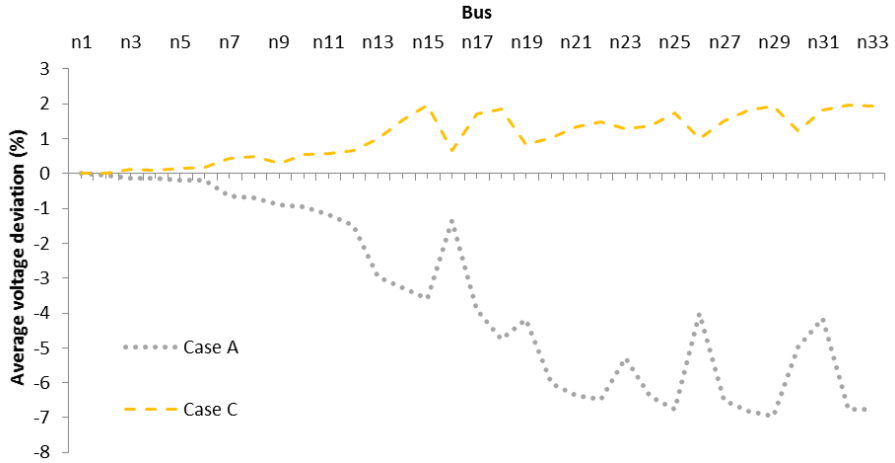

Figure 5.62: Average voltage deviation in Case C

state. Analysing the Case C hourly losses, in particular, is possible to see the loss values fluctuate between 0.15MWh and 0.2MWh, when in Case B the values where always above 0.2MWh.

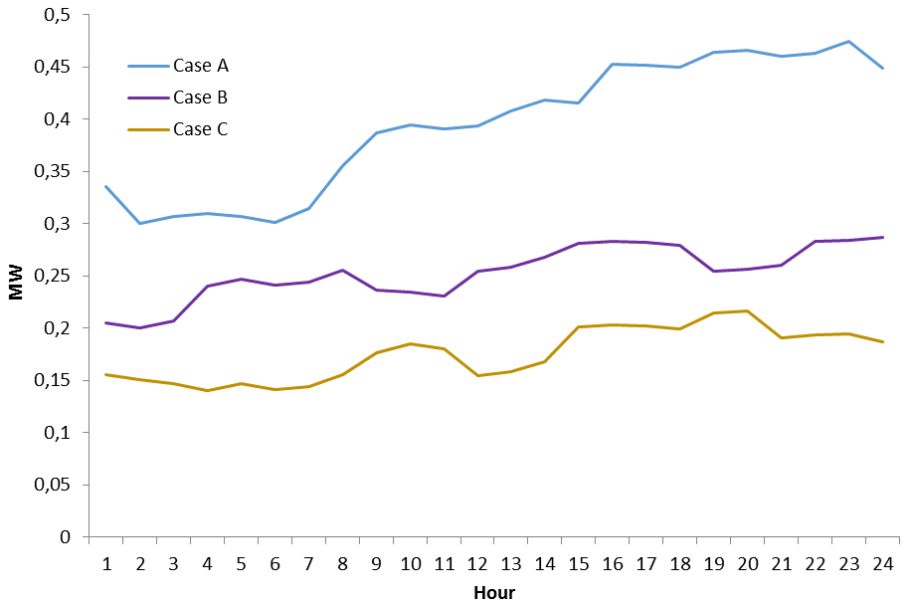

Figure 5.63: Case A, Case B and Case C system losses

Therefore, the integration of DGs in the system considerably the energy matrix and this effect can be seen in the comparison analysis of Case A and Case C. This analysis allows not only comparing the variation of the power supplied by the original source but the real impact of DGs in the system. Figure 5.64 (Case A) has a simple correlation between demand and PSS due to the fact that the substation is the only power source. In Figure 5.65 can be seen the Case C energy matrix. In this case there are, mainly, two different periods, one where wind DG is the main energy source, between the hour 1 and 10, approximately, and a second period, from hour 10 to 24, where the substation is the main source. DGs from the PV type are less relevant in the overall analysis, although they fulfill a reasonable part of the demand between hour 10 and 15, which are, usually, the hours with the most sun exposure. It is also relevant to notice that a part of the renewable

energy produced is not used. The great impact and advantages in economic and environmental terms to the system are subject to analysis in subsection 5.3.5.

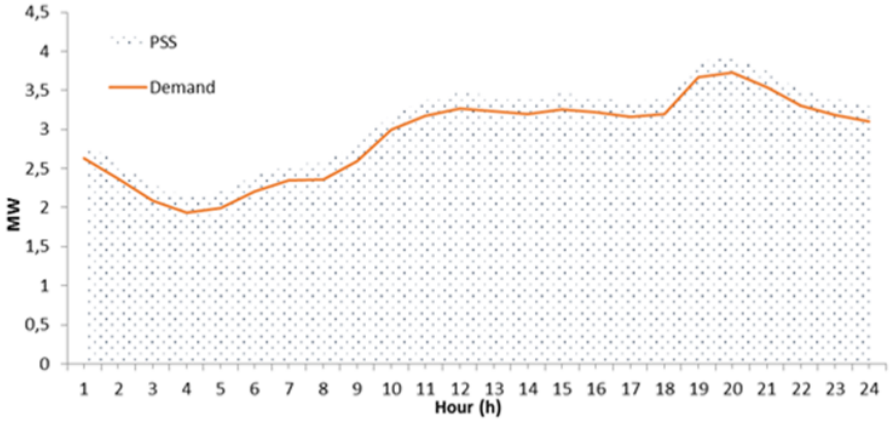

Figure 5.64: Case A energy matrix

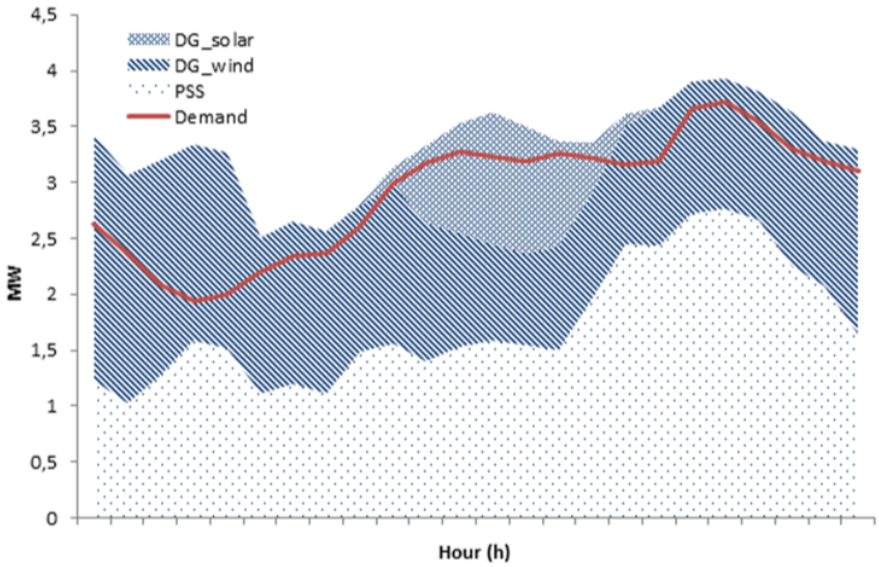

Figure 5.65: Case C energy matrix

5.3.4 Case D – Considering Dynamic Reconfiguration, Distributed Energy Resources and Energy Storage Systems

Finally Case D, presents the most complex case study in this work, where all technologies are considered (dynamic reconfiguration, distributed energy resources (wind and PV) and energy storage systems). The system dynamic reconfiguration for this case study can be seen from Figure C.73 to Figure C.96 in the Appendix C. Similarly to all cases analysed so far when considering reconfiguration, all nodes are fed and the radial configuration is maintained at all times, considering all the scenarios, through the less congested path and with the lower R / X. Also it is relevant to notice that hourly topology is different from the previous to the next hour.

Average voltage deviations of Cases A, C and D are presented in Figure 5.66. Case D presents the best voltage deviation profile (because of the introduction of the ESSs) when comparing to Case C. Comparing boyh cases it is possible to see a 1% decrease in the further nodes because the demand it is supplied locally, presenting a big system operation improvement.

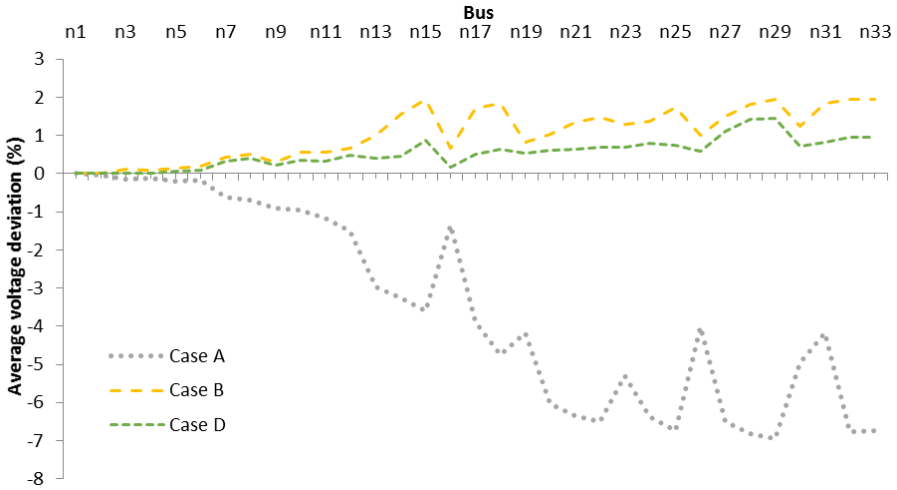

Figure 5.66: Average voltage deviation of the Cases A, C and D

The active losses for all cases are presented in Figure 5.67. As expected when analysing the average voltage deviation, Case D presents the lowest losses, which is justified, when comparing with Case C, due to the integration of ESSs, since this technology charge some of the power that would be otherwise lost by curtailment. That is, ESSs will charge in periods where there are excess of renewable production (which can be seen later when analysing the energy matrix), and/or when energy price is at its lowest. The discharge is done in the opposite case, which is, when renewable production is lower and/or when the energy price is at its highest, helping to satisfy the demand in the best way at all time. This has a large effect in the system operation, because it reduces the peak hours effect, making the operation healthier and closer to its optimal point.

Total active losses for Case D are equal to 3.29MW, representing a decrease of 21.83%, 45.90% and 65.30% from Case C, B and A, respectively. The losses in this case fluctuate between 0.10MWh and 0.15MWh, being this losses value always lower than Case C which, is justified by the use of ESSs.

The energy matrix for this case is presented in Figure 5.68. As mentioned before, the ESSs charge period represents a shallow peak and, consequently, a period where renewable production is not utilized (from hour 1 to hour 8). On the other hand, the discharge period is equal to the period with higher demand (from hour 9 to hour 23). In this period ESSs provide a steady and helpful energy supplement (from wind and PV DGs energy stored), making the dependence from the up-stream grid much lower and allowing for greater integration of renewable energy. In a general way, the energy matrix, as well as active losses and voltage deviation resulting from the grid operation show the increase in the efficiency and quality of the system operation. This improvement comes from the integration of several key technologies in the system, working in a coordinated way.

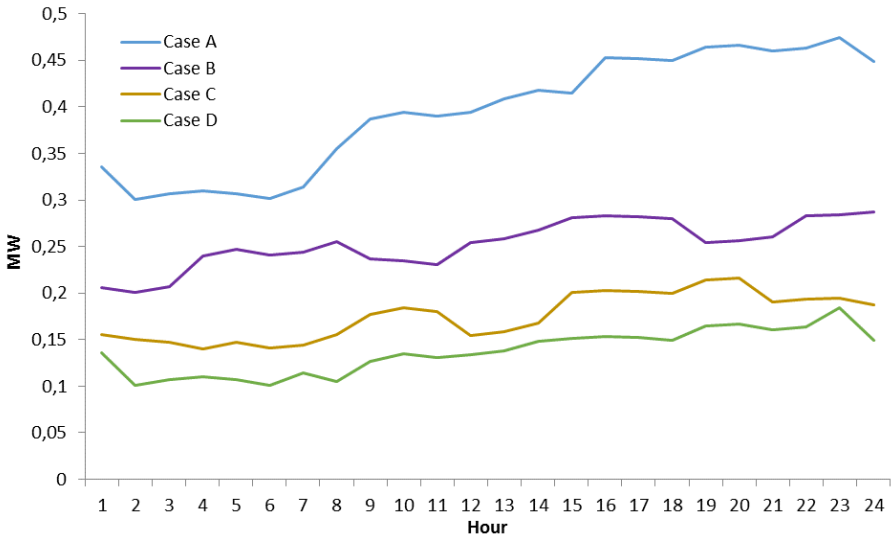

Figure 5.67: System losses for all cases

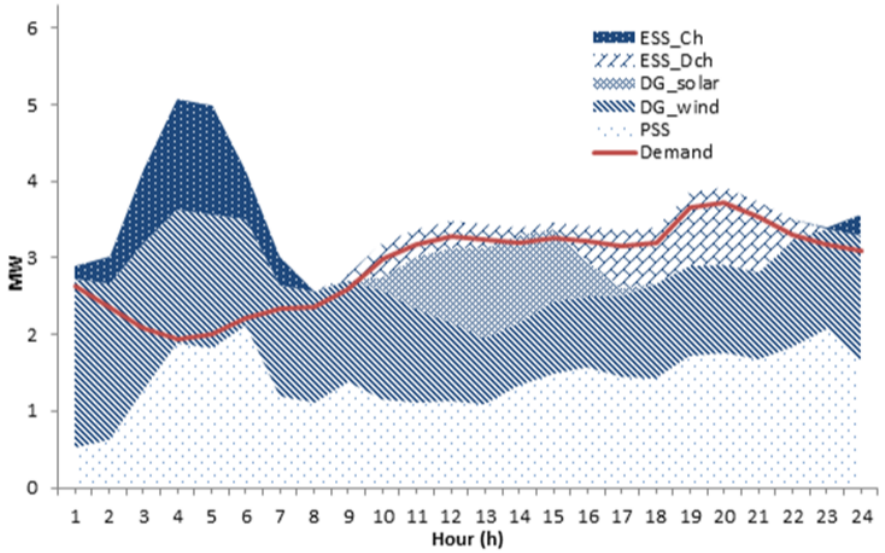

Figure 5.68: Case D energy matrix

5.3.5 Cost Analysis

In Table 5.3 is summarized the Lagoa Test System Costs for the different case studies (A to D) as well as the losses. The results follow the same pattern as the 119 bus test system, which reveals the study effectiveness and relevance. From the results presented in this table it is possible to see the significant differences in terms of costs between the different case studies. As expected, the Base Case, Case A, presents not only the highest total cost but also the highest values in terms of energy, emissions and power not served costs, as well as the highest system losses. All of these factors have a huge weight in the total costs, therefore the value being so high. In Case B (where dynamic reconfiguration is used), the system presents a significant total costs reduction (approximately 12,09%) considering already the switching line costs. Also losses were reduced by 35,86% in relation to the Base Case.

Table 5.3: Lagoa Test System: Different Case Studies Costs

	Case A	Case B	Case C	Case D
Total Cost [€]	5627,86	4947,45	4556,23	3993,00
Reconfiguration Cost [€]	0	620	540	610
Energy Cost [€]	5188,02	4087,42	3841,92	3272,32
Emission Cost [€]	348,36	187,78	139,65	110,68
Power not served [€]	91,48	52,25	33,66	0
P Losses [MW]	9,47	6,07	4,20	3,29
Q Losses [MVAR]	5,94	4,63	3,69	3,08

In Case C (where DGs are integrated in the system together with dynamic reconfiguration), the total cost is reduced on 481,22€ in comparison with Case B (approximately 9,73%) being the cost term with the most significant decrease, the energy cost. The reduction in terms of emission costs does not have the same relevance but is also easily noticed. Finally, Case D is the case that has the integration of all technologies considered in this dissertation. The total cost reduction remains approximately the same as the previous case (473,23€), but has a much more relevant situation to analyse, which is the power not served being 0MW. This is explained due to the integration of ESSs, taking advantage of the shallow hours in order to charge itself, with the excess of production that can be observed in the energy matrix shown in Figure 5.68. As a result, the introduction of all technologies results in a healthier system operation and also leads to a significant reduction of the total costs.

5.4 Chapter Summary

In this chapter were presented and analysed the results of two test systems considered (the 119 Bus Test System and the Lagoa Test System), in terms of dynamic network reconfiguration, voltage deviation profiles, energy losses, energy matrix and total cost of each solution. The results showed that the introduction of DER and dynamic reconfiguration, providing a healthier and smoother operational system.

The results obtained specifically in Case D, in both test systems showed encouraging results, with tremendous efficiency in terms of losses and costs reduction. In this case the production of energy to supply the system demand, comes mainly from DER and ESSs role in the grid, not letting the energy produced in excess by DGs in shallow hours to be wasted, storing this energy, using it in peak hours, supplanting the excess of demand without the need to highly increase the value of imported energy from the substation. This leads to a system that depends much less in the imported energy, which has a significant higher cost. As a result, the use of dynamic reconfiguration allowed a reduction of the system energy losses, costs and the improvement of the system reliability.

Chapter 6

Conclusions and Future Works

In this chapter, the main conclusions of the dissertation are presented and some directions of future work are also discussed. Finally, the contributions of this work are highlighted by presenting the publication, a result of this dissertation work.

6.1 Conclusions

In this dissertation an improved dynamic system reconfiguration model aiming to optimize system operation was presented, allowing greater integration of distributed energy sources in the system. The main contributions of this work derive from the stochastic model formulation, which takes into account the stochastic nature of renewables sources, the wind and PV uncertainty and intermittency, as well as the demand. In this model ESSs were also used in order to understand their impact and importance when incorporating them simultaneously with DGs and dynamic reconfiguration. The objective function is to minimize the sum of all costs, the expected costs of operation, emissions and unserved power, considering the most important technical and economic constraints. The computational tool was tested in two different systems, the IEEE 119-bus network system, a theoretical case, and the system of Lagoa, in São Miguel Island, Azores, representing a real system, operating both systems in a reliable and stable way.

The results obtained for both cases show that the deployment of all the technologies mentioned results in a substantial improvement regarding costs, voltage profiles and losses, translating into an improved and healthier system operation for both the Distribution System Operator (DSO) and the customer. The introduction of dynamic reconfiguration alone translates into a significant improvement in voltage deviation which directly turns into a total operation cost reduction, which is even greater when DGs are added in dynamic reconfiguration. Regarding the use of ESSs, this technology presents a small improvement in terms of voltage profile. However, ESSs has a great impact on the amount of RES energy stored and injected into the power system that would, otherwise, would be lost. The overproduction could not be utilized when necessary, which means that when demand is high, the imported energy will be also higher, translating into bigger losses and higher costs, as tested in Case A for both simulations.

Dynamic reconfiguration increases the system operation reliability and helps to integrate higher levels of renewable energy, as can be seen in the real system on Case D, which represents the case where all technologies are present. In here, DGs and ESSs fulfill close to 59% of the demand, presenting an encouraging set of results for these systems future.

Therefore, the proposed model has revealed to be an efficient operation optimization tool; in particular, in the real system it is possible to verify that the integration of dynamic reconfiguration together with the other technologies exploited in this work, leads to a significant improvement of the system, either at the level of renewables accommodation or reliability and stability of the system. Regardless this system, in its current state, does not have such technologies but with such encouraging results, it should be considered by the DSO to study their installation.

6.2 Future Works

The following points may be further studied in order to broaden the understanding of the topics treated in this dissertation:

- The integration of switchable capacitor banks was not considered, as well as the analysis of the reactive power flow in the system, which could be subject to further study.
- Perform a study on the optimal position and sizing of ESSs in the real system, as well as an analysis on the different ESSs types that can be implemented.
- Develop a new methodology based in the present model, to update the conventional switches to automated switched, considering the number of reconfiguration and the presence in different reconfigurations topology's.

6.3 Works Resulting from this Dissertation

This dissertation has resulted in one IEEE conference paper that has already been submitted at the 18th IEEE International Conference on Environment and Electrical Engineering — EEEIC 2017 (technically co-sponsored by IEEE), Palermo, 12-15 June 2017.

J. Pogeira, S.F. Santos, D.Z. Fitiwi, J.P.S. Catalão, "*Implementing Dynamic System Reconfiguration with Renewables Considering Future Grid Technologies: A Real Case Study*", in: Proceedings of the 18th International Conference on Environment and Electrical Engineering – EEEIC 2018, Palermo, Italy, 12-15 June, 2018

Appendix A

SOS2 - Piecewise Linearization

In this dissertation was chosen an appropriate linearization model to be able to integrate the calculation of the optimal power flow (OPF) in distribution systems. The selected model is presented in [81] and is a model that is based on the use of Special Ordered Sets of type 2 (SOS2), being selected due to its great accuracy in estimated losses and because it does not create a big computational effort and complexity.

It is defined as a piecewise linear function, usually modeled by introducing a set of positive variables $Z\_P_l^{pt}$ where $pt \in (0,1,2,3,4,5)$, that will form an *SOS2*. It is important to note that *pt* represents the intersection points between the linear approximation and the quadratic function. The $Z\_P_l^{pt}$ variable acts as a weight associated to the points, having the purpose to force, at the most, two consecutive variables to have non-zero values, which can be seen in equation (A.1).

Each flow partition is calculated by the product of the number of each partition *(pt)* and the line capacity is divided by the total number of intersection points considered, thus being able to obtain equally spaced intersection points. In equation (A.2), the absolute power flow in a line is expressed by the sum of the products of $Z\_P_l^{pt}$ variables and flow values at the partitions. This guarantees that power flow values correspond to a certain point in one of the linear segments between two consecutive intersection points. The quadratic power flow is expressed as in equation (A.3), similarly to equation (A.2). The reactive power flow and the quadratic reactive flow can be calculated in a similar way to what is done for the active power flow and quadratic power flow, in equations (A.2) and (A.3).

$$\sum_{pt=0}^{PT} Z\_P_l^{pt} = 1 \tag{A.1}$$

$$P_{l,s,h} = \sum_{pt=0}^{PT} Z\_P_l^{pt} * \left(\frac{LineCap}{5} * pt \right) \tag{A.2}$$

$$P_{l,s,h}^2 = \sum_{pt=0}^{PT} Z\_P_l^{pt} * \left(\frac{LineCap}{5} * pt \right)^2 \tag{A.3}$$

Appendix B

System Data

B.1 IEEE 119 Bus Distribution System

Table B.1: Parameters of the IEEE 119 bus test system

Lines	FROM	TO	R [Ω]	X [Ω]	S^{max}	Node	Active Power [kW]	Reactive Power [kVAr]
line1	1	2	0,036	0,01296	1200	2	133,84	101,14
line2	2	3	0,033	0,01188	400	3	16,214	11,292
line3	2	4	0,045	0,0162	1200	4	34,415	21,845
line4	4	5	0,015	0,054	800	5	73,016	63,602
line 5	5	6	0,015	0,054	800	6	144,2	68,604
line 6	6	7	0,015	0,0125	800	7	104,47	61,725
line 7	7	8	0,018	0,014	400	8	28,547	11,503
line 8	8	9	0,021	0,063	400	9	82,547	51,073
line 9	2	10	0,166	0,1344	400	10	198,2	106,77
line 10	10	11	0,112	0,07889	400	11	146,8	75,995
line 11	11	12	0,187	0,313	400	12	26,04	18,687
line 12	12	13	0,142	0,1512	400	13	52,1	23,22
line 13	13	14	0,18	0,118	400	14	141,9	117,5
line 14	14	15	0,15	0,045	400	15	21,87	28,79
line 15	15	16	0,16	0,18	400	16	33,37	26,45
line 16	16	17	0,157	0,171	400	17	32,43	25,23
line 17	11	18	0,218	0,285	400	18	20,234	11,906
line 18	18	19	0,118	0,185	400	19	156,94	78,523
line 19	19	20	0,16	0,196	400	20	546,29	351,4
line 20	20	21	0,12	0,189	400	21	180,31	164,2
line 21	21	22	0,12	0,0789	400	22	93,167	54,594
line 22	22	23	1,41	0,723	400	23	85,18	39,65
line 23	23	24	0,293	0,1348	400	24	168,1	95,178
line 24	24	25	0,133	0,104	400	25	125,11	150,22
line 25	25	26	0,178	0,134	400	26	16,03	24,62
line 26	26	27	0,178	0,134	400	27	26,03	24,62
line 27	4	29	0,015	0,0296	800	29	594,56	522,62
line 28	29	30	0,012	0,0276	800	30	120,62	59,117
line 29	30	31	0,12	0,2766	800	31	102,38	99,554

Lines	FROM	TO	R [Ω]	X [Ω]	S^{max}	Node	Active Power [kW]	Reactive Power [kVAr]
line 30	31	32	0,21	0,243	400	32	513,4	318,5
line 31	32	33	0,12	0,054	400	33	475,25	456,14
line 32	33	34	0,178	0,234	400	34	151,43	136,79
line 33	34	35	0,178	0,234	400	35	205,38	83,302
line 34	35	36	0,154	0,162	400	36	131,6	93,082
line 35	31	37	0,187	0,261	400	37	448,4	369,79
line 36	37	38	0,133	0,099	400	38	440,52	321,64
line 37	30	40	0,33	0,194	400	40	112,54	55,134
line 38	40	41	0,31	0,194	400	41	53,963	38,998
line 39	41	42	0,13	0,194	400	42	393,05	342,6
line 40	42	43	0,28	0,15	400	43	326,74	278,56
line 41	43	44	1,18	0,85	400	44	536,26	240,24
line 42	44	45	0,42	0,2436	400	45	76,247	66,562
line 43	45	46	0,27	0,0972	400	46	53,52	39,76
line 44	46	47	0,339	0,1221	400	47	40,328	31,964
line 45	47	48	0,27	0,1779	400	48	39,653	20,758
line 46	36	49	0,21	0,1383	400	49	66,195	42,361
line 47	49	50	0,12	0,0789	400	50	73,904	51,653
line 48	50	51	0,15	0,0987	400	51	114,77	57,965
line 49	51	52	0,15	0,0987	400	52	918,37	1205,1
line 50	52	53	0,24	0,1581	400	53	210,3	146,66
line 51	53	54	0,12	0,0789	400	54	66,68	56,608
line 52	54	55	0,405	0,1458	400	55	42,207	40,184
line 53	54	56	0,405	0,1458	400	56	433,74	283,41
line 54	30	58	0,391	0,141	400	58	62,1	26,86
line 55	58	59	0,406	0,1461	400	59	92,46	88,38
line 56	59	60	0,406	0,1461	400	60	85,188	55,436
line 57	60	61	0,706	0,5461	400	61	345,3	332,4
line 58	61	62	0,338	0,1218	400	62	22,5	16,83
line 59	62	63	0,338	0,1218	400	63	80,551	49,156
line 60	63	64	0,207	0,0747	400	64	95,86	90,758
line 61	64	65	0,247	0,8922	400	65	62,92	47,7
line 62	1	66	0,028	0,0418	1200	66	478,8	463,74
line 63	66	67	0,117	0,2016	1200	67	120,94	52,006
line 64	67	68	0,255	0,0918	800	68	139,11	100,11
line 65	68	69	0,21	0,0759	400	69	391,78	193,5
line 66	69	70	0,383	0,138	400	70	27,741	26,713
line 67	70	71	0,504	0,3303	400	71	52,814	25,257
line 68	71	72	0,406	0,1641	400	72	66,89	38,713
line 69	72	73	0,962	0,761	400	73	467,5	395,14

Lines	FROM	TO	R [Ω]	X [Ω]	S^{max}	Node	Active Power [kW]	Reactive Power [kVAr]
line 70	73	74	0,165	0,06	400	74	594,85	239,74
line 71	74	75	0,303	0,1092	400	75	132,5	84,363
line 72	75	76	0,303	0,1092	400	76	52,669	22,482
line 73	76	77	0,206	0,144	400	77	869,79	614,775
line 74	77	78	0,233	0,084	400	78	31,349	29,817
line 75	78	79	0,591	0,1773	400	79	192,39	122,43
line 76	79	80	0,126	0,0453	400	80	65,75	45,37
line 77	67	81	0,559	0,3678	800	81	238,15	223,22
line 78	81	82	0,186	0,1227	800	82	294,55	162,47
line 79	82	83	0,186	0,1227	400	83	485,57	437,92
line 80	83	84	0,26	0,139	400	84	243,53	183,03
line 81	84	85	0,154	0,148	400	85	243,53	183,03
line 82	85	86	0,23	0,128	400	86	134,25	119,29
line 83	86	87	0,252	0,106	400	87	22,71	27,96
line 84	87	88	0,18	0,148	400	88	49,513	26,515
line 85	82	89	0,16	0,182	400	89	383,78	257,16
line 86	89	90	0,2	0,23	400	90	49,64	20,6
line 87	90	91	0,16	0,393	400	91	22,473	11,806
line 88	68	93	0,669	0,2412	400	93	62,93	42,96
line 89	93	94	0,266	0,1227	400	94	30,67	34,93
line 90	94	95	0,266	0,1227	400	95	62,53	66,79
line 91	95	96	0,266	0,1227	400	96	114,57	81,748
line 92	96	97	0,266	0,1227	400	97	81,292	66,526
line 93	97	98	0,233	0,115	400	98	31,733	15,96
line 94	98	99	0,496	0,138	400	99	33,32	60,48
line 95	95	100	0,196	0,18	400	100	531,28	224,85
line 96	100	101	0,196	0,18	400	101	507,03	367,42
line 97	101	102	0,1866	0,122	400	102	26,39	11,7
line 98	102	103	0,0746	0,318	400	103	45,99	30,392
line 99	1	105	0,0625	0,0265	800	105	100,66	47,572
line 100	105	106	0,1501	0,234	800	106	456,48	350,3
line 101	106	107	0,1347	0,0888	800	107	522,56	449,29
line 102	107	108	0,2307	0,1203	400	108	408,43	168,46
line 103	108	109	0,447	0,1608	400	109	141,48	134,25

Lines	FROM	TO	R [Ω]	X [Ω]	S^{max}	Node	Active Power [kW]	Reactive Power [kVAr]
line 104	109	110	0,1632	00588	400	110	104,43	66,024
line 105	110	111	0,33	0,099	400	111	96,793	83,647
line 106	111	112	0,156	0,0561	400	112	493,92	419,34
line 107	112	113	0,3819	0,1374	400	113	225,38	135,88
line 108	113	114	0,1626	0,0585	400	114	509,21	387,21
line 109	114	115	0,3819	0,1374	400	115	188,5	173,46
line 110	115	116	0,2445	0,0879	400	116	918,03	898,55
line 111	115	117	0,2088	0,0753	400	117	305,08	215,37
line 112	117	118	0,2301	0,0828	400	118	54,38	40,97
line 113	105	119	0,6102	0,2196	400	119	211,14	192,9
line 114	119	120	0,1866	0,127	400	120	67,009	53,336
line 115	120	121	0,3732	0,246	400	121	162,07	90,321
line 116	121	122	0,405	0,367	400	122	48,795	29,156
line 117	122	123	0,489	0,489	400	123	33,9	18,98

B.2 Installed capacity of DGs and their placement

Table B.2: Installed capacity of DGs and their placement

DG Type	Node	Installed Power [MW]
PV	32	2
PV	38	2
Wind	14	1
Wind	19	1
Wind	20	2
Wind	24	1
Wind	32	1
Wind	33	1
Wind	34	1
Wind	37	1
Wind	38	1
Wind	42	2
Wind	44	2
Wind	52	2
Wind	53	1
Wind	56	1
Wind	61	1
Wind	69	1
Wind	73	1
Wind	74	1
Wind	77	1
Wind	79	1
Wind	82	1
Wind	83	1
Wind	85	1
Wind	89	1
Wind	96	1
Wind	101	2
Wind	106	1
Wind	108	1
Wind	112	1
Wind	114	1
Wind	116	3
Wind	117	1
Wind	119	1
	Total MW	44

B.3 Installed capacity of ESSs and their placement

Table B.3: Installed capacity of ESSs and their placement

Node	Installed Power [MW]
20	1
29	2
33	1
43	1
52	2
56	1
61	1
66	1
69	1
73	1
77	1
83	1
89	1
100	1
107	1
112	1
116	1
Total MW	19

B.4 Lagoa Test System

Table B.4: Parameters of the Lagoa test system

Lines	FROM	TO	R [Ω]	X [Ω]	S^{max}	Node	Active Power [kW]	Reactive Power [kVAr]
line 1	1	2	0,0992	0,047	6,986	2	97,974	43,869
line 2	2	3	0,493	0,2511	6,986	3	85,238	38,166
line 3	3	4	0,366	0,1864	6,986	4	33,213	14,871
line 4	4	5	0,3811	0,1941	6,986	5	64,663	28,954
line 5	4	6	0,819	0,707	6,986	6	30,445	13,632
line 6	1	7	0,1872	0,6188	6,986	7	62,703	28,076
line 7	7	8	0,7114	0,2351	6,986	8	48,987	21,935
line 8	7	9	1,03	0,74	6,986	9	112,67	50,449
line 9	7	10	1,044	0,74	6,986	10	68,582	30,708
line 10	10	11	0,1966	0,065	6,986	11	122,468	54,836
line 11	11	12	0,3744	0,1238	6,986	12	92,096	41,237
line 12	12	13	1,468	1,155	6,986	13	28,6	12,806
line 13	13	14	0,5416	0,7129	6,986	14	78,379	35,095
line 14	14	15	0,591	0,526	6,986	15	102,873	46,062
line 15	1	16	0,7463	0,545	6,986	16	43,109	19,302
line 16	16	17	1,289	1,721	6,986	17	237,289	91,298
line 17	17	18	0,732	0,547	6,986	18	243,007	93,498
line 18	17	19	0,164	0,1565	6,986	19	190,18	73,172
line 19	19	20	1,5042	1,3554	6,986	20	154,238	59,343
line 20	20	21	0,4095	0,4784	6,986	21	211,311	81,302
line 21	21	22	0,7089	0,9373	6,986	22	232,442	89,433
line 22	22	23	0,4512	0,3083	6,986	23	225,425	86,733
line 23	22	24	0,898	0,7091	6,986	24	189,831	73,038
line 24	24	25	0,896	0,7011	6,986	25	213,56	82,168
line 25	25	26	0,203	0,1034	6,986	26	166,103	63,908
line 26	24	27	0,2842	0,1447	6,986	27	179,614	69,107
line 27	27	28	1,059	0,9337	6,986	28	78,960	40,11
line 28	28	29	0,8042	0,7006	6,986	29	71,44	36,29
line 29	28	30	0,5075	0,2585	6,986	30	82,72	42,02
line 30	30	31	0,9744	0,963	6,986	31	75,2	38,2
line 31	28	32	0,3105	0,3619	6,986	32	67,68	34,38
line 32	32	33	0,341	0,5302	6,986	33	232,442	89,433

B.5 Lagoa System : Installed capacity of DGs and their placement

Table B.5: Installed capacity of DGs and their placement

DG Type	Node	Installed Power [MW]
PV	4	2
PV	27	2
Wind	10	1
Wind	13	1
Wind	24	1
	Total MW	7

B.6 Lagoa System : Installed capacity of ESSs and their placement

Table B.6: Installed capacity of ESSs and their placement

Node	Installed Power [MW]
3	1
13	1
28	1
Total MW	3

Appendix C

Reconfiguraton Schemes

C.1 IEEE 119-bus test system Case C

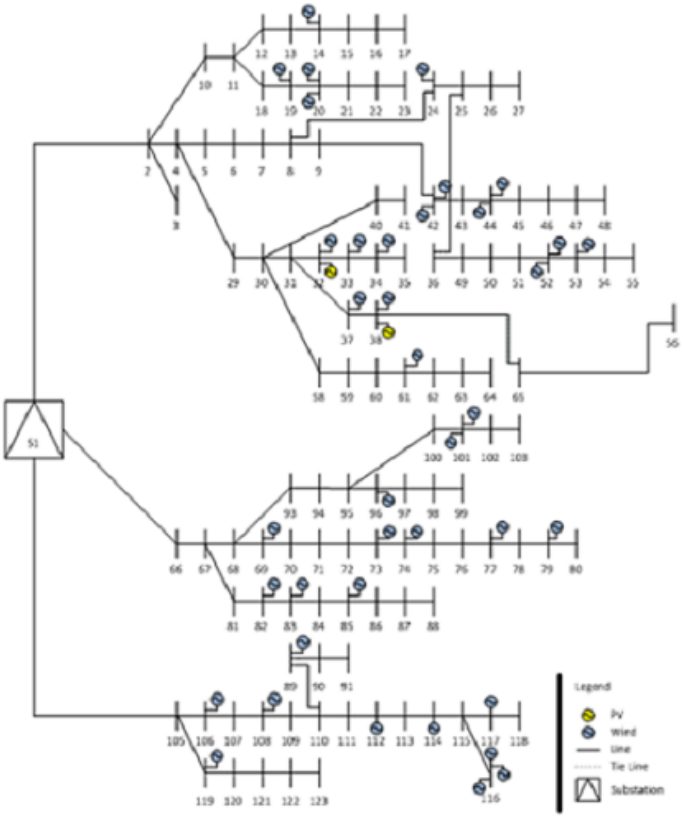

Figure C.1: 119 Bus test system reconfiguration for h=1

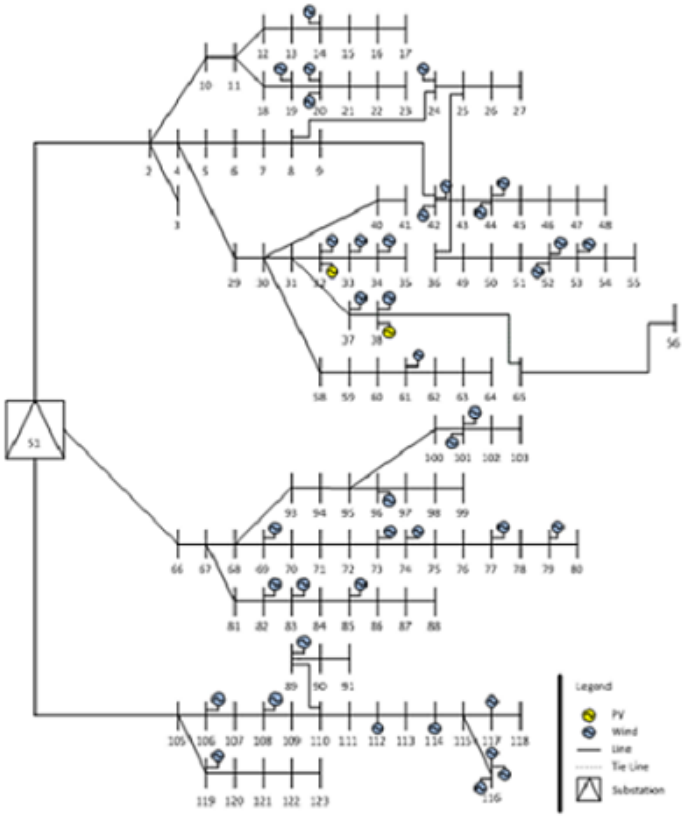

Figure C.2: 119 Bus test system reconfiguration for h=2

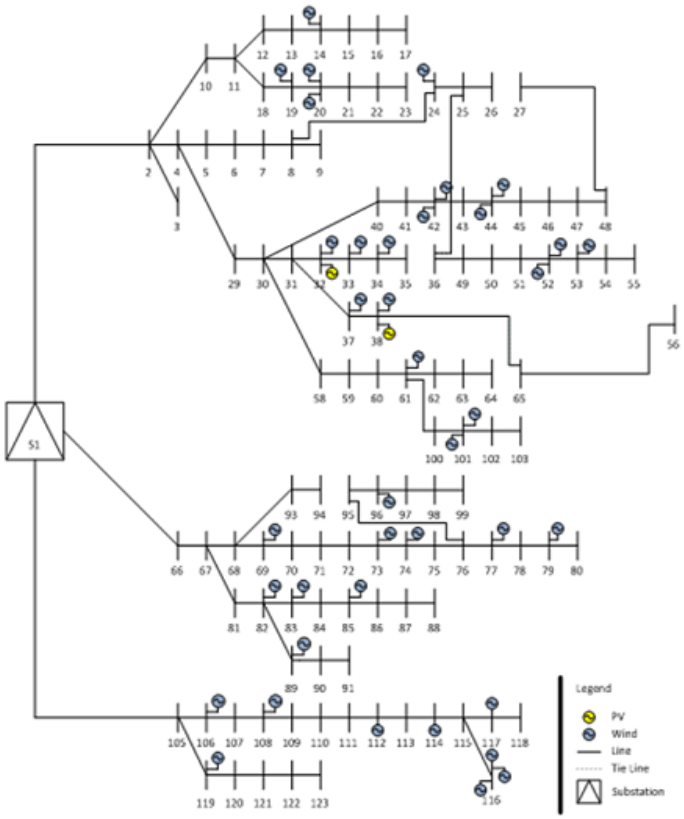

Figure C.3: 119 Bus test system reconfiguration for h=3

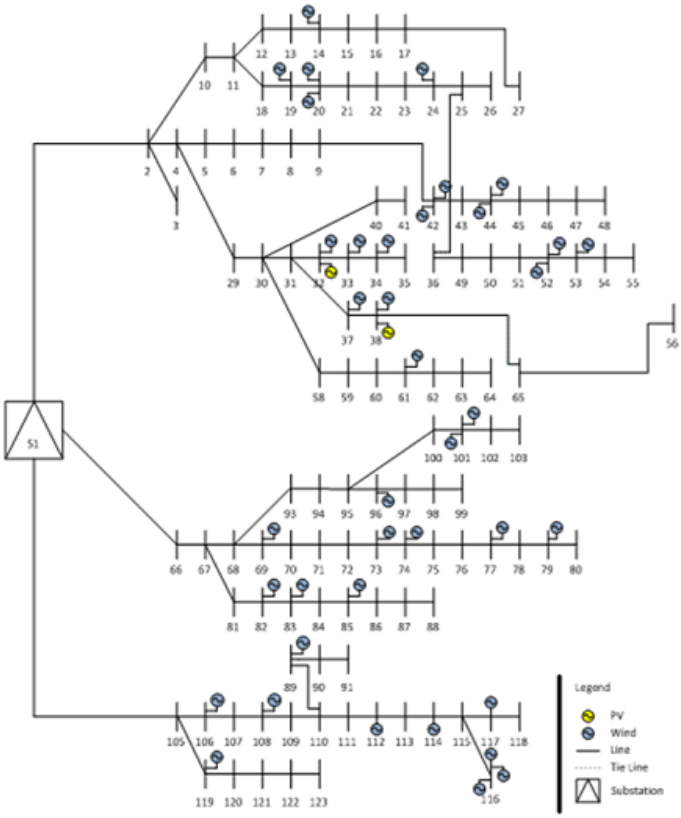

Figure C.4: 119 Bus test system reconfiguration for h=4

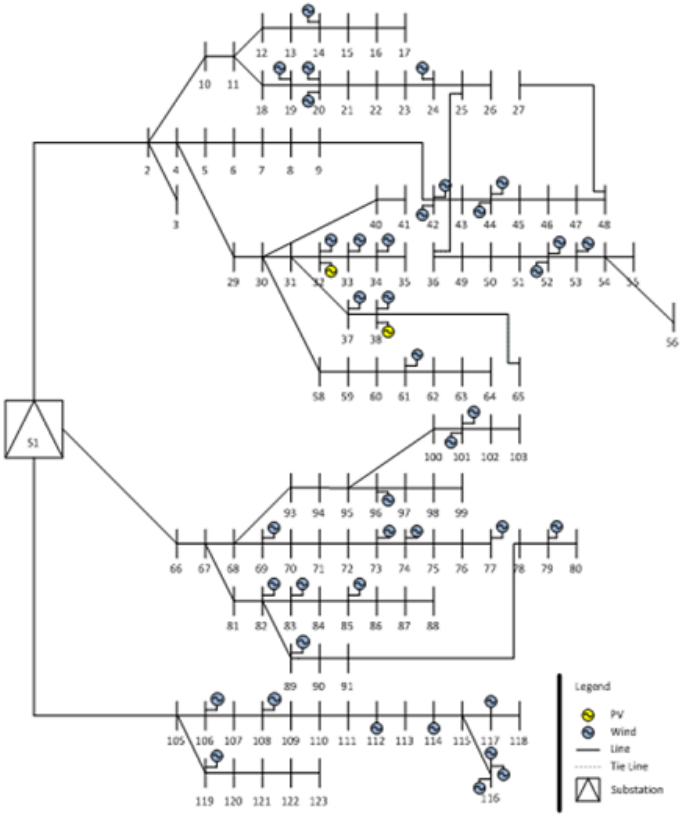

Figure C.5: 119 Bus test system reconfiguration for h=5

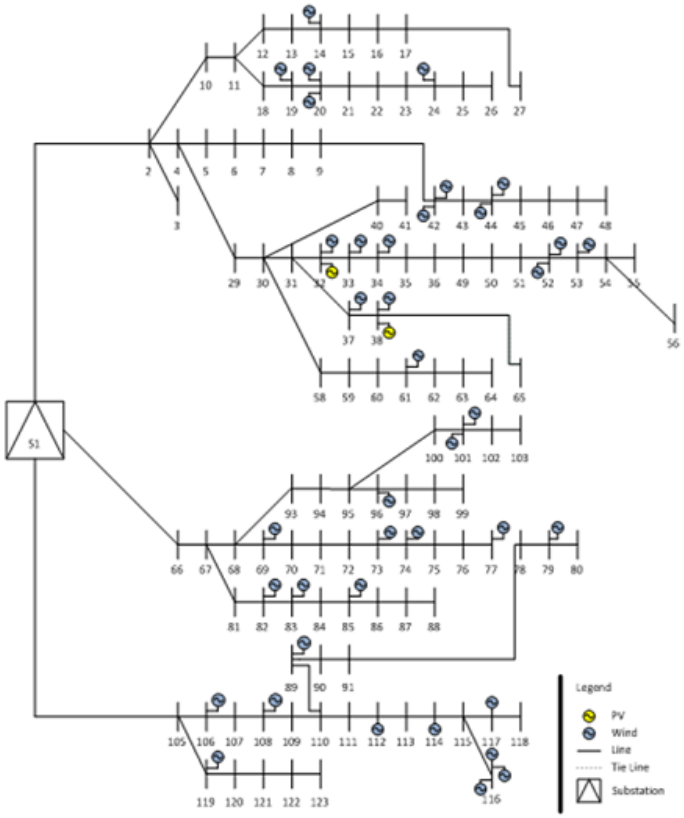

Figure C.6: 119 Bus test system reconfiguration for h=6

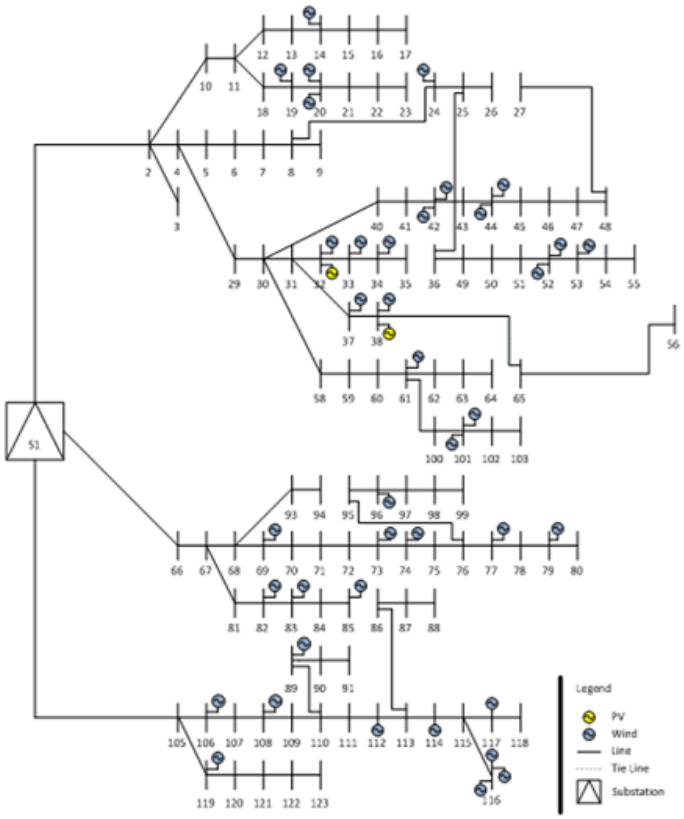

Figure C.7: 119 Bus test system reconfiguration for h=7

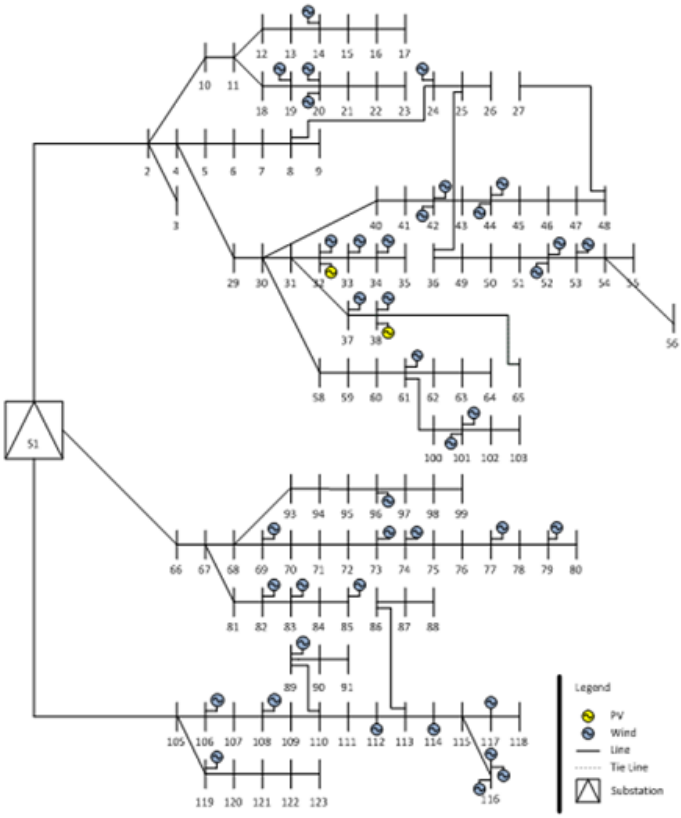

Figure C.8: 119 Bus test system reconfiguration for h=8

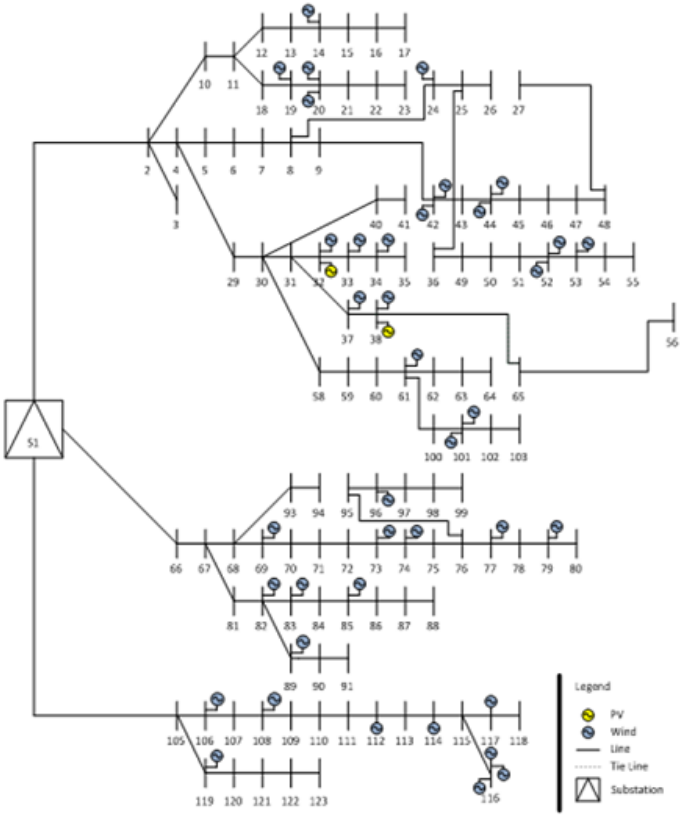

Figure C.9: 119 Bus test system reconfiguration for h=9

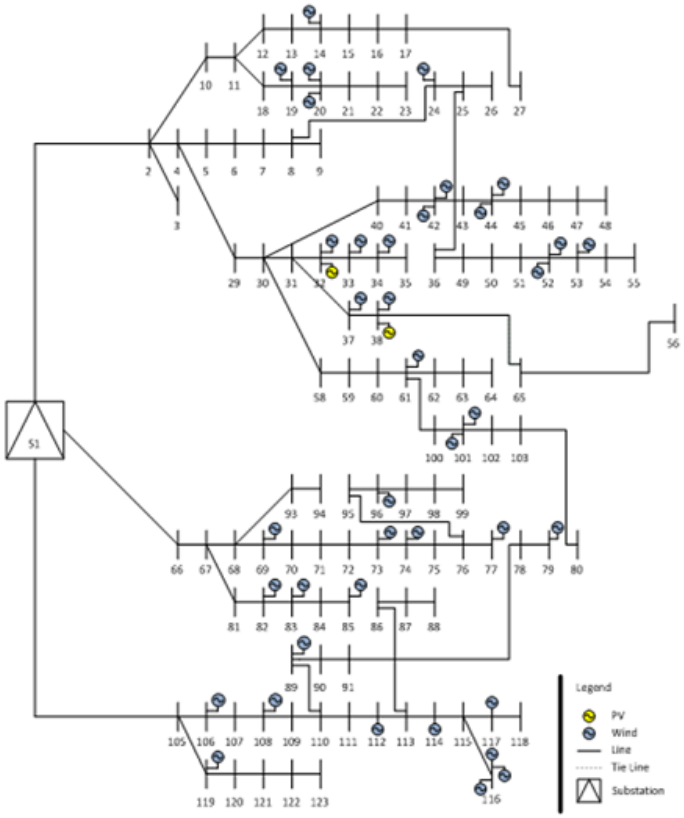

Figure C.10: 119 Bus test system reconfiguration for h=10

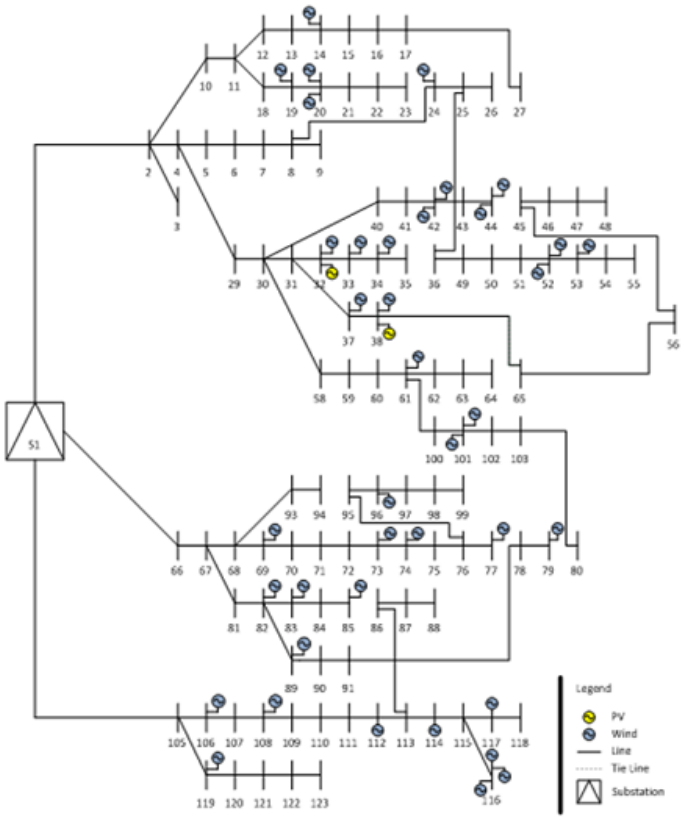

Figure C.11: 119 Bus test system reconfiguration for h=11

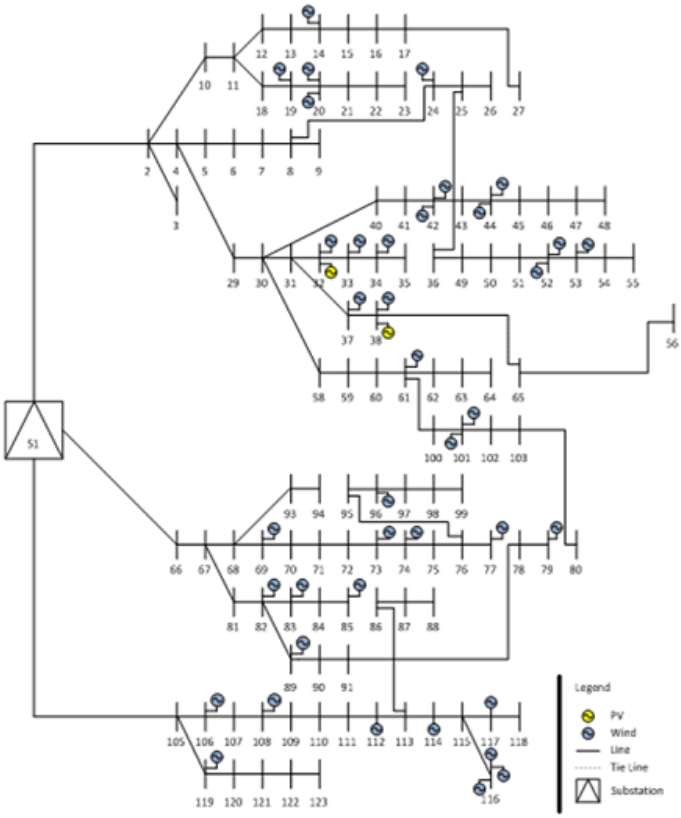

Figure C.12: 119 Bus test system reconfiguration for h=12

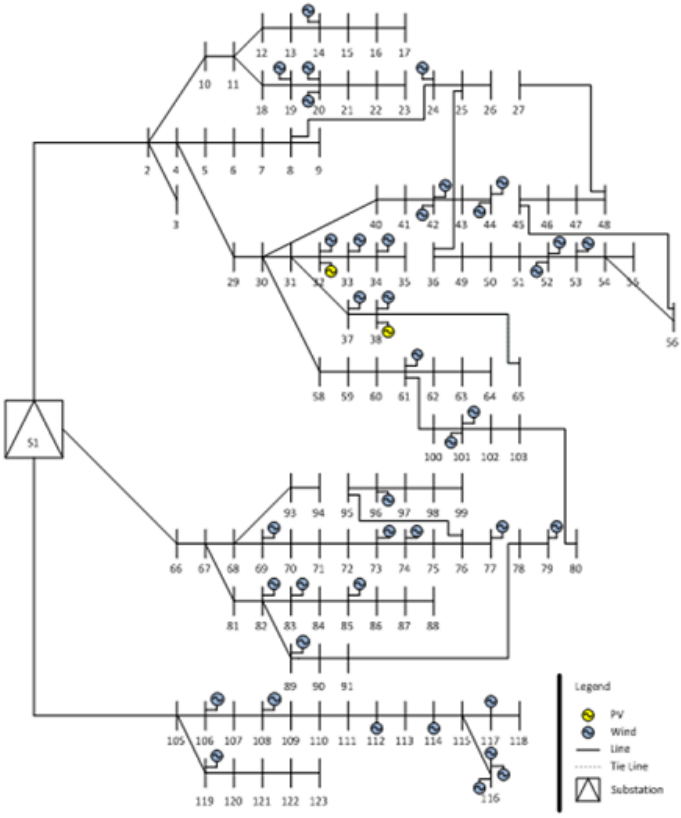

Figure C.13: 119 Bus test system reconfiguration for h=13

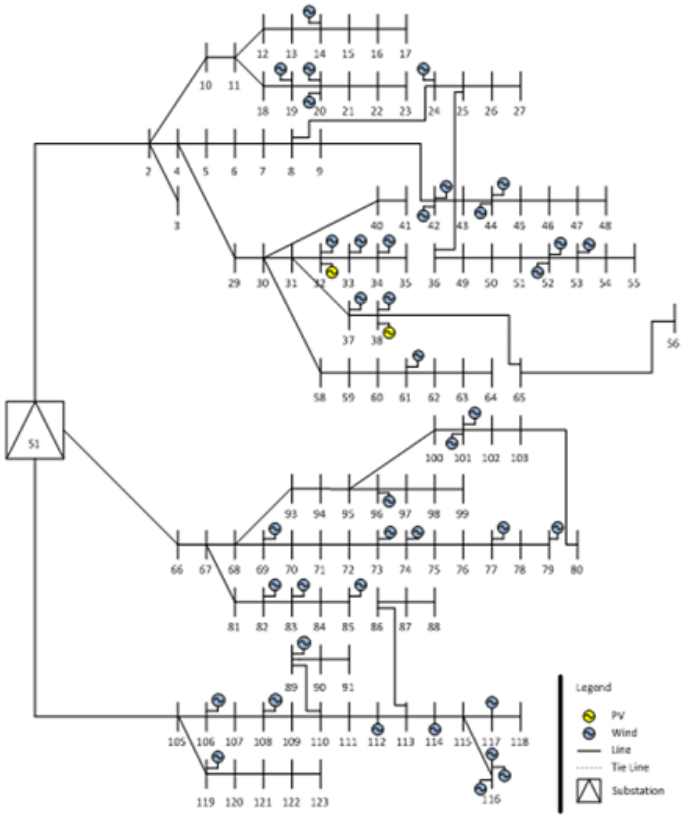

Figure C.14: 119 Bus test system reconfiguration for h=14

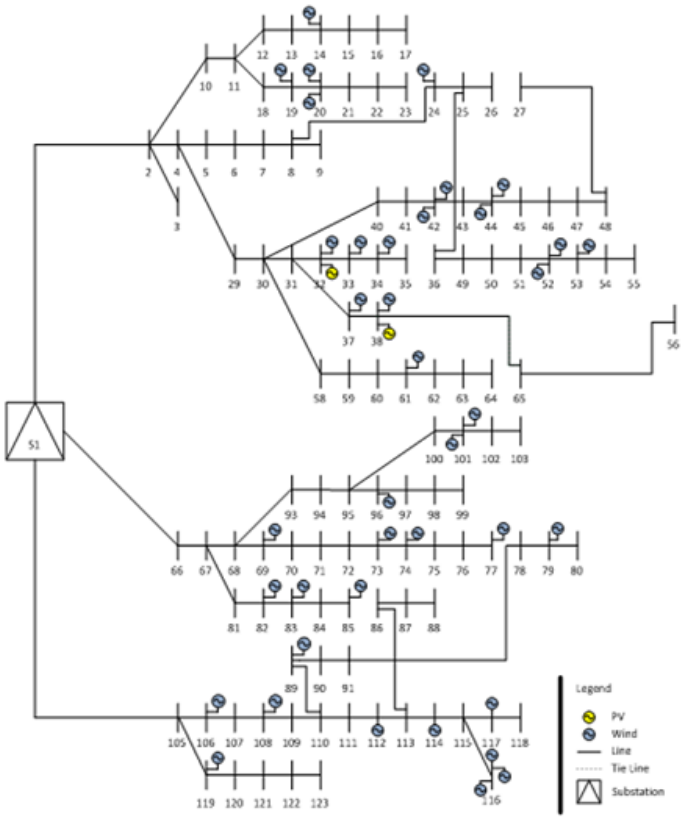

Figure C.15: 119 Bus test system reconfiguration for h=15

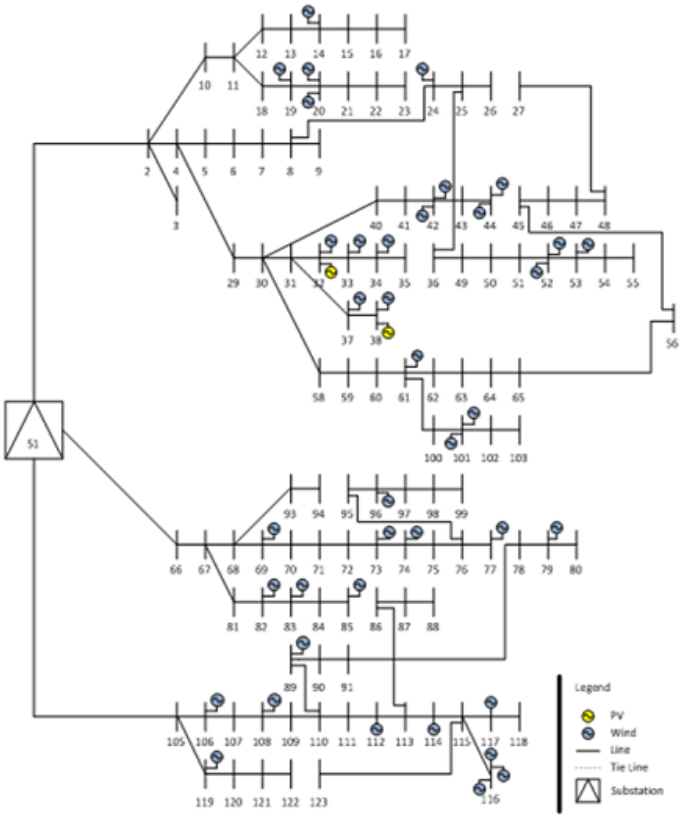

Figure C.16: 119 Bus test system reconfiguration for h=16

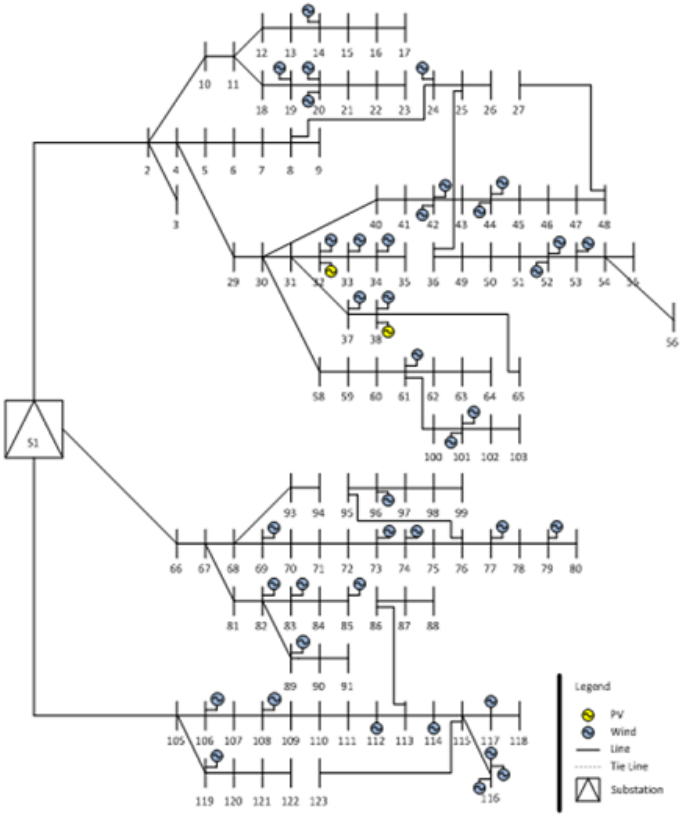

Figure C.17: 119 Bus test system reconfiguration for h=17

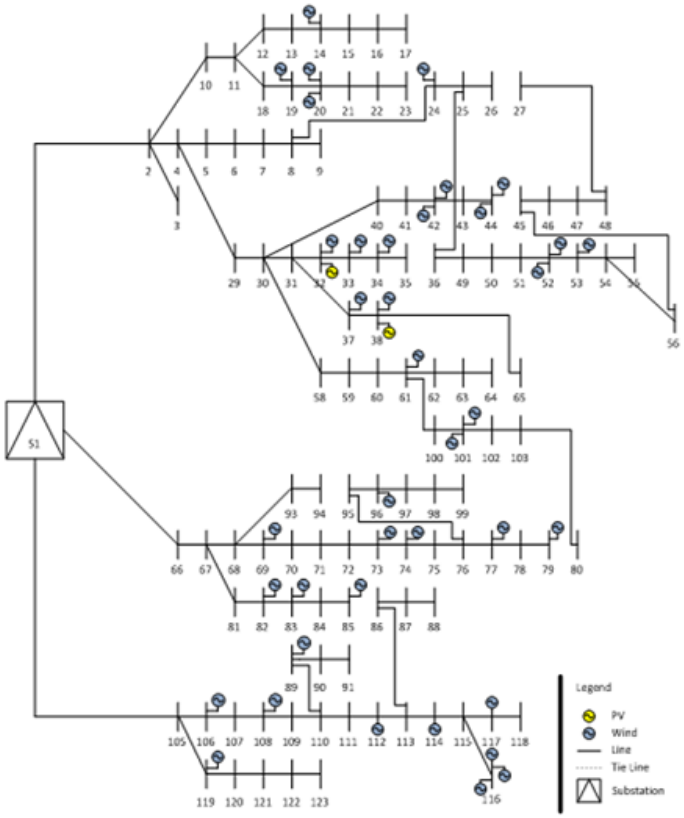

Figure C.18: 119 Bus test system reconfiguration for h=18

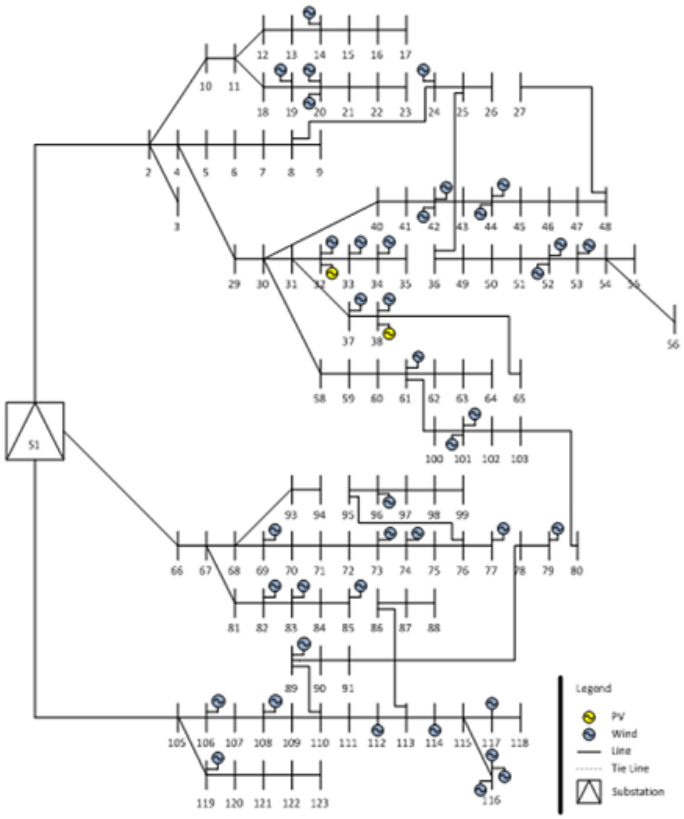

Figure C.19: 119 Bus test system reconfiguration for h=19

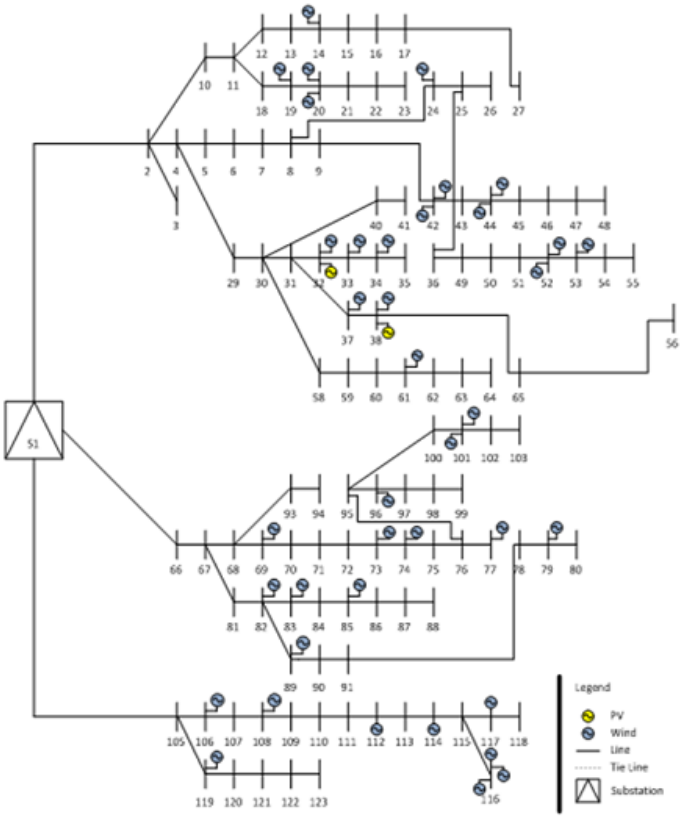

Figure C.20: 119 Bus test system reconfiguration for h=20

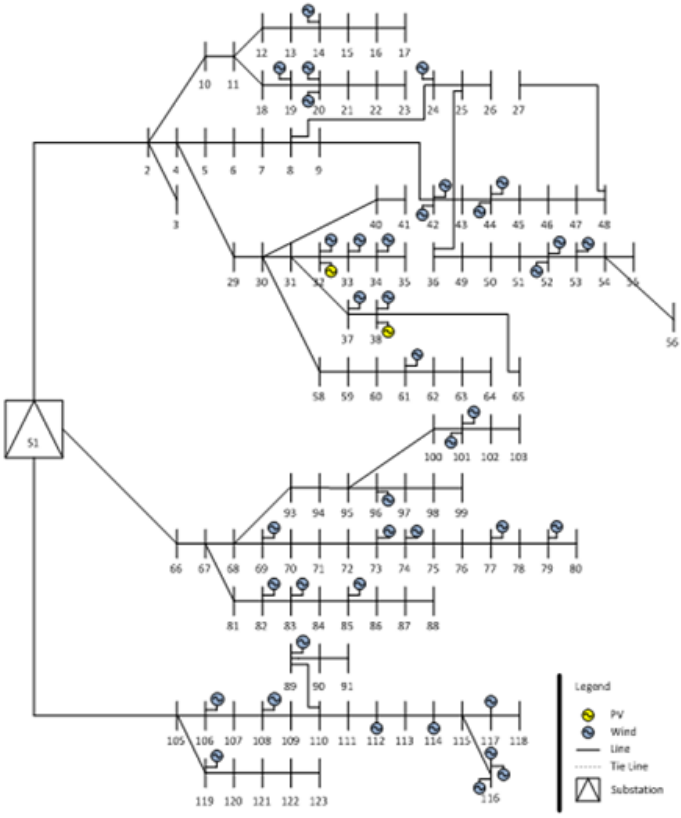

Figure C.21: 119 Bus test system reconfiguration for h=21

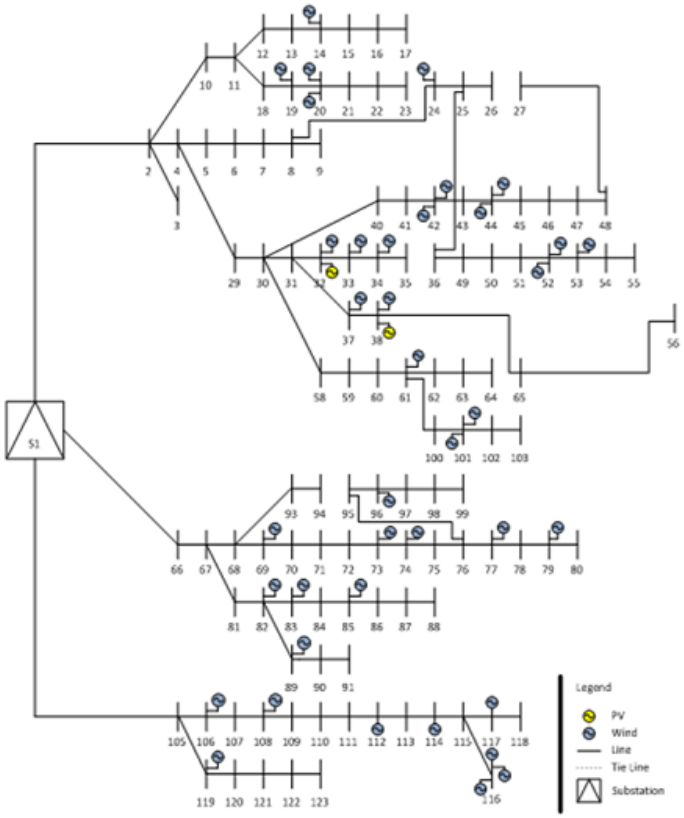

Figure C.22: 119 Bus test system reconfiguration for h=22

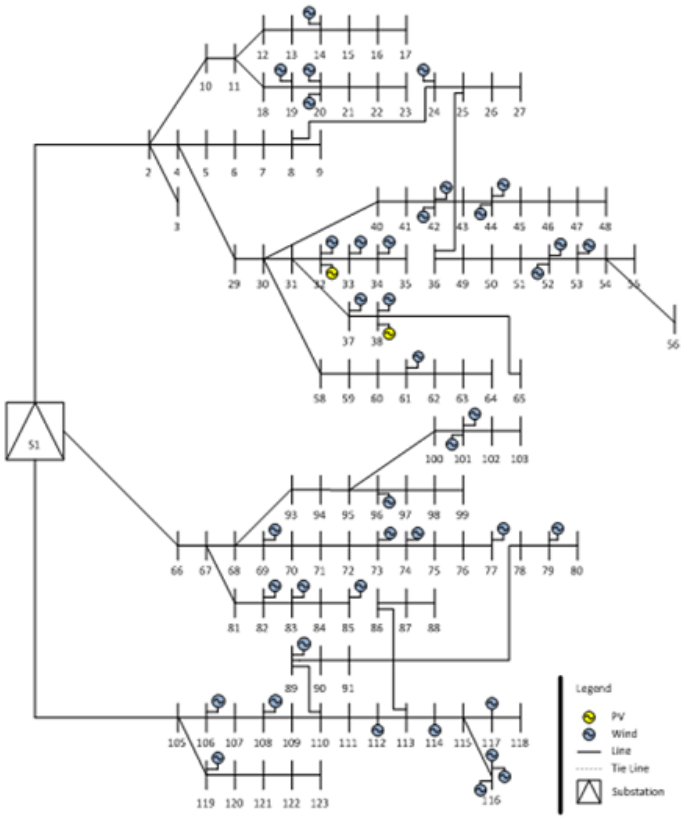

Figure C.23: 119 Bus test system reconfiguration for h=23

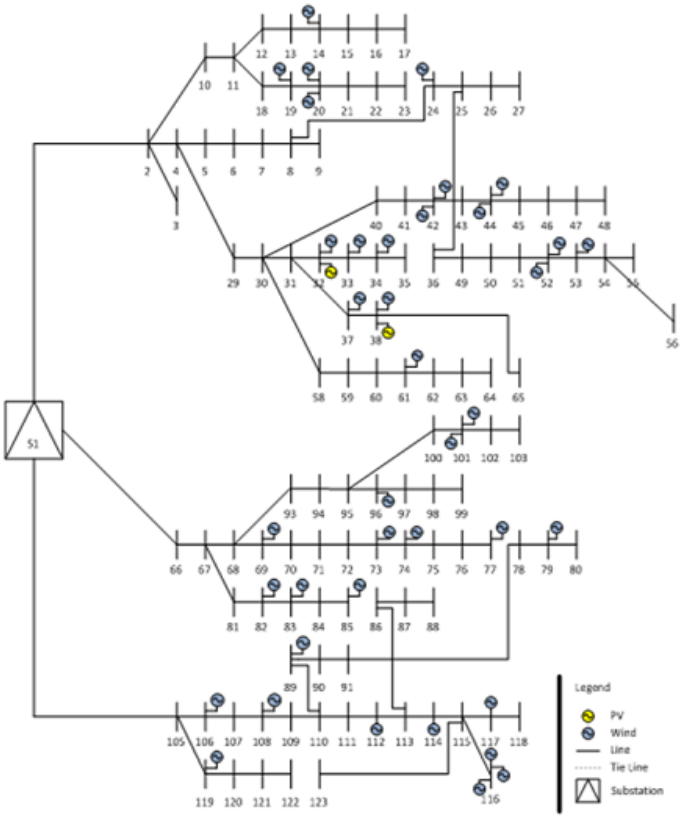

Figure C.24: 119 Bus test system reconfiguration for h=24

C.2 IEEE 119-bus test system Case D

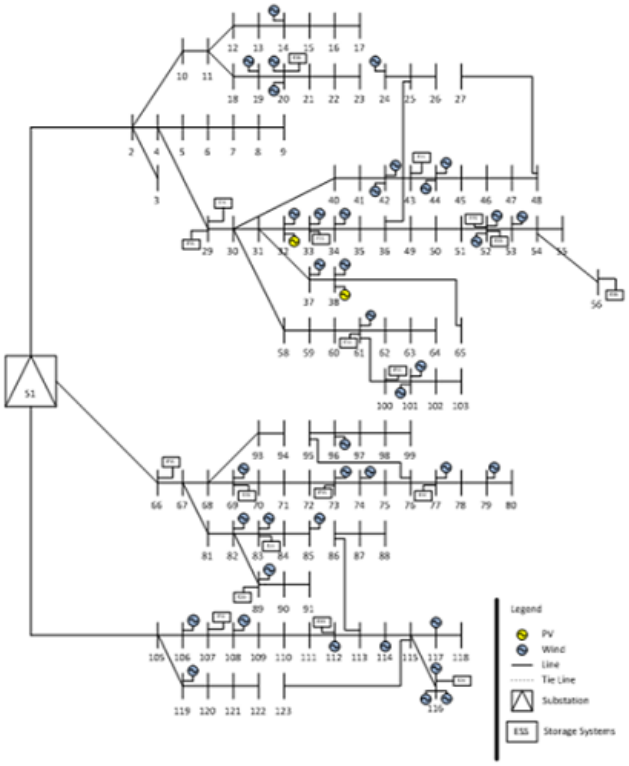

Figure C.25: 119 Bus test system reconfiguration for h=1

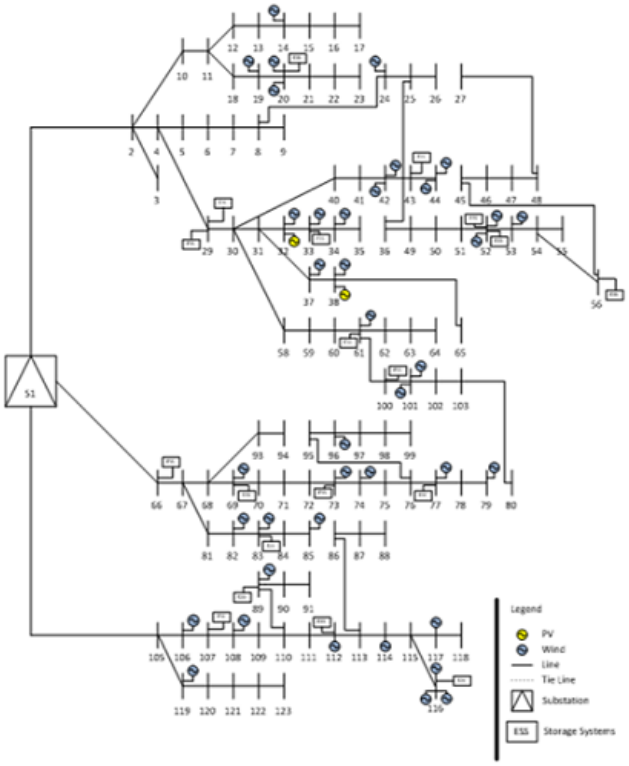

Figure C.26: 119 Bus test system reconfiguration for h=2

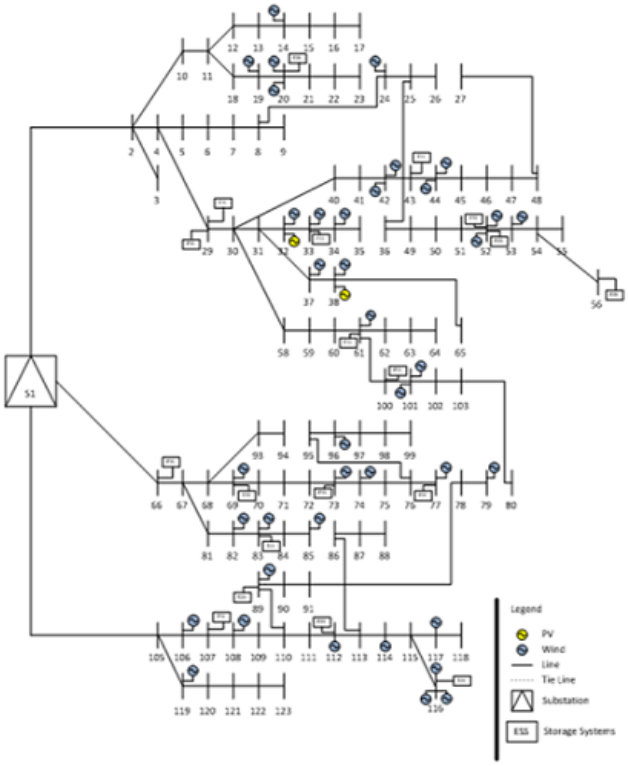

Figure C.27: 119 Bus test system reconfiguration for h=3

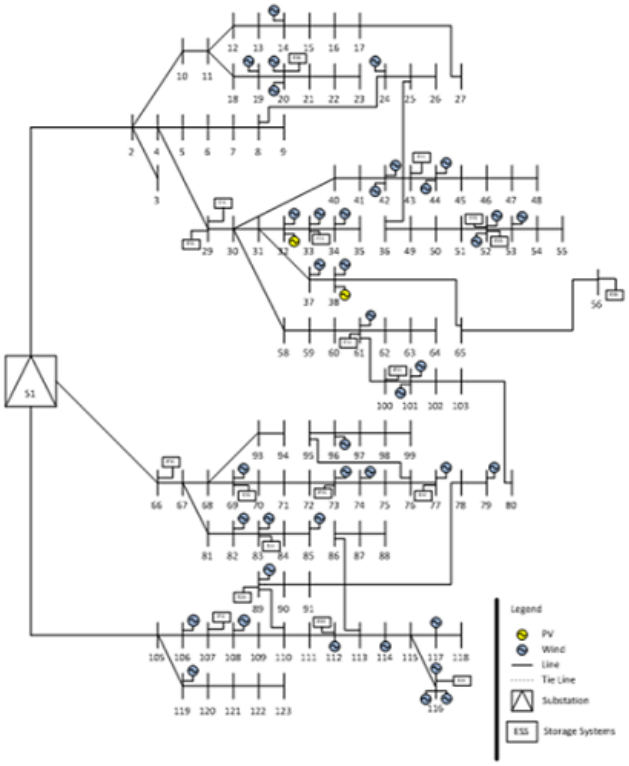

Figure C.28: 119 Bus test system reconfiguration for h=4

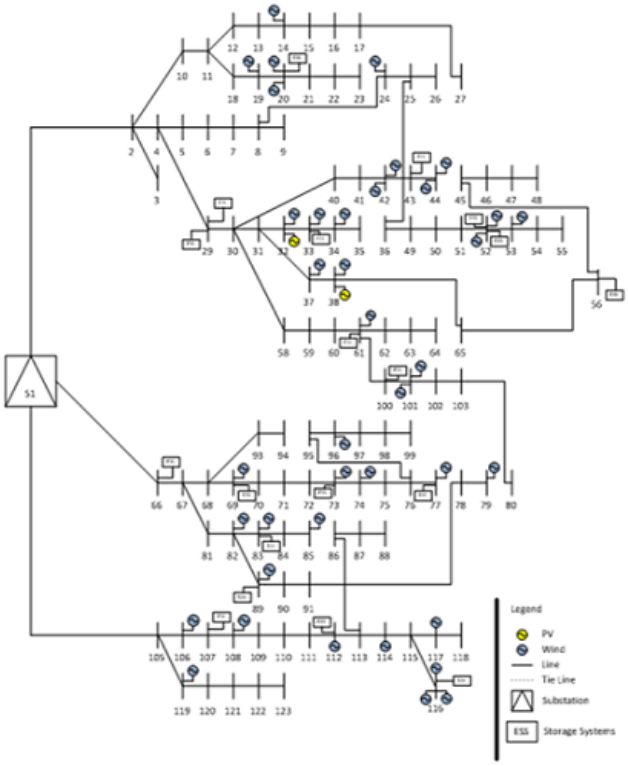

Figure C.29: 119 Bus test system reconfiguration for h=5

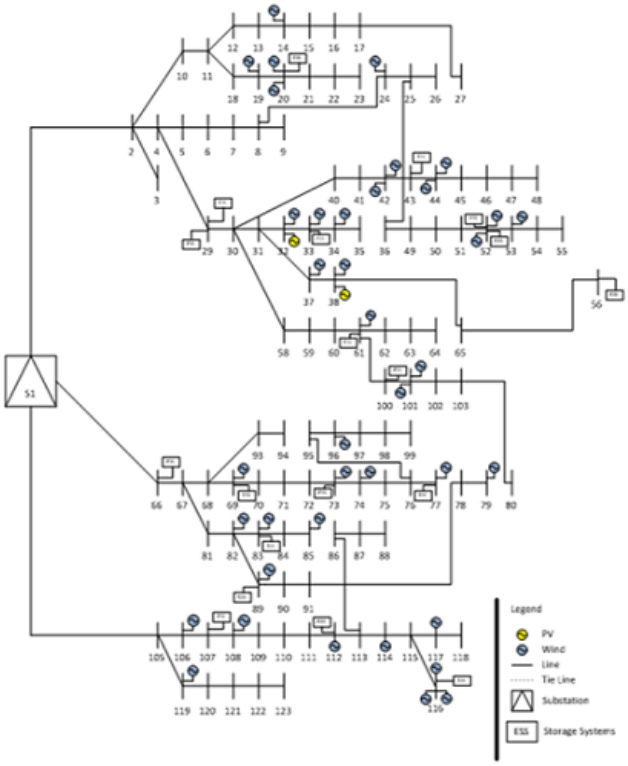

Figure C.30: 119 Bus test system reconfiguration for h=6

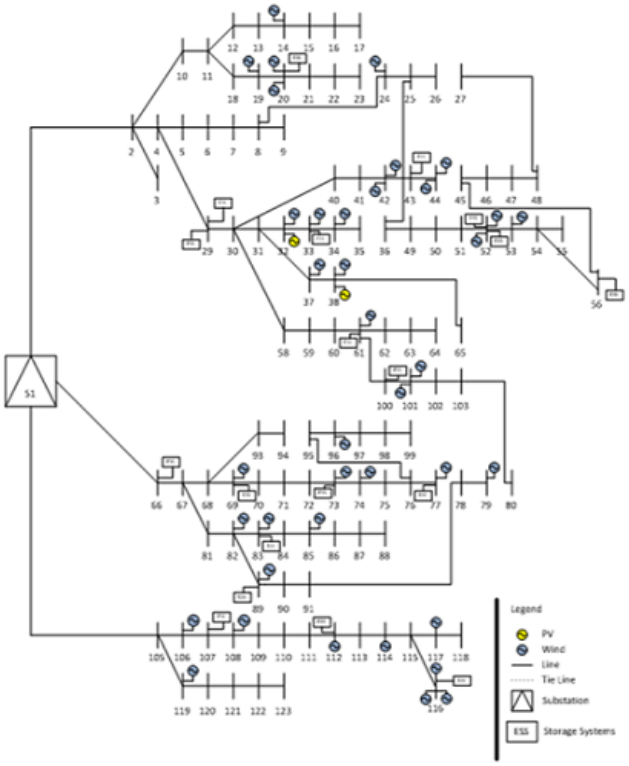

Figure C.31: 119 Bus test system reconfiguration for h=7

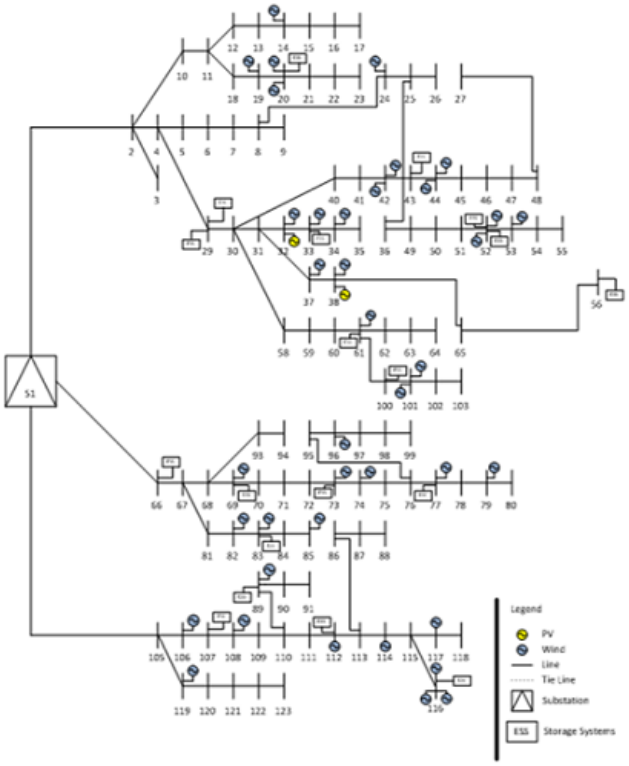

Figure C.32: 119 Bus test system reconfiguration for h=8

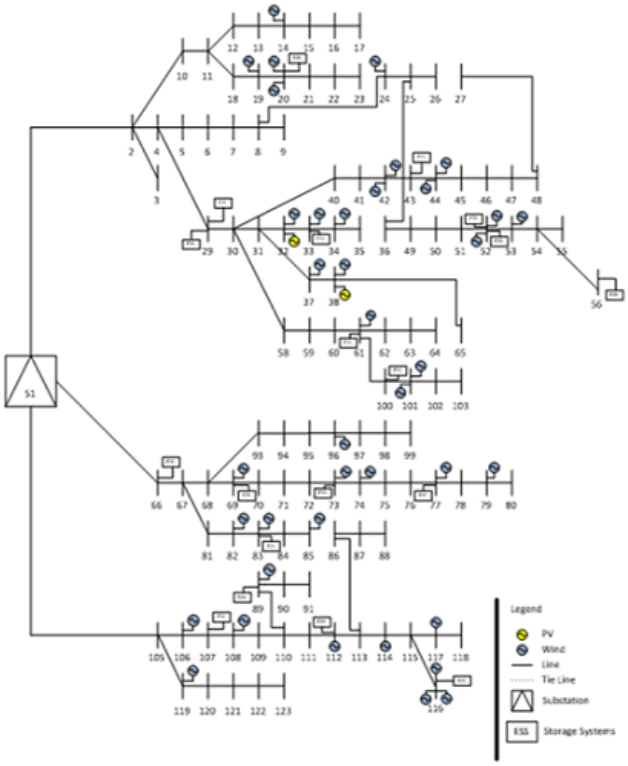

Figure C.33: 119 Bus test system reconfiguration for h=9

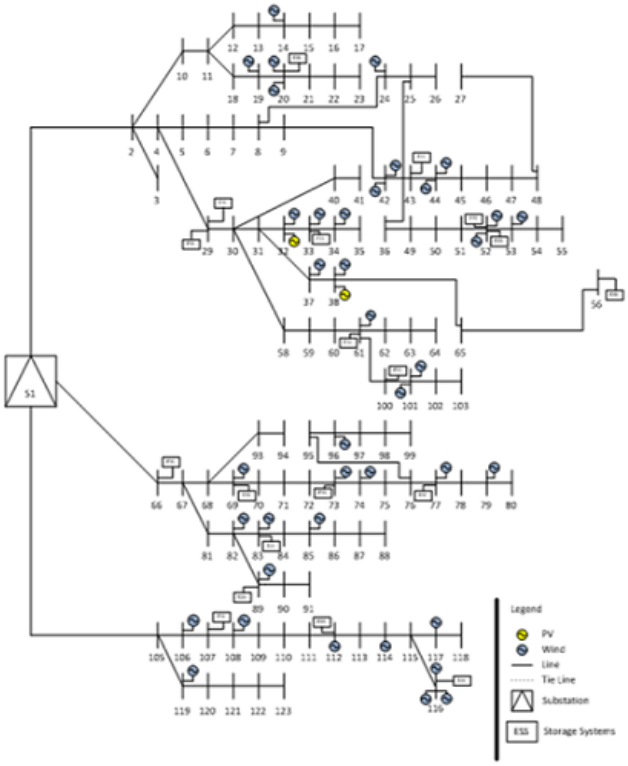

Figure C.34: 119 Bus test system reconfiguration for h=10

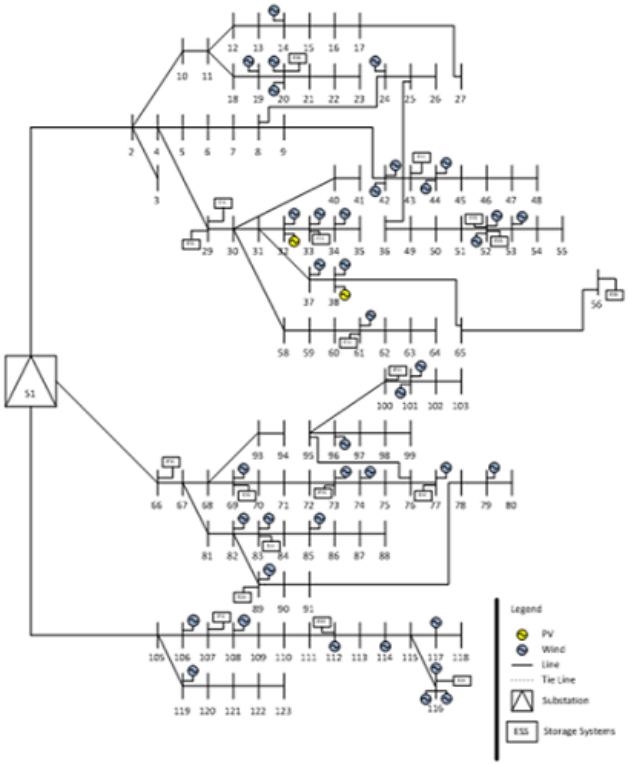

Figure C.35: 119 Bus test system reconfiguration for h=11

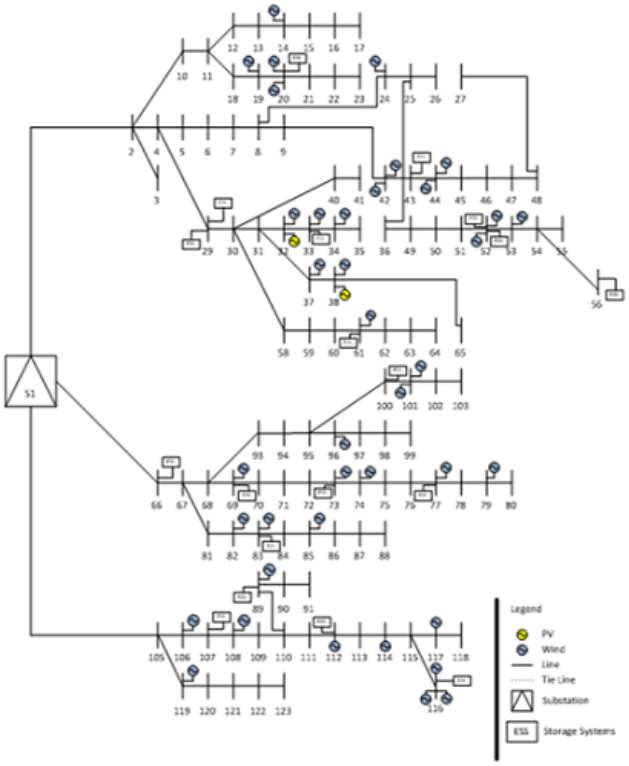

Figure C.36: 119 Bus test system reconfiguration for h=12

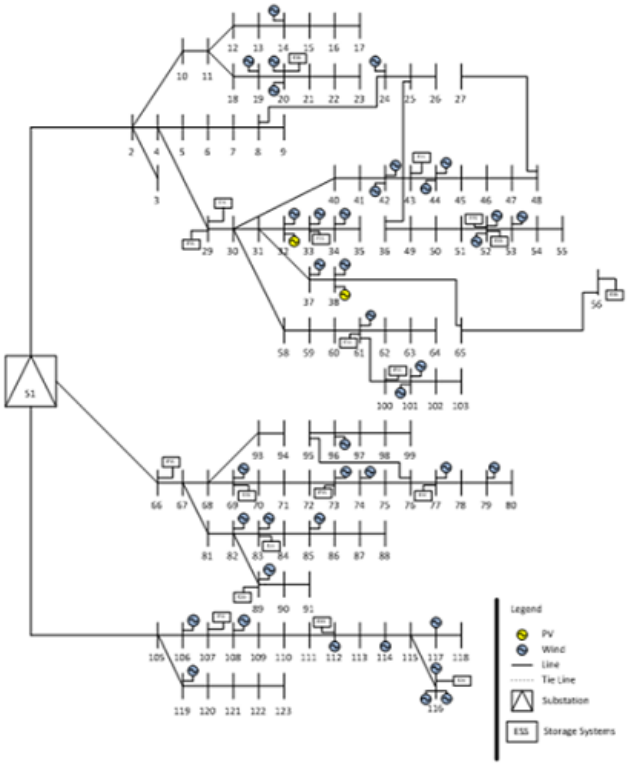

Figure C.37: 119 Bus test system reconfiguration for h=13

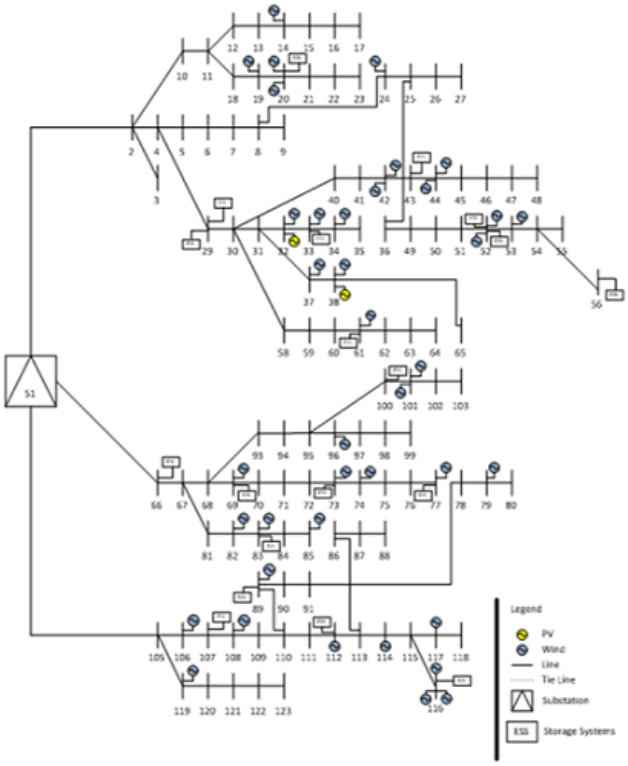

Figure C.38: 119 Bus test system reconfiguration for h=14

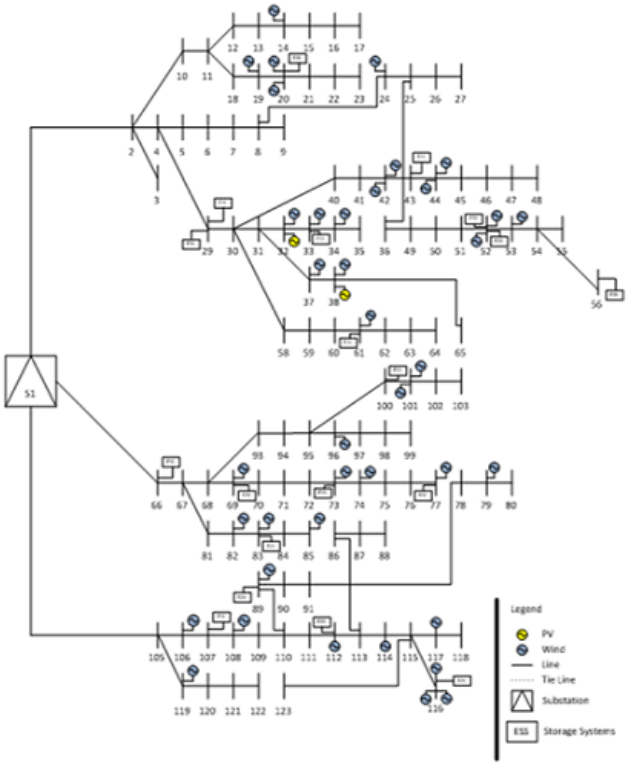

Figure C.39: 119 Bus test system reconfiguration for h=15

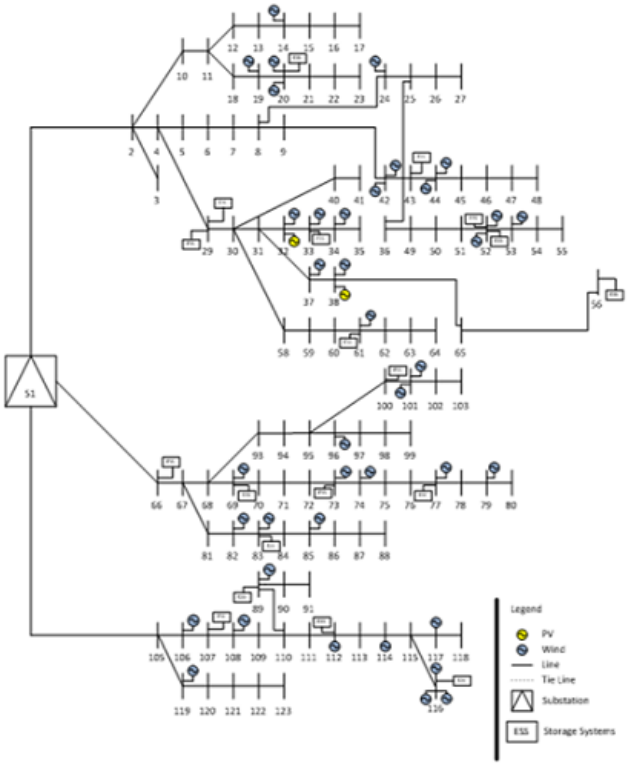

Figure C.40: 119 Bus test system reconfiguration for h=16

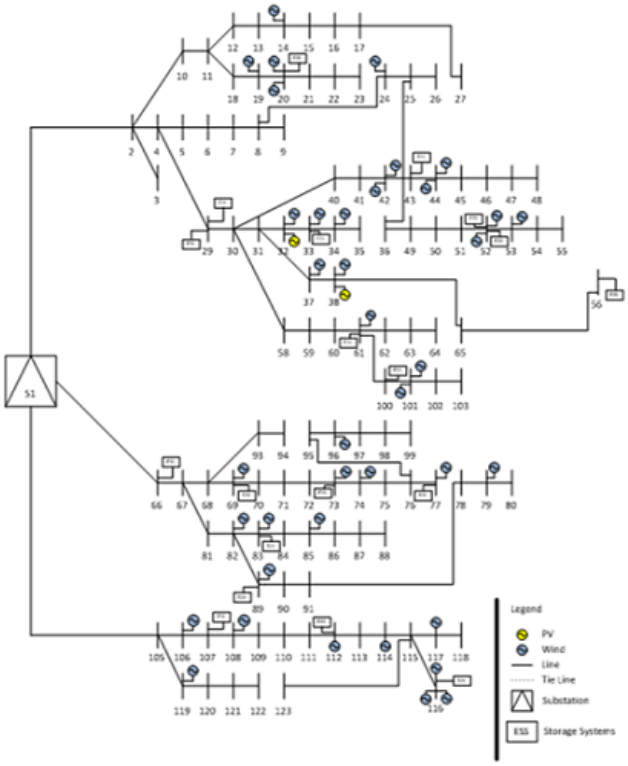

Figure C.41: 119 Bus test system reconfiguration for h=17

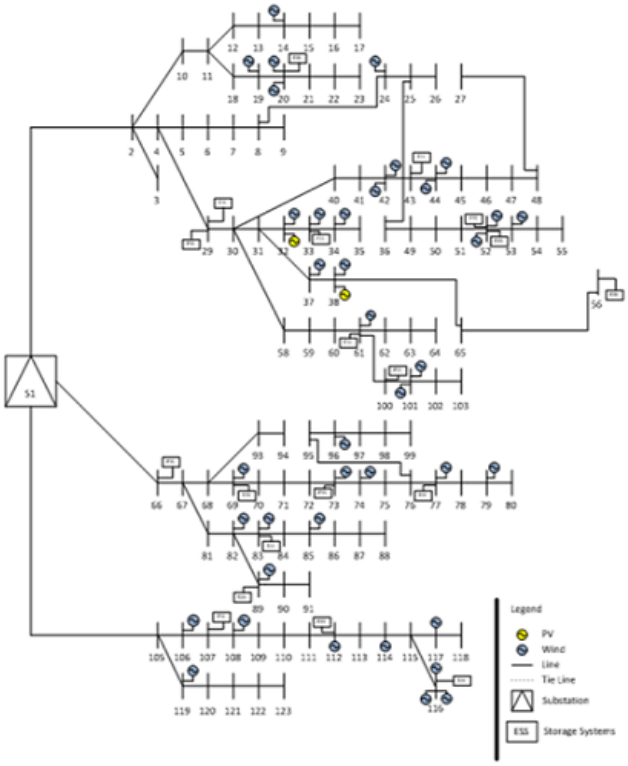

Figure C.42: 119 Bus test system reconfiguration for h=18

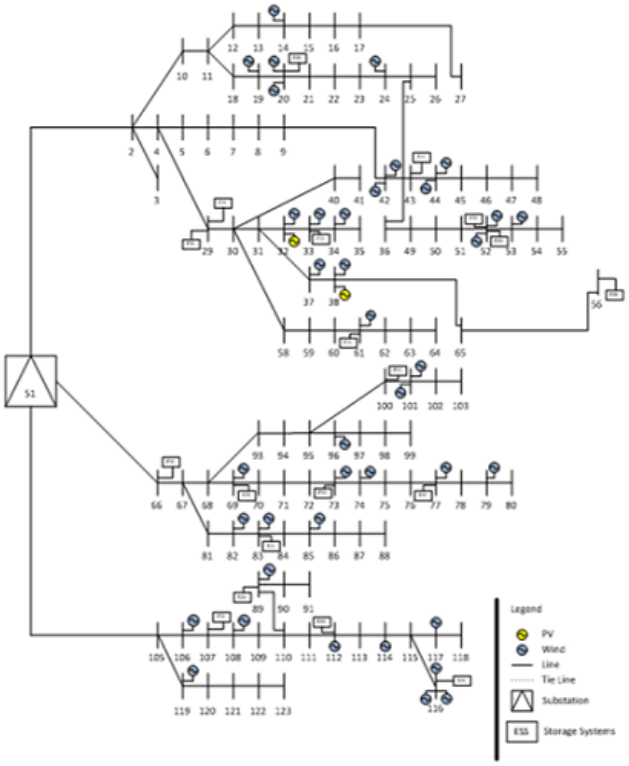

Figure C.43: 119 Bus test system reconfiguration for h=19

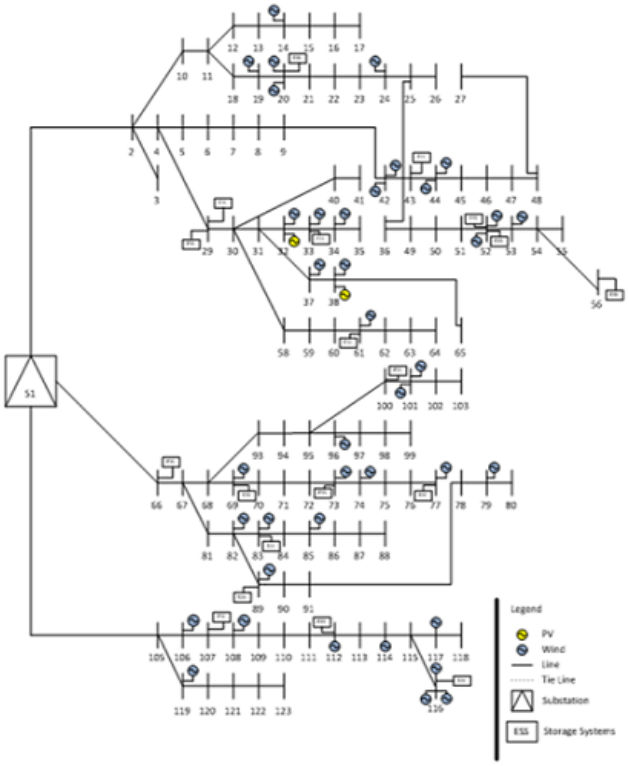

Figure C.44: 119 Bus test system reconfiguration for h=20

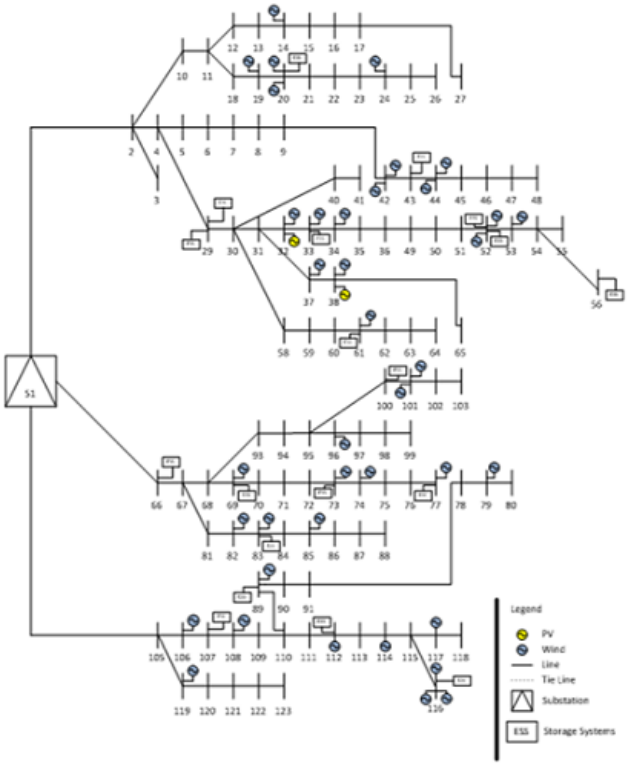

Figure C.45: 119 Bus test system reconfiguration for h=21

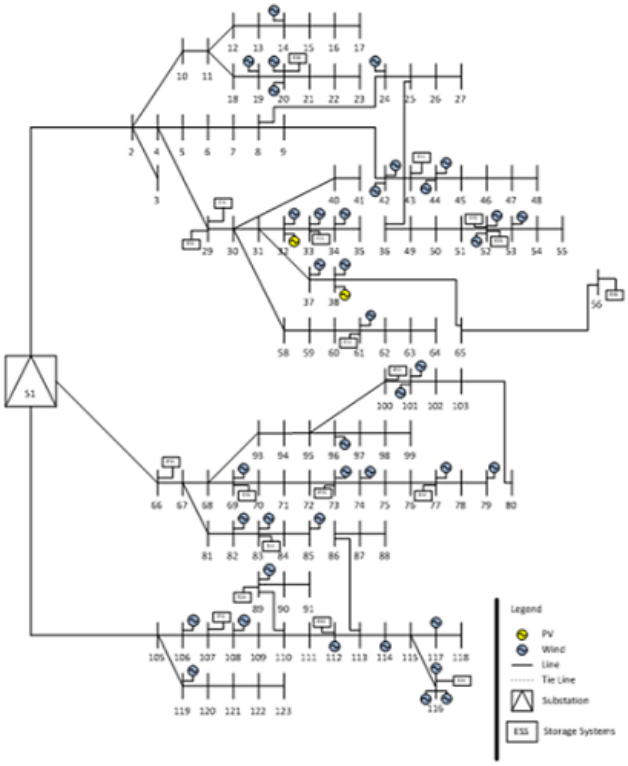

Figure C.46: 119 Bus test system reconfiguration for h=22

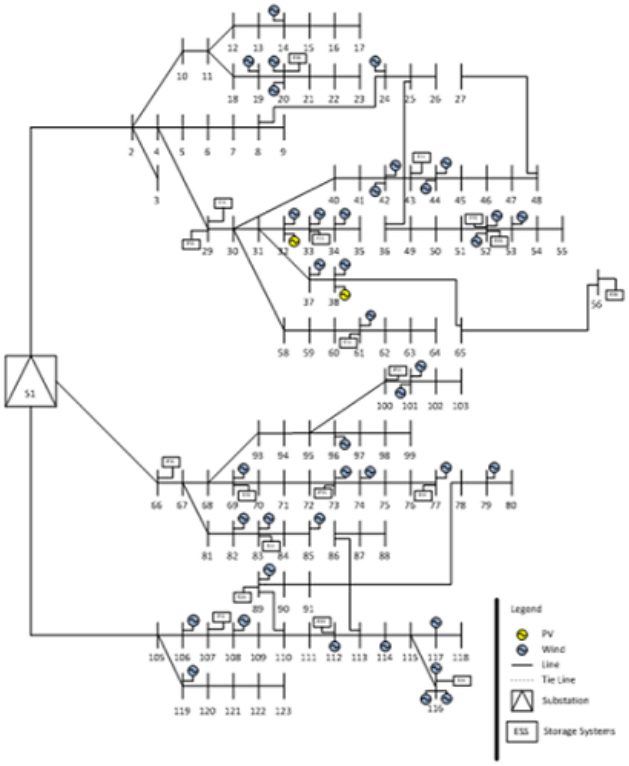

Figure C.47: 119 Bus test system reconfiguration for h=23

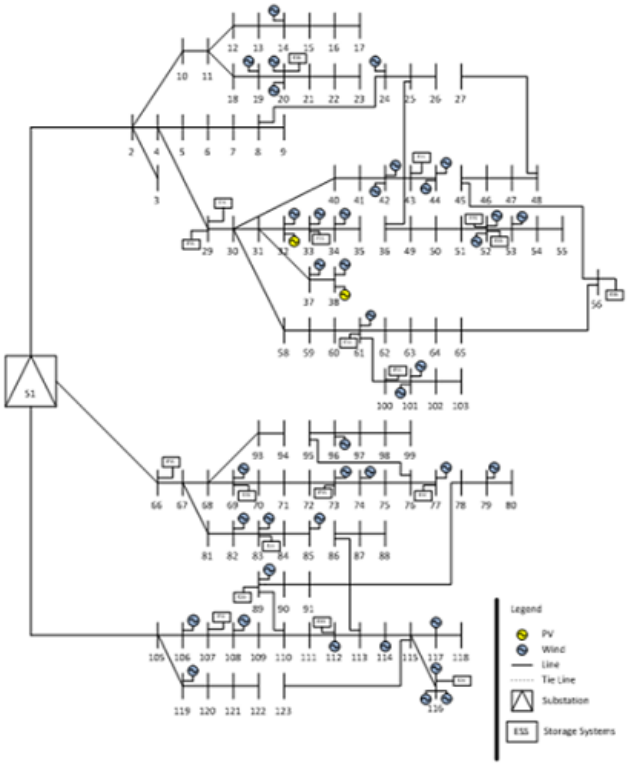

Figure C.48: 119 Bus test system reconfiguration for h=24

C.3 Lagoa System Case C

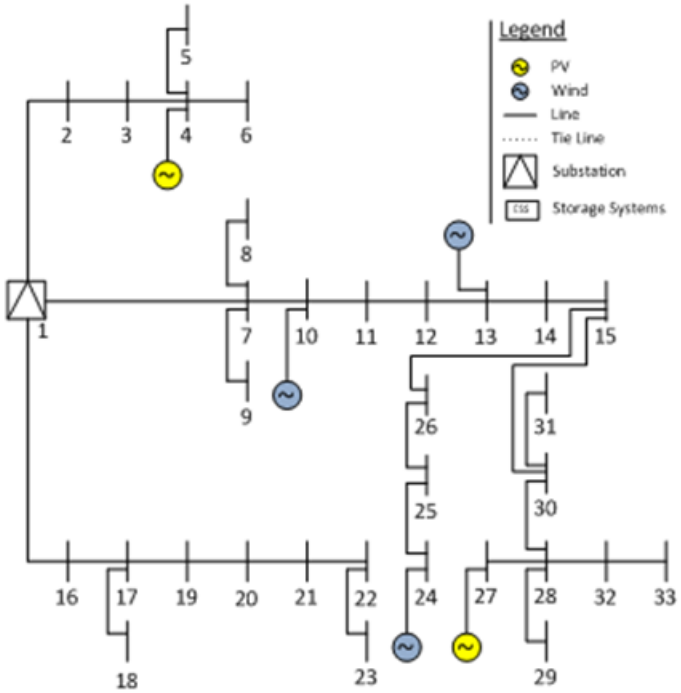

Figure C.49: 119 Bus test system reconfiguration for h=1

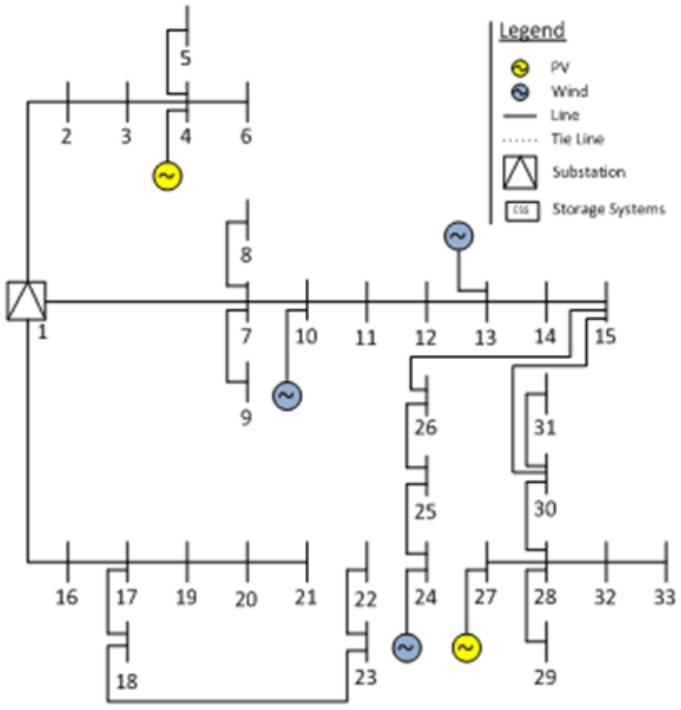

Figure C.50: 119 Bus test system reconfiguration for h=2

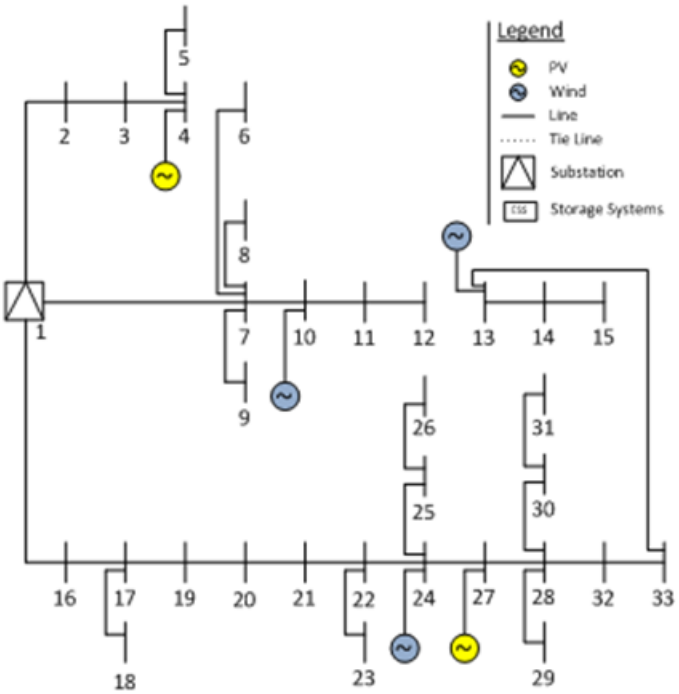

Figure C.51: 119 Bus test system reconfiguration for h=3

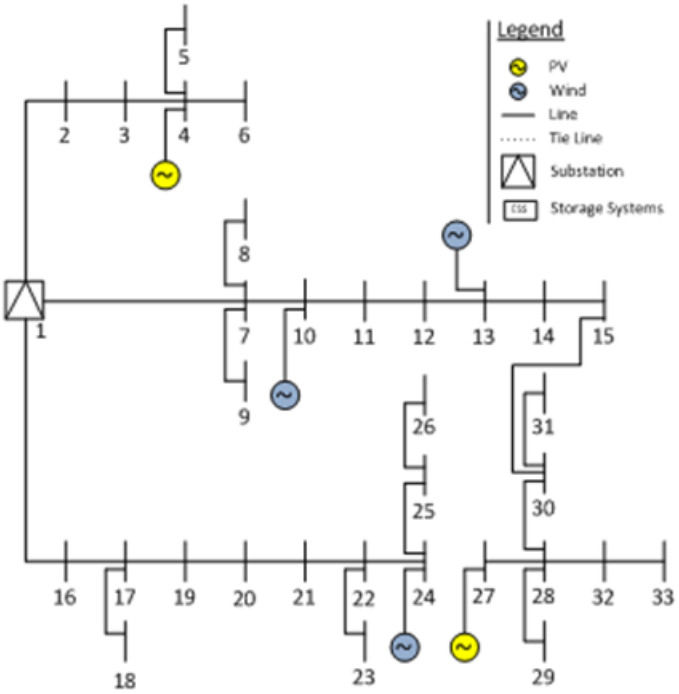

Figure C.52: 119 Bus test system reconfiguration for h=4

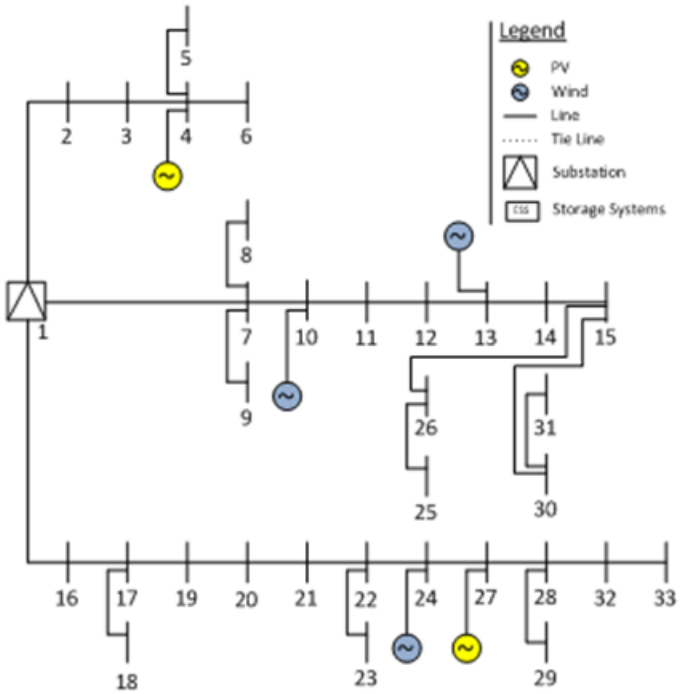

Figure C.53: 119 Bus test system reconfiguration for h=5

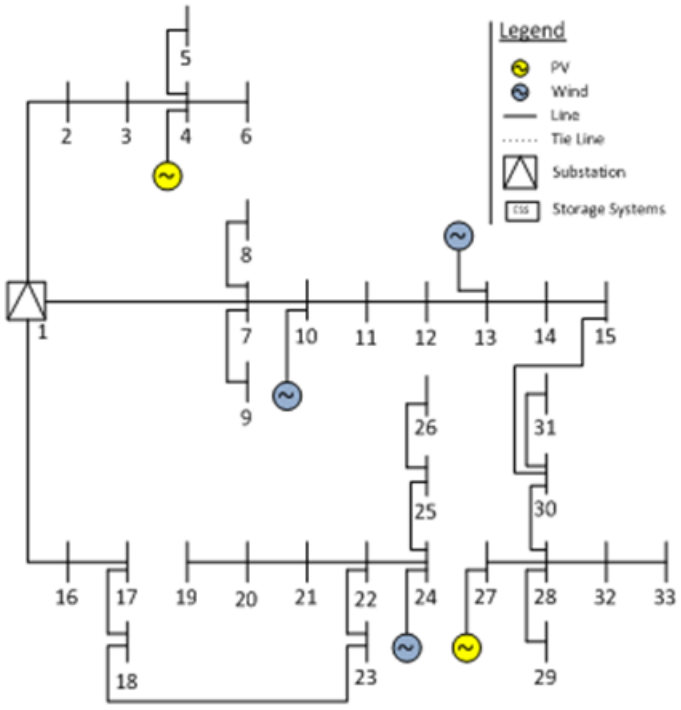

Figure C.54: 119 Bus test system reconfiguration for h=6

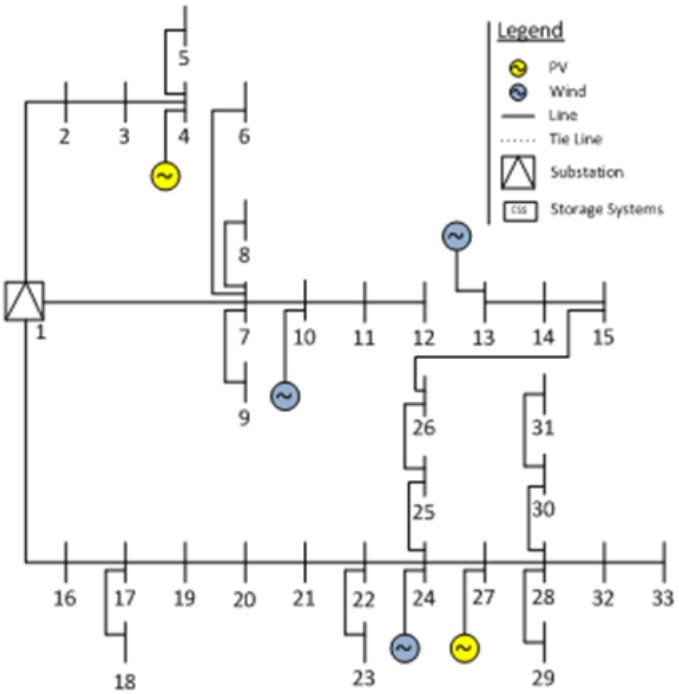

Figure C.55: 119 Bus test system reconfiguration for h=7

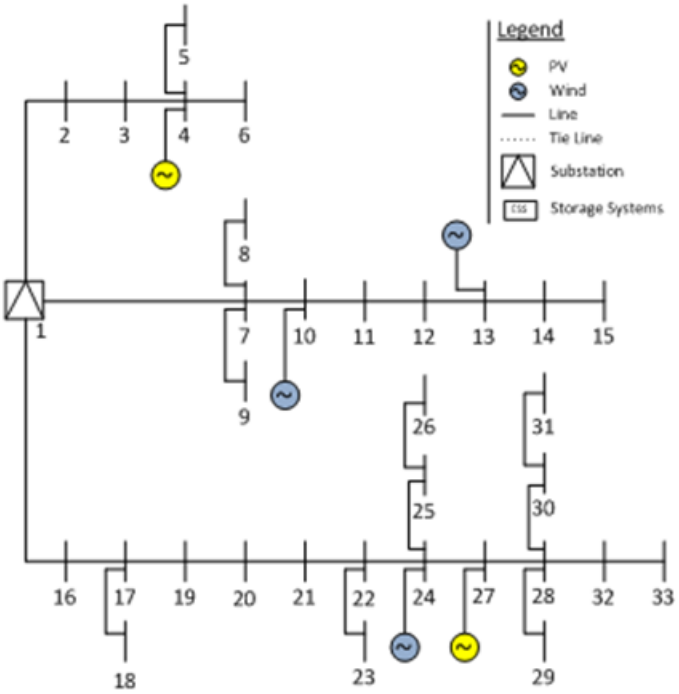

Figure C.56: 119 Bus test system reconfiguration for h=8

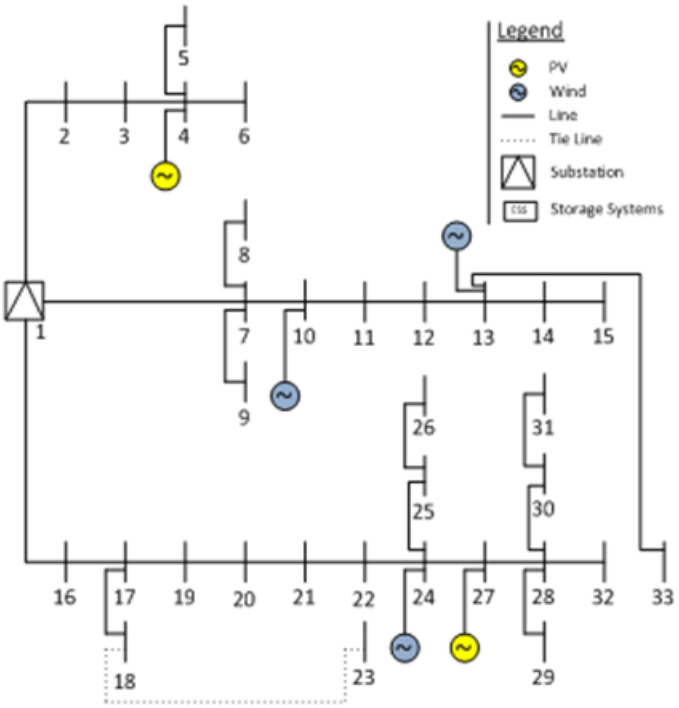

Figure C.57: 119 Bus test system reconfiguration for h=9

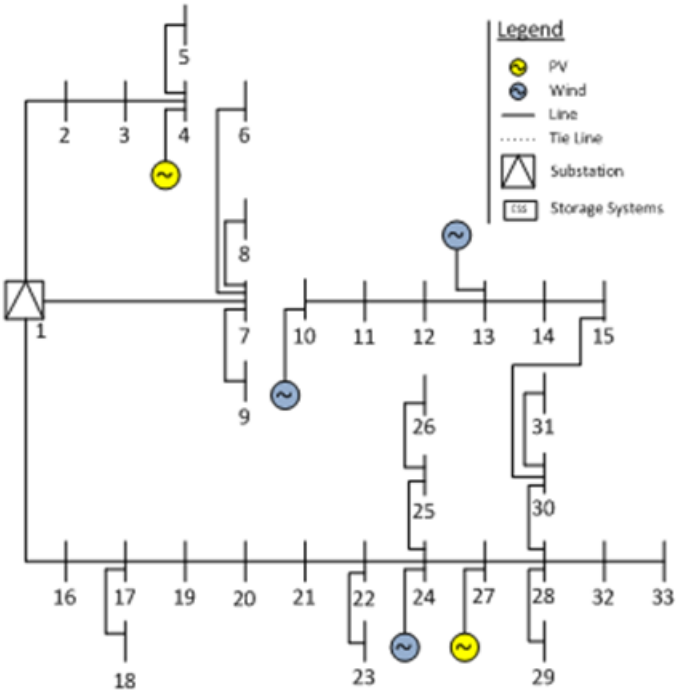

Figure C.58: 119 Bus test system reconfiguration for h=10

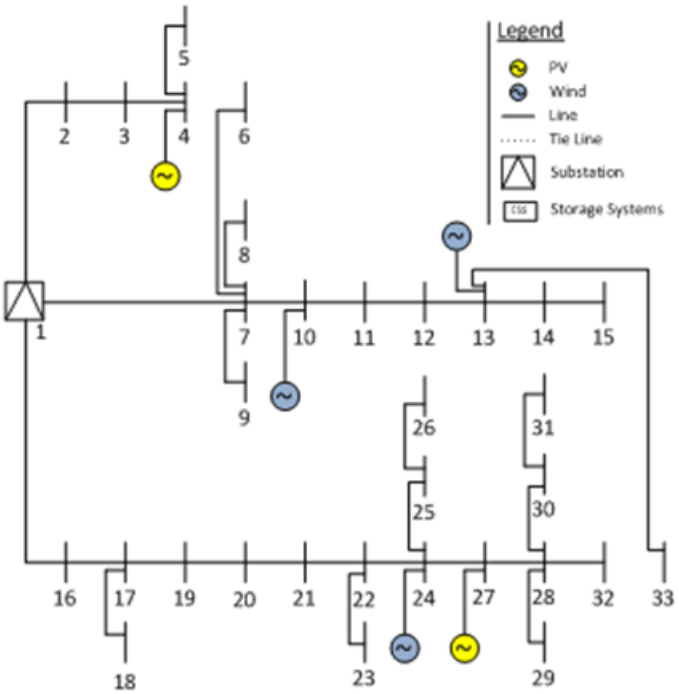

Figure C.59: 119 Bus test system reconfiguration for h=11

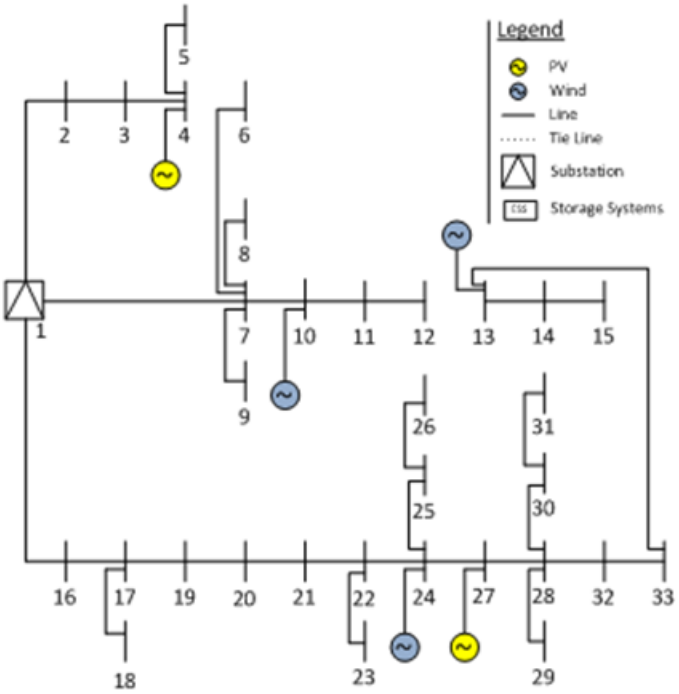

Figure C.60: 119 Bus test system reconfiguration for h=12

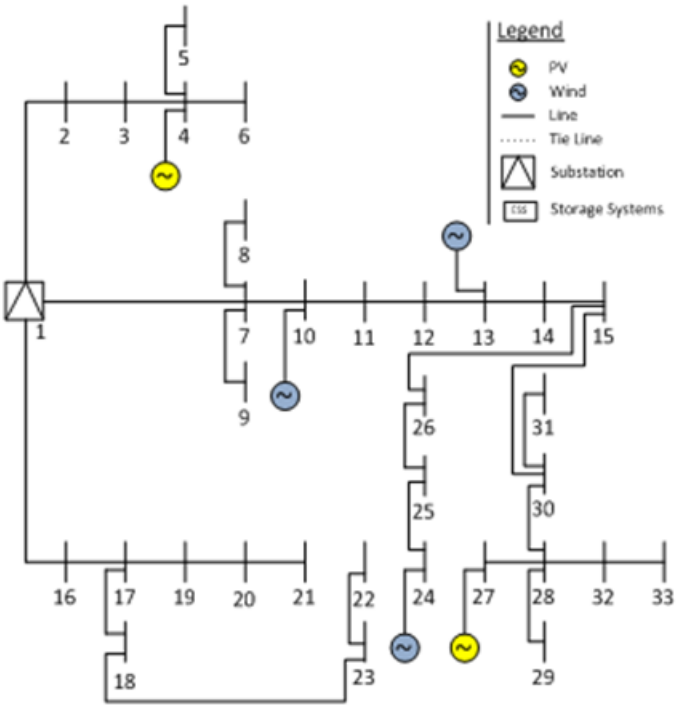

Figure C.61: 119 Bus test system reconfiguration for h=13

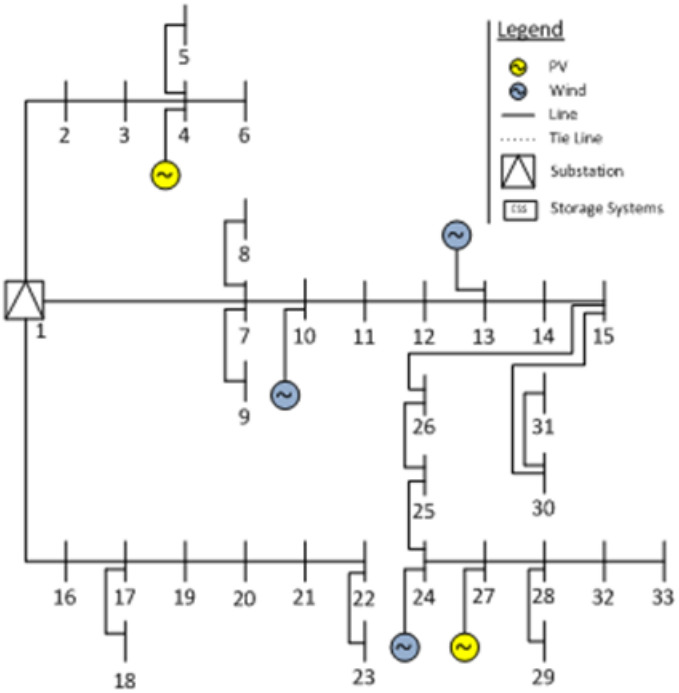

Figure C.62: 119 Bus test system reconfiguration for h=14

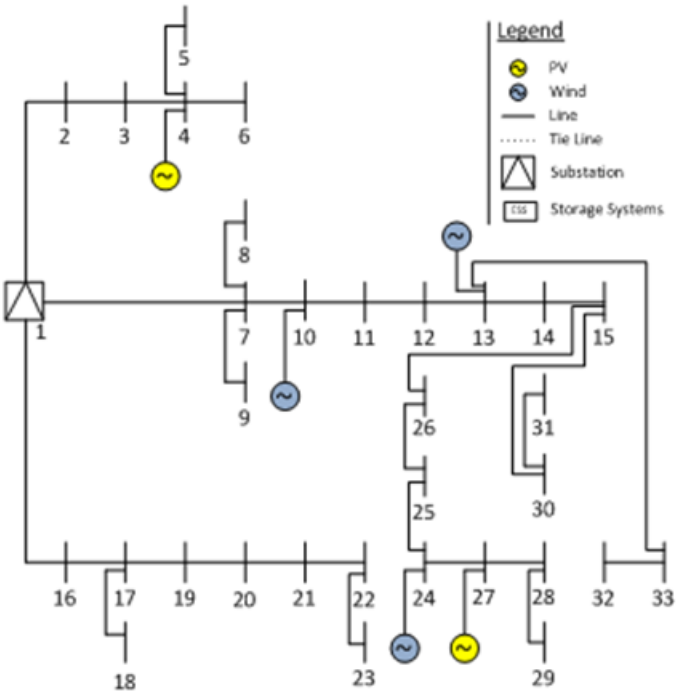

Figure C.63: 119 Bus test system reconfiguration for h=15

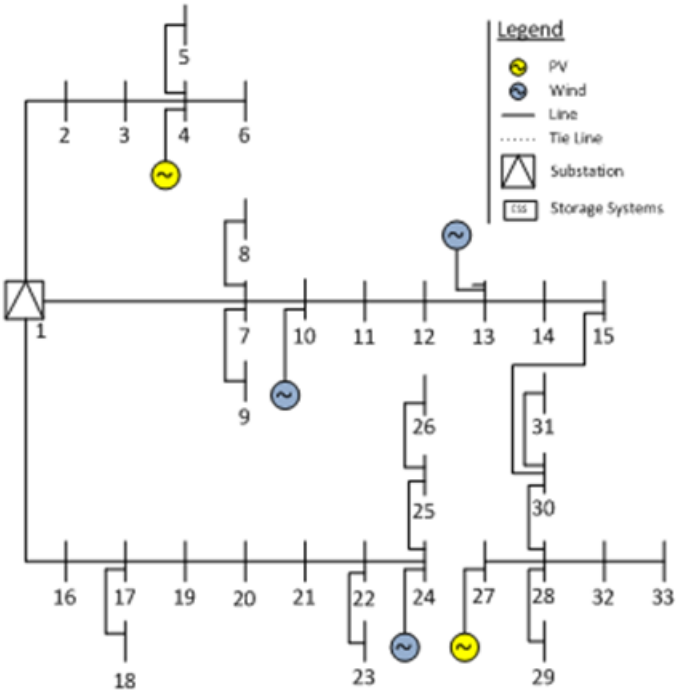

Figure C.64: 119 Bus test system reconfiguration for h=16

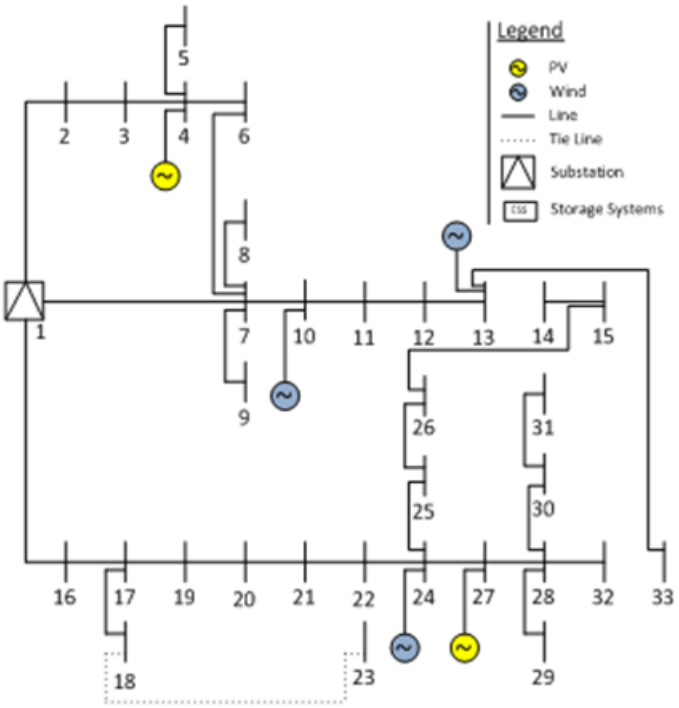

Figure C.65: 119 Bus test system reconfiguration for h=17

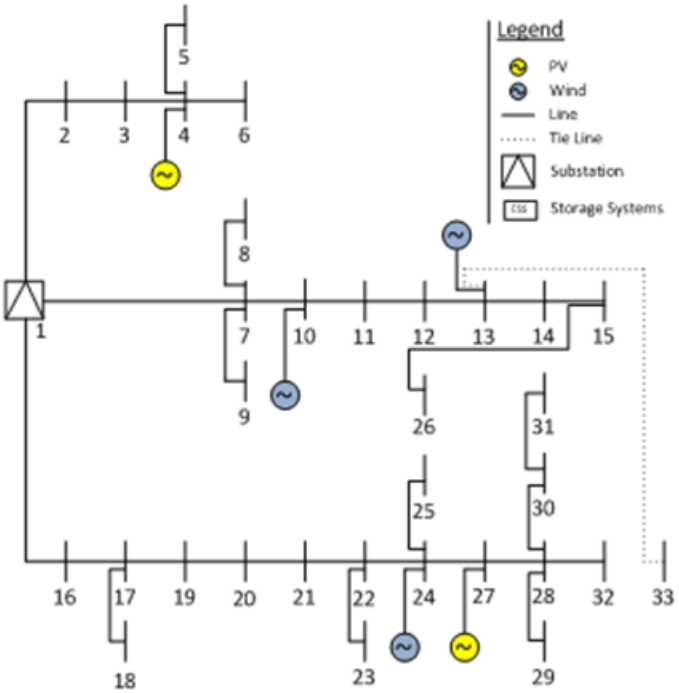

Figure C.66: 119 Bus test system reconfiguration for h=18

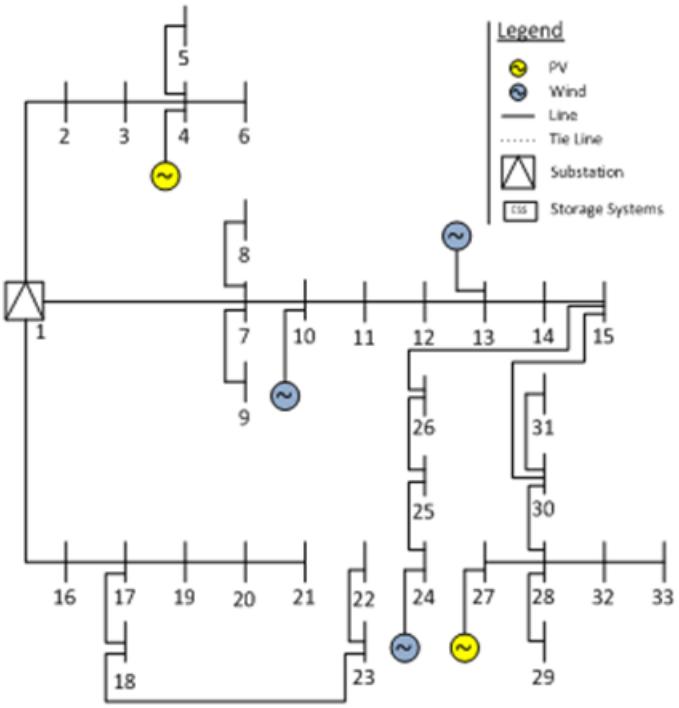

Figure C.67: 119 Bus test system reconfiguration for h=19

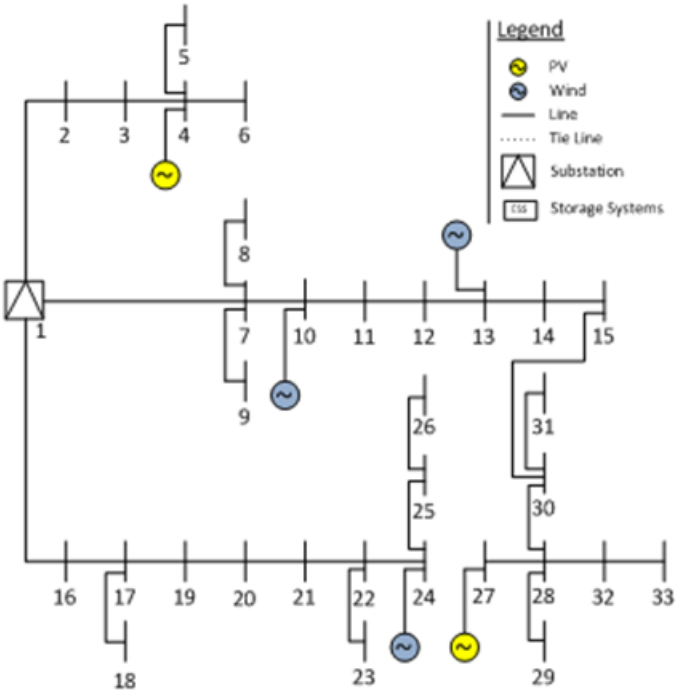

Figure C.68: 119 Bus test system reconfiguration for h=20

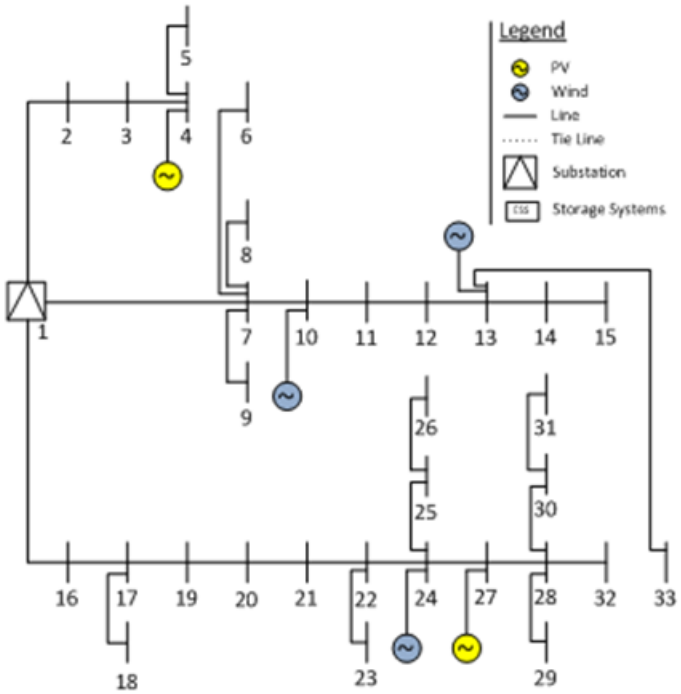

Figure C.69: 119 Bus test system reconfiguration for h=21

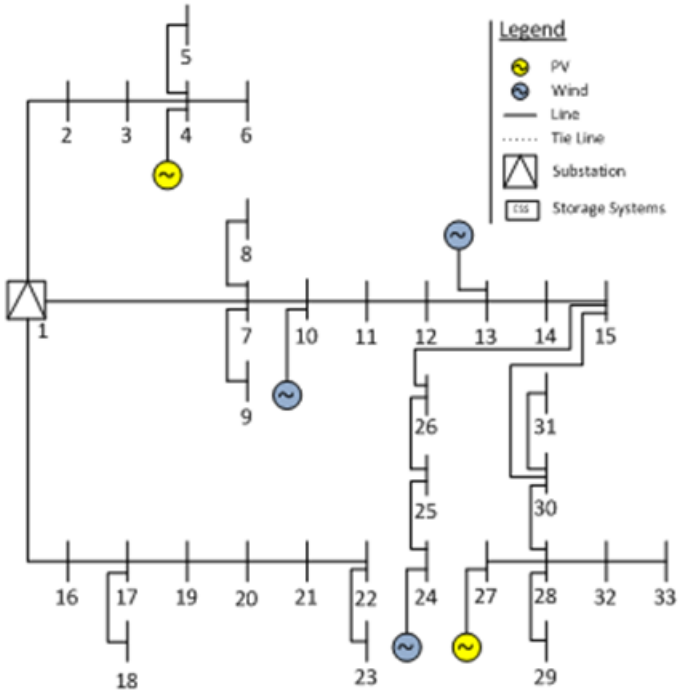

Figure C.70: 119 Bus test system reconfiguration for h=22

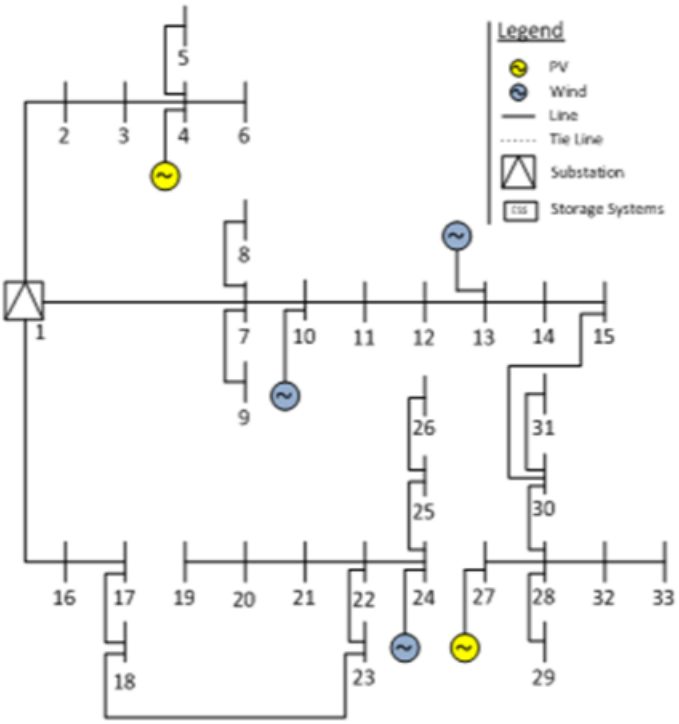

Figure C.71: 119 Bus test system reconfiguration for h=23

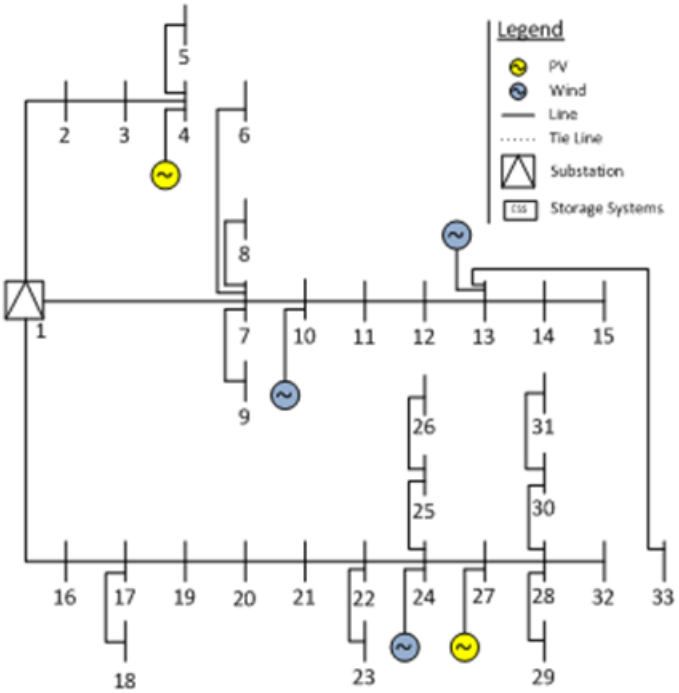

Figure C.72: 119 Bus test system reconfiguration for h=24

C.4 Lagoa System Case D

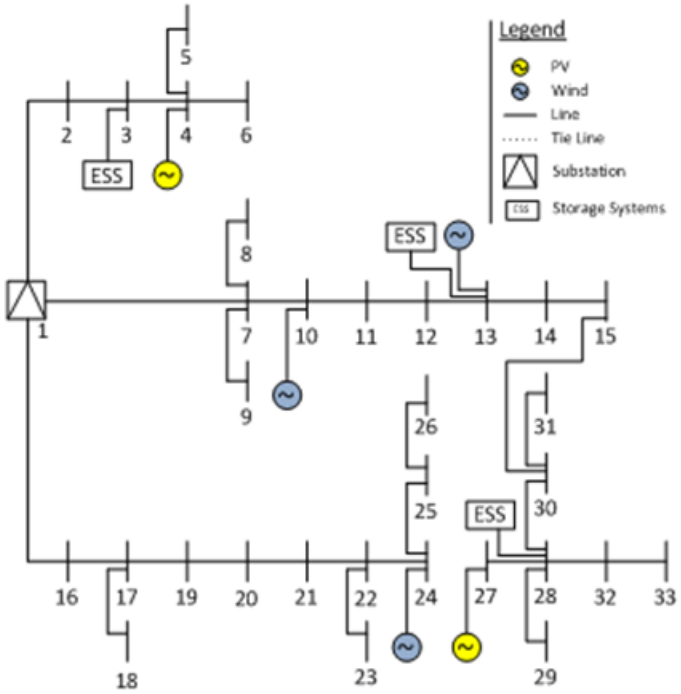

Figure C.73: 119 Bus test system reconfiguration for h=1

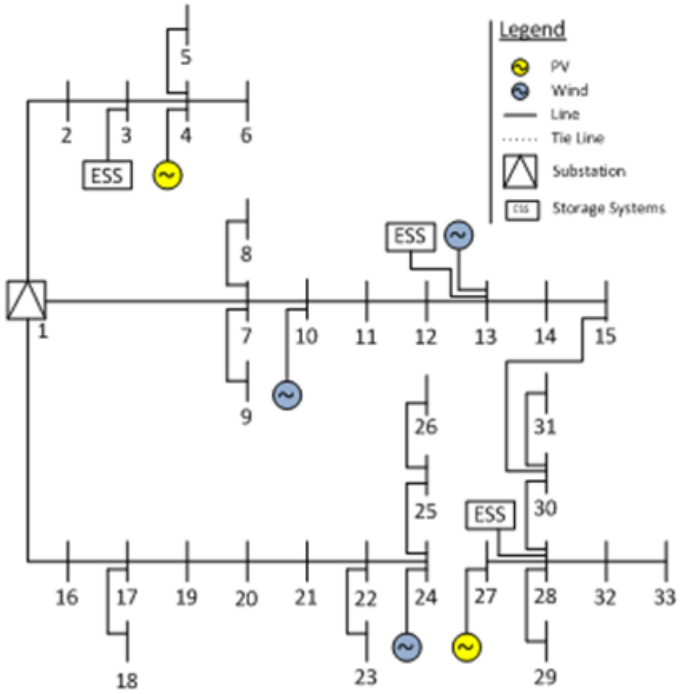

Figure C.74: 119 Bus test system reconfiguration for h=2

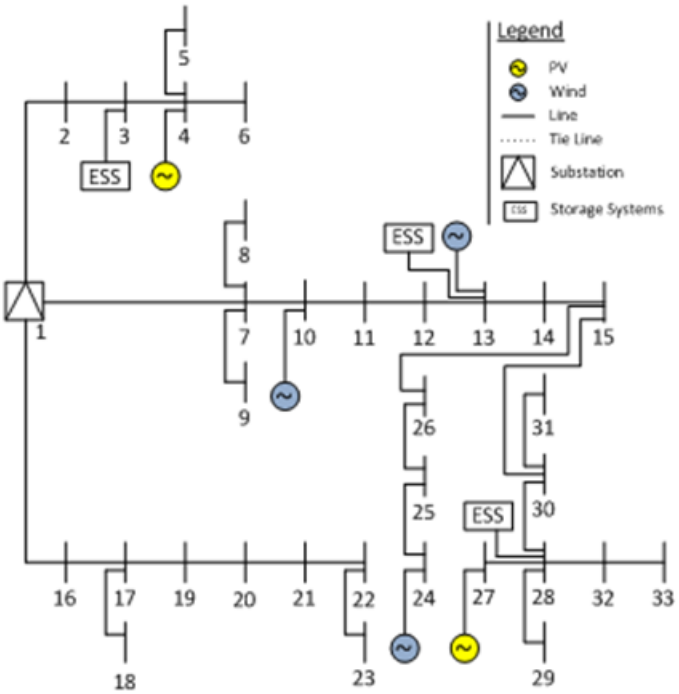

Figure C.75: 119 Bus test system reconfiguration for h=3

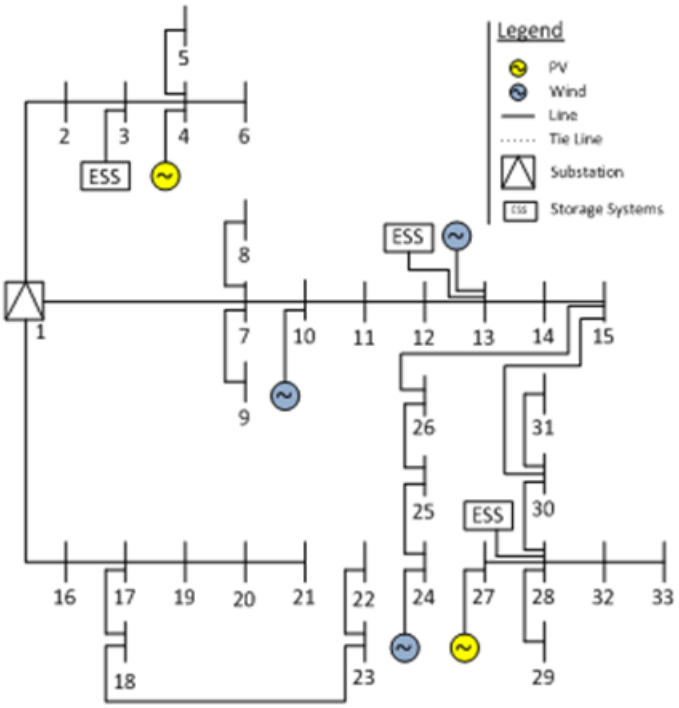

Figure C.76: 119 Bus test system reconfiguration for h=4

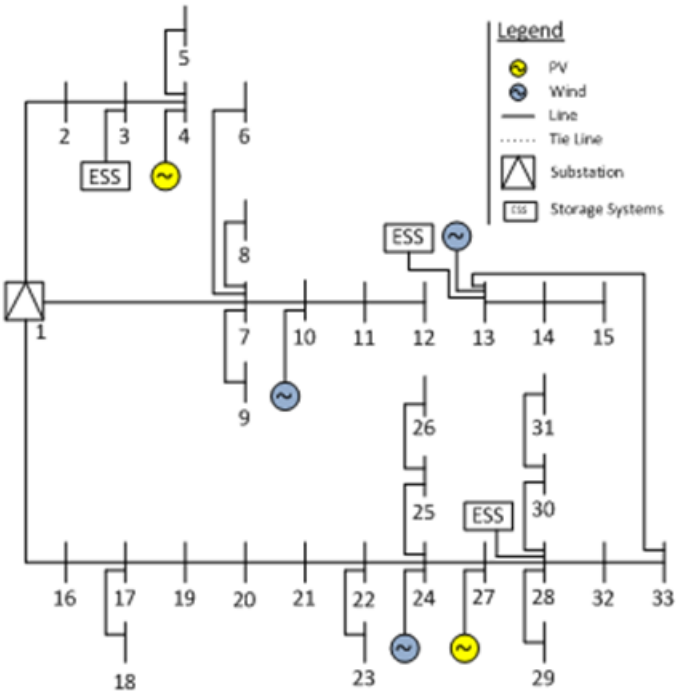

Figure C.77: 119 Bus test system reconfiguration for h=5

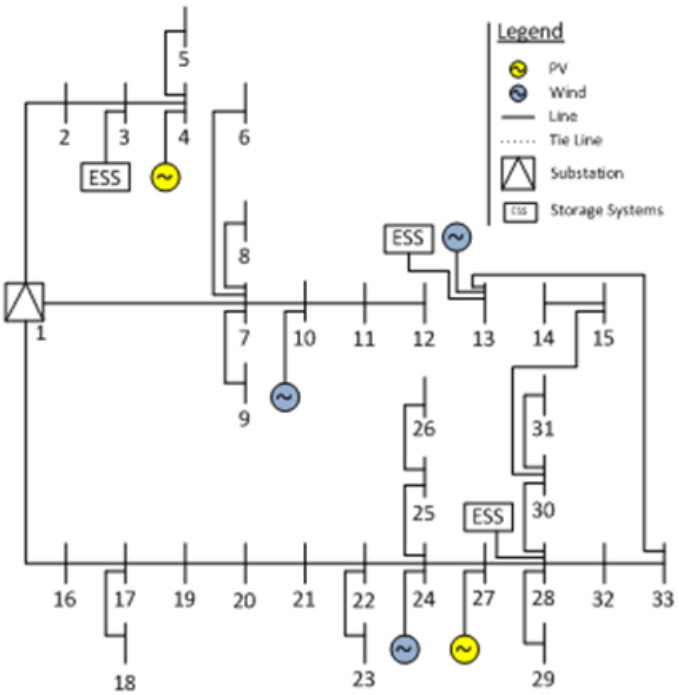

Figure C.78: 119 Bus test system reconfiguration for h=6

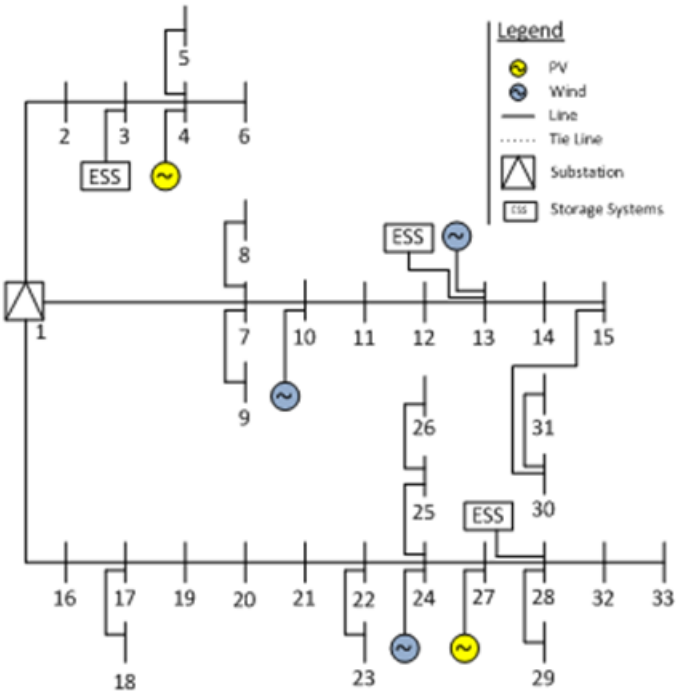

Figure C.79: 119 Bus test system reconfiguration for h=7

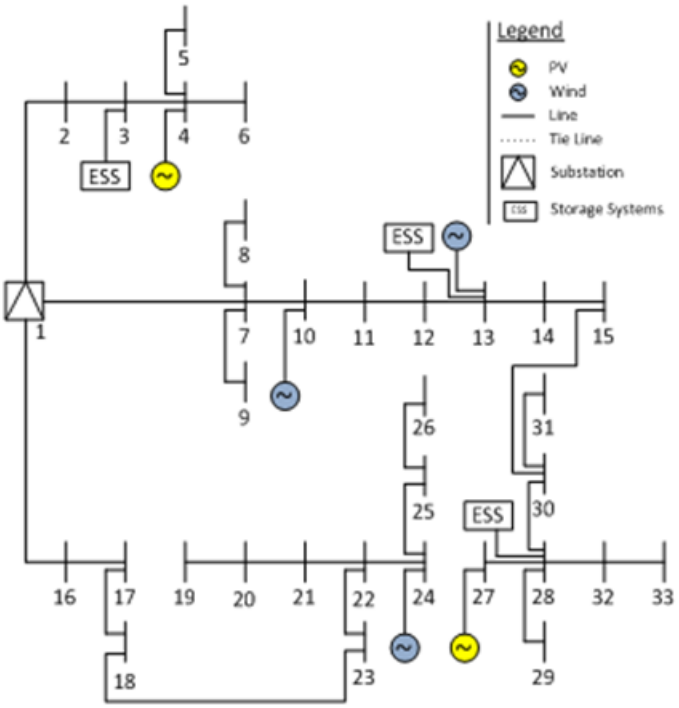

Figure C.80: 119 Bus test system reconfiguration for h=8

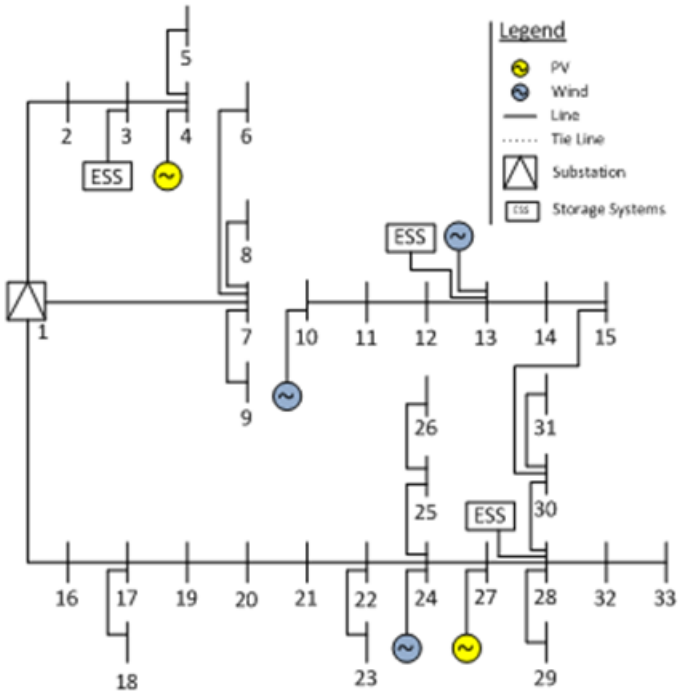

Figure C.81: 119 Bus test system reconfiguration for h=9

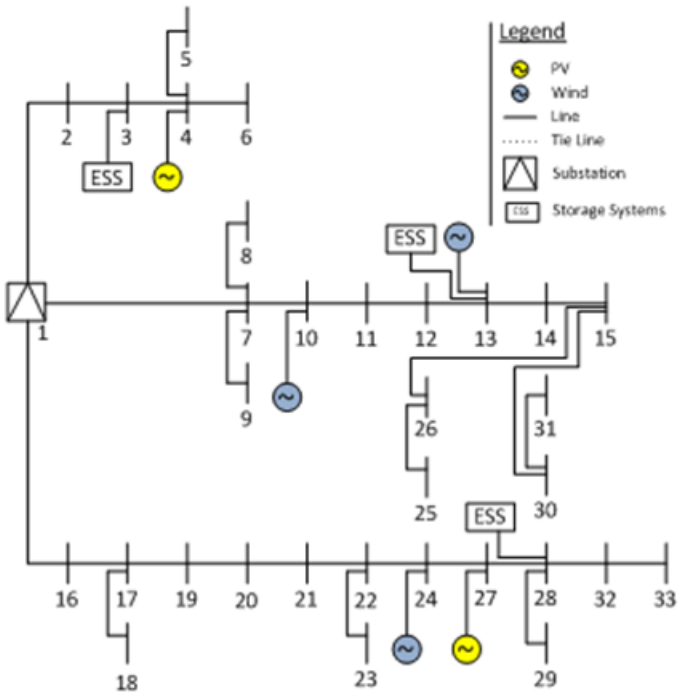

Figure C.82: 119 Bus test system reconfiguration for h=10

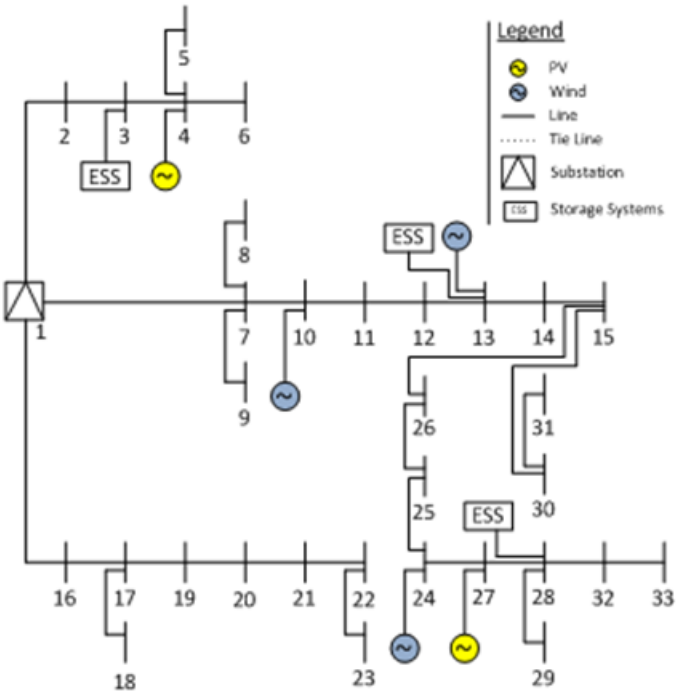

Figure C.83: 119 Bus test system reconfiguration for h=11

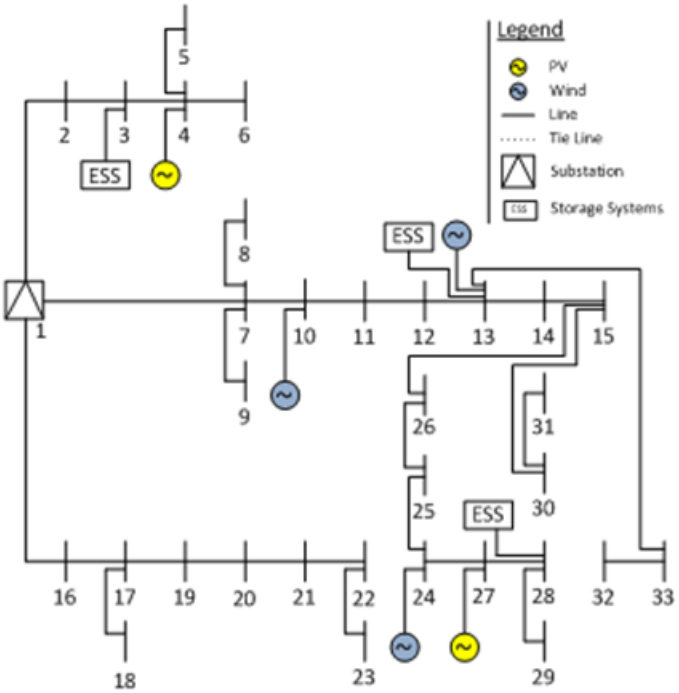

Figure C.84: 119 Bus test system reconfiguration for h=12

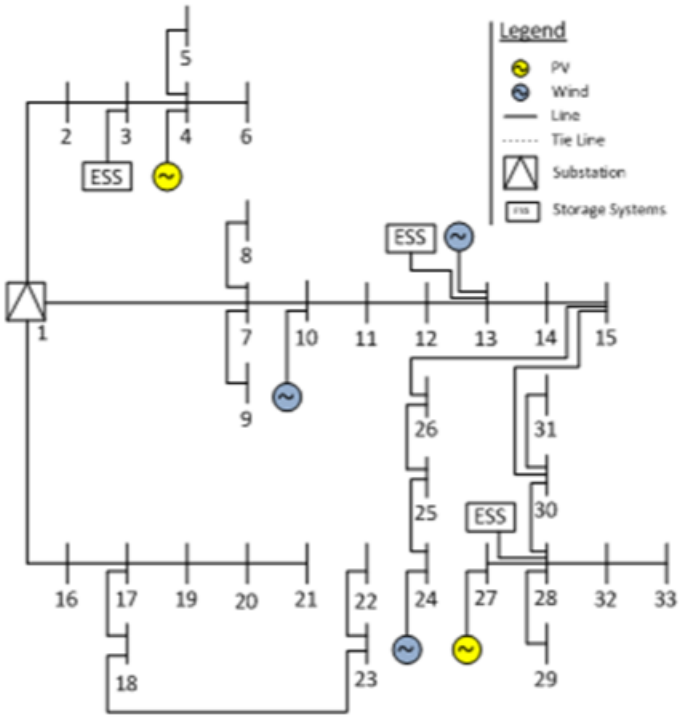

Figure C.85: 119 Bus test system reconfiguration for h=13

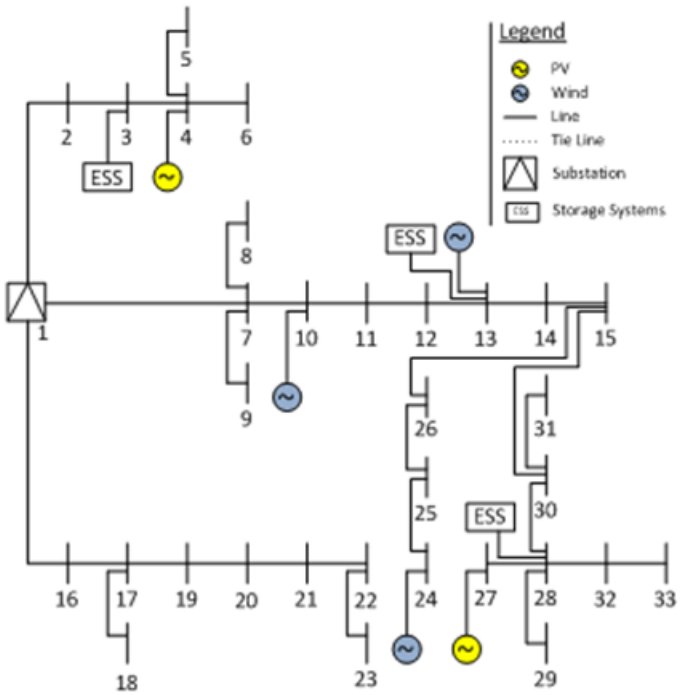

Figure C.86: 119 Bus test system reconfiguration for h=14

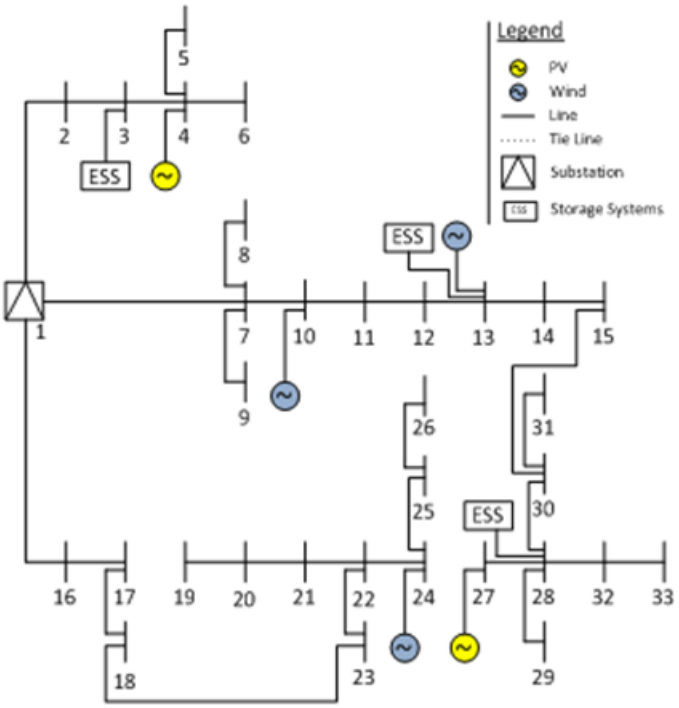

Figure C.87: 119 Bus test system reconfiguration for h=15

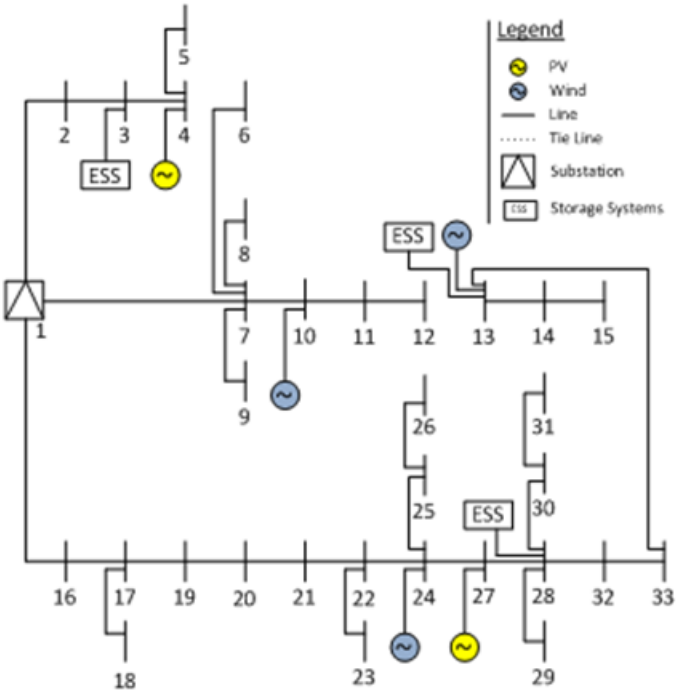

Figure C.88: 119 Bus test system reconfiguration for h=16

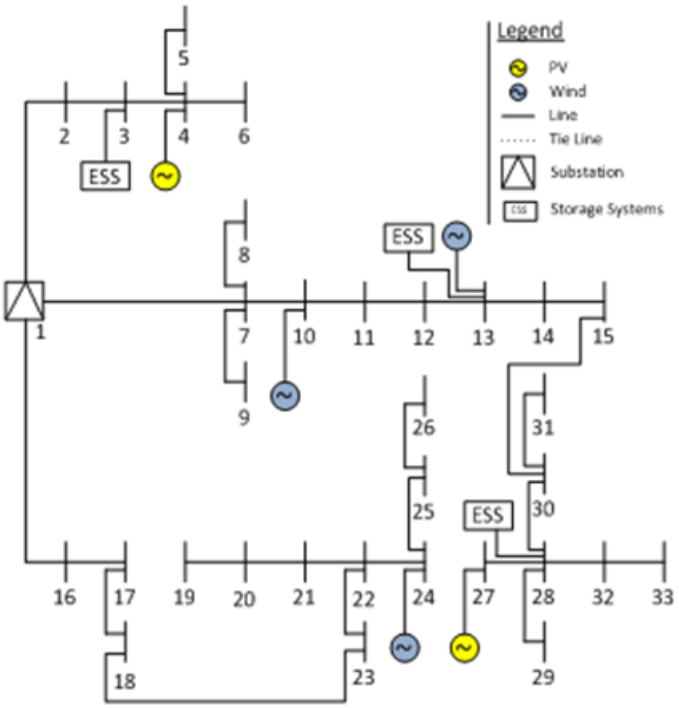

Figure C.89: 119 Bus test system reconfiguration for h=17

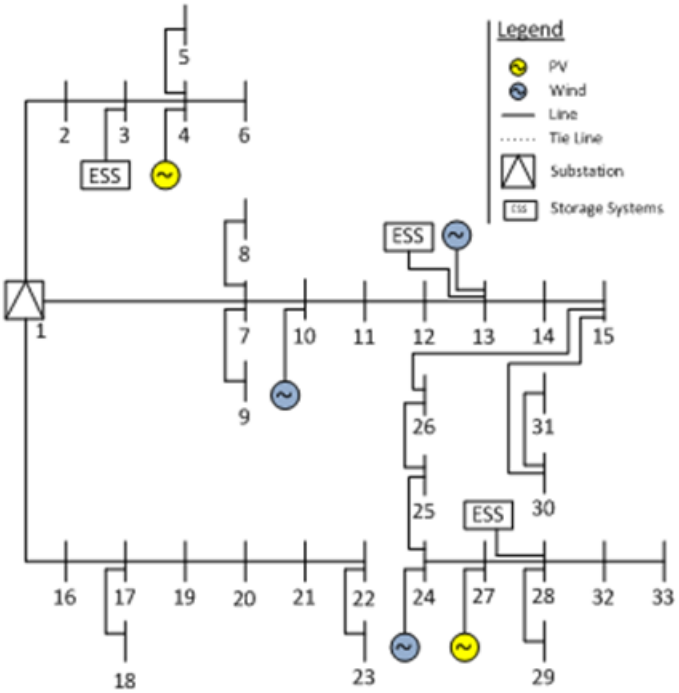

Figure C.90: 119 Bus test system reconfiguration for h=18

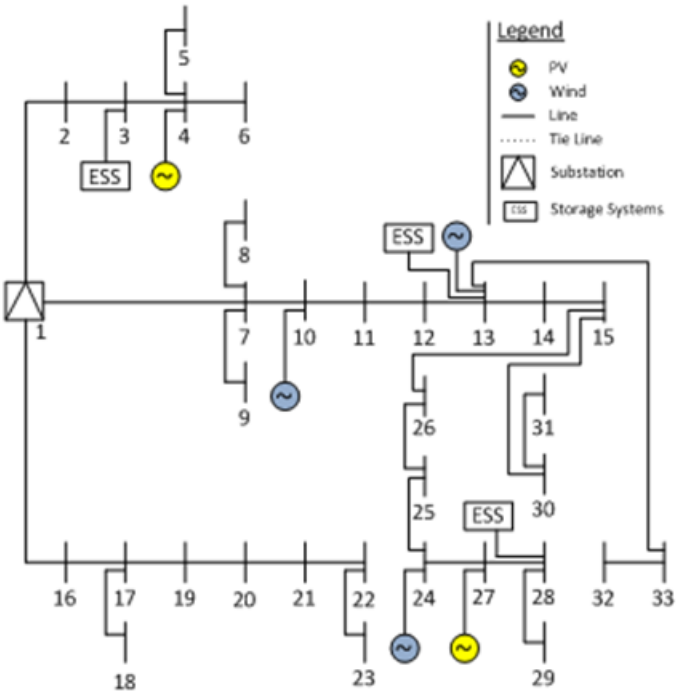

Figure C.91: 119 Bus test system reconfiguration for h=19

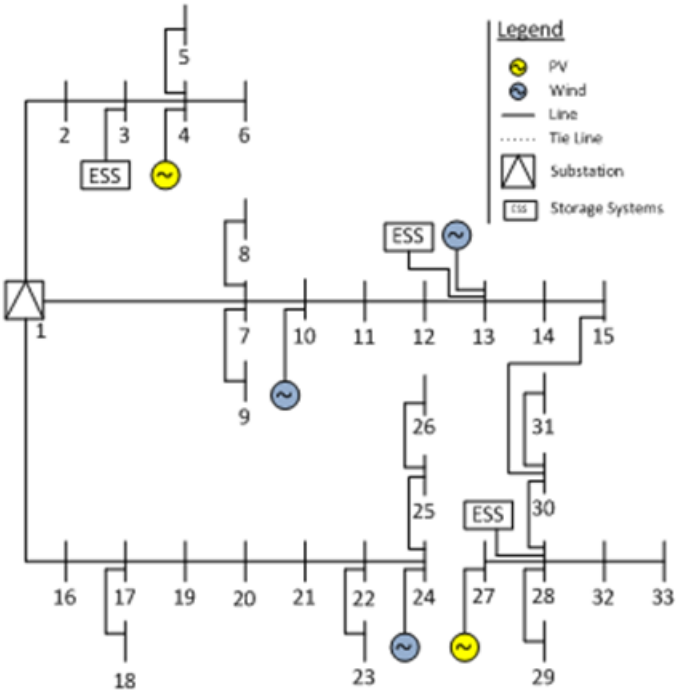

Figure C.92: 119 Bus test system reconfiguration for h=20

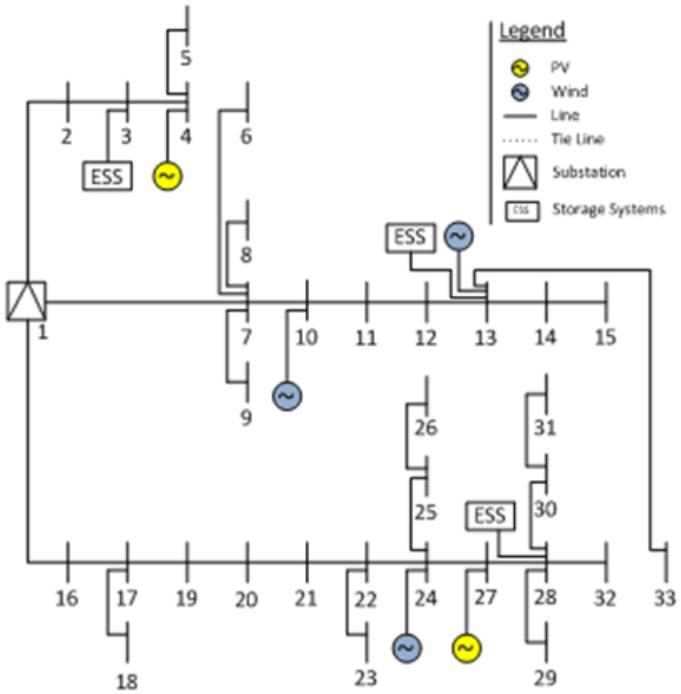

Figure C.93: 119 Bus test system reconfiguration for h=21

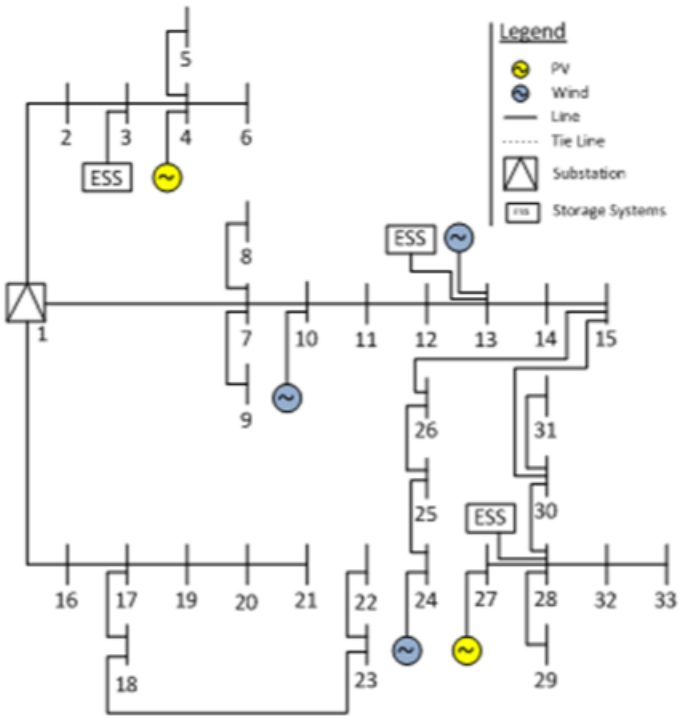

Figure C.94: 119 Bus test system reconfiguration for h=22

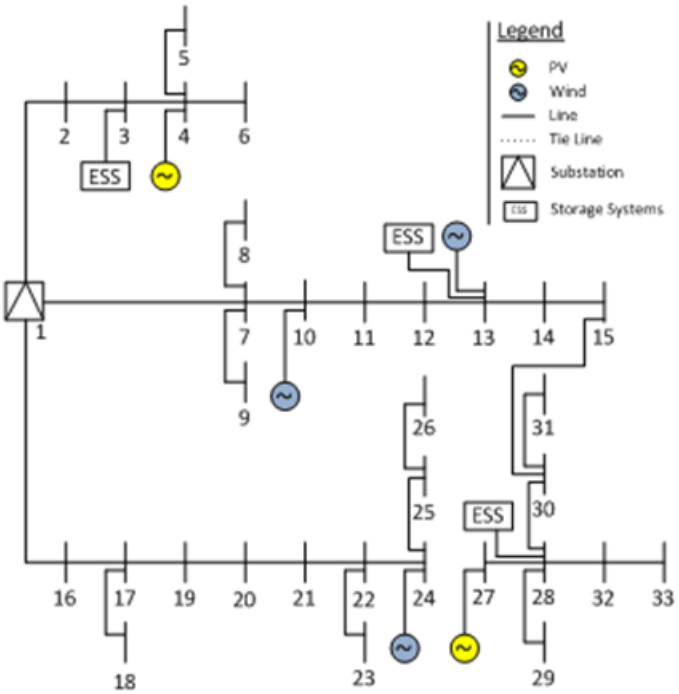

Figure C.95: 119 Bus test system reconfiguration for h=23

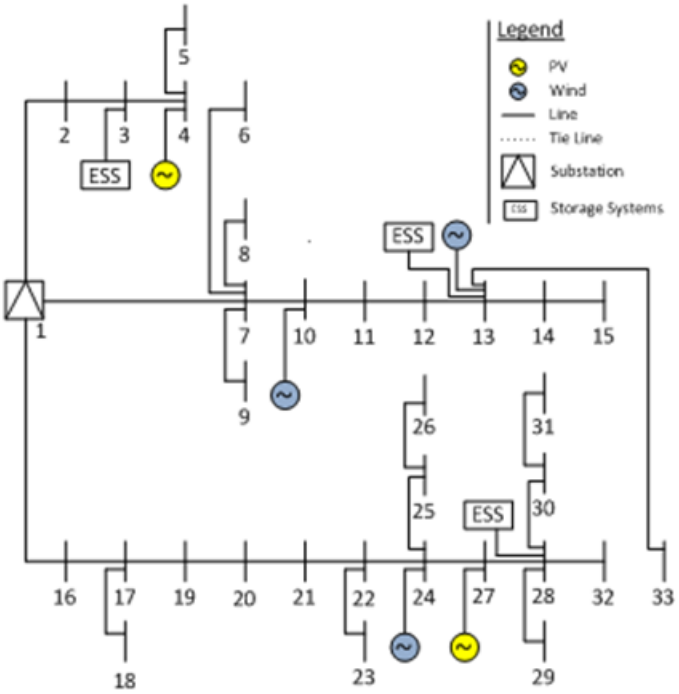

Figure C.96: 119 Bus test system reconfiguration for h=24

References

[1] M. Nicolini and M. Tavoni, "Are renewable energy subsidies effective? Evidence from Europe," *Renewable and Sustainable Energy Reviews*, vol. 74, pp. 412–423, Jul. 2017.

[2] T. Khanam, A. Rahman, B. Mola-Yudego, P. Pelkonen, Y. Perez, and J. Pykäläinen, "Achievable or unbelievable? Expert perceptions of the European Union targets for emissions, renewables, and efficiency," *Energy Research & Social Science*, vol. 34, pp. 144–153, Dec. 2017.

[3] K. P. Kumar and B. Saravanan, "Recent techniques to model uncertainties in power generation from renewable energy sources and loads in microgrids – A review," *Renewable and Sustainable Energy Reviews*, vol. 71, pp. 348–358, May 2017.

[4] S. B. Karanki and D. Xu, "Optimal capacity and placement of battery energy storage systems for integrating renewable energy sources in distribution system," in *Power Systems Conference (NPSC), 2016 National*. IEEE, 2016, pp. 1–6.

[5] S. F. Santos, D. Z. Fitiwi, M. Cruz, C. M. P. Cabrita, and J. P. S. Catalão, "Impacts of optimal energy storage deployment and network reconfiguration on renewable integration level in distribution systems," vol. 185, Jan. 2017, pp. 44–55.

[6] X. Liang, "Emerging Power Quality Challenges Due to Integration of Renewable Energy Sources," *IEEE Transactions on Industry Applications*, vol. 53, no. 2, pp. 855–866, Mar. 2017.

[7] C. L. T. Borges, "An overview of reliability models and methods for distribution systems with renewable energy distributed generation," *Renewable and Sustainable Energy Reviews*, vol. 16, no. 6, pp. 4008–4015, Aug. 2012.

[8] W. L. Theo, J. S. Lim, W. S. Ho, H. Hashim, and C. T. Lee, "Review of distributed generation (DG) system planning and optimisation techniques: Comparison of numerical and mathematical modelling methods," *Renewable and Sustainable Energy Reviews*, vol. 67, pp. 531–573, Jan. 2017.

[9] P. T. Manditereza and R. Bansal, "Renewable distributed generation: The hidden challenges – A review from the protection perspective," *Renewable and Sustainable Energy Reviews*, vol. 58, pp. 1457–1465, May 2016.

[10] M. Abdullah, A. Agalgaonkar, and K. Muttaqi, "Assessment of energy supply and continuity of service in distribution network with renewable distributed generation," *Applied Energy*, vol. 113, pp. 1015–1026, Jan. 2014.

[11] B. Muruganantham, R. Gnanadass, and N. Padhy, "Challenges with renewable energy sources and storage in practical distribution systems," *Renewable and Sustainable Energy Reviews*, vol. 73, pp. 125–134, Jun. 2017.

[12] R. E. Brown, "Impact of smart grid on distribution system design," in *Power and Energy Society General Meeting-Conversion and Delivery of Electrical Energy in the 21st Century, 2008 IEEE*. IEEE, 2008, pp. 1–4.

[13] S. Tiba and A. Omri, "Literature survey on the relationships between energy, environment and economic growth," *Renewable and Sustainable Energy Reviews*, vol. 69, pp. 1129–1146, Mar. 2017.

[14] T. Lehtola and A. Zahedi, "Sustainable energy supply using renewable sources supported by storage technology," in *Innovative Smart Grid Technologies-Asia (ISGT-Asia), 2016 IEEE*. IEEE, 2016, pp. 71–74.

[15] D. Eltigani and S. Masri, "Challenges of integrating renewable energy sources to smart grids: A review," *Renewable and Sustainable Energy Reviews*, vol. 52, pp. 770–780, Dec. 2015.

[16] A. Huda and R. Živanović, "Large-scale integration of distributed generation into distribution networks: Study objectives, review of models and computational tools," *Renewable and Sustainable Energy Reviews*, vol. 76, pp. 974–988, Sep. 2017.

[17] S. Montoya-Bueno, J. Muñoz-Hernández, and J. Contreras, "Uncertainty management of renewable distributed generation," *Journal of Cleaner Production*, vol. 138, pp. 103–118, Dec. 2016.

[18] M. Håberg and G. Doorman, "A Stochastic Mixed Integer Linear Programming Formulation for the Balancing Energy Activation Problem Under Uncertainty." IEEE, Jun. 2017, pp. 1–6.

[19] P. H. Nguyen, N. Blaauwbroek, C. Nguyen, X. Zhang, A. Flueck, and X. Wang, "Interfacing applications for uncertainty reduction in smart energy systems utilizing distributed intelligence," *Renewable and Sustainable Energy Reviews*, vol. 80, pp. 1312–1320, Dec. 2017.

[20] H. S. Farmad and S. Biglar, "Integration of demand side management, distributed generation, renewable energy sources and energy storages," 2012.

[21] M. Žnidarec, D. Šljivac, and D. Topić, "Influence of distributed generation from renewable energy sources on distribution network hosting capacity." Budapest, Hungary: IEEE, Jun. 2017, pp. 1–7.

[22] X. Luo, J. Wang, M. Dooner, and J. Clarke, "Overview of current development in electrical energy storage technologies and the application potential in power system operation," *Applied Energy*, vol. 137, pp. 511–536, Jan. 2015.

[23] G. Haddadian, N. Khalili, M. Khodayar, and M. Shahidehpour, "Optimal coordination of variable renewable resources and electric vehicles as distributed storage for energy sustainability," *Sustainable Energy, Grids and Networks*, vol. 6, pp. 14–24, Jun. 2016.

[24] H. Fathabadi, "Utilization of electric vehicles and renewable energy sources used as distributed generators for improving characteristics of electric power distribution systems," vol. 90, pp. 1100–1110, Oct. 2015.

[25] S. Montoya-Bueno, J. I. Muñoz, and J. Contreras, "Optimal expansion model of renewable distributed generation in distribution systems," in *Power Systems Computation Conference (PSCC), 2014*. IEEE, 2014, pp. 1–7.

[26] P. Paliwal, N. Patidar, and R. Nema, "Planning of grid integrated distributed generators: A review of technology, objectives and techniques," *Renewable and Sustainable Energy Reviews*, vol. 40, pp. 557–570, Dec. 2014.

[27] N. Mahmud and A. Zahedi, "Review of control strategies for voltage regulation of the smart distribution network with high penetration of renewable distributed generation," *Renewable and Sustainable Energy Reviews*, vol. 64, pp. 582–595, Oct. 2016.

[28] O. Badran, S. Mekhilef, H. Mokhlis, and W. Dahalan, "Optimal reconfiguration of distribution system connected with distributed generations: A review of different methodologies," *Renewable and Sustainable Energy Reviews*, vol. 73, pp. 854–867, Jun. 2017.

[29] B. Sultana, M. Mustafa, U. Sultana, and A. R. Bhatti, "Review on reliability improvement and power loss reduction in distribution system via network reconfiguration," *Renewable and Sustainable Energy Reviews*, vol. 66, pp. 297–310, Dec. 2016.

[30] L. Xu, R. Cheng, Z. He, J. Xiao, and H. Luo, "Dynamic Reconfiguration of Distribution Network Containing Distributed Generation," in *Computational Intelligence and Design (ISCID), 2016 9th International Symposium On*, vol. 1. IEEE, 2016, pp. 3–7.

[31] X. Meng, L. Zhang, P. Cong, W. Tang, X. Zhang, and D. Yang, "Dynamic reconfiguration of distribution network considering scheduling of DG active power outputs," in *Power System Technology (POWERCON), 2014 International Conference On*. IEEE, 2014, pp. 1433–1439.

[32] T. Thakur and Jaswanti, "Study and Characterization of Power Distribution Network Reconfiguration." IEEE, 2006, pp. 1–6.

[33] A. W. Bizuayehu, A. A. S. de la Nieta, J. Catalao, P. M. de Quevedo, and J. Contreras, "Distribution system reconfiguration in economic dispatch with high wind penetration," in *Power & Energy Society General Meeting, 2015 IEEE*. IEEE, 2015, pp. 1–5.

[34] P. Meneses de Quevedo, J. Contreras, M. J. Rider, and J. Allahdadian, "Contingency Assessment and Network Reconfiguration in Distribution Grids Including Wind Power and Energy Storage," *IEEE Transactions on Sustainable Energy*, vol. 6, no. 4, pp. 1524–1533, Oct. 2015.

[35] F. Capitanescu, L. F. Ochoa, H. Margossian, and N. D. Hatziargyriou, "Assessing the Potential of Network Reconfiguration to Improve Distributed Generation Hosting Capacity in Active Distribution Systems," *IEEE Transactions on Power Systems*, vol. 30, no. 1, pp. 346–356, Jan. 2015.

[36] J. M. Andújar, F. Segura, and T. Domínguez, "Study of a renewable energy sources-based smart grid. requirements, targets and solutions," in *Power Engineering and Renewable Energy (ICPERE), 2016 3rd Conference On*. IEEE, 2016, pp. 45–50.

[37] S. Kakran and S. Chanana, "Smart operations of smart grids integrated with distributed generation: A review," *Renewable and Sustainable Energy Reviews*, vol. 81, pp. 524–535, Jan. 2018.

[38] H. Shirzeh, F. Naghdy, P. Ciufo, and M. Ros, "Stochastic energy balancing of renewable sources in a smart grid," in *Power Engineering Conference (AUPEC), 2015 Australasian Universities*. IEEE, 2015, pp. 1–6.

[39] P. Crespo Del Granado, Z. Pang, and S. W. Wallace, "Synergy of smart grids and hybrid distributed generation on the value of energy storage," *Applied Energy*, vol. 170, pp. 476–488, May 2016.

[40] "Government Technology: State & Local Government News Articles," http://www.govtech.com, [Accessed: 17-October-2017].

[41] A. Elmitwally, M. Elsaid, M. Elgamal, and Z. Chen, "A Fuzzy-Multiagent Service Restoration Scheme for Distribution System With Distributed Generation," *IEEE Transactions on Sustainable Energy*, vol. 6, no. 3, pp. 810–821, Jul. 2015.

[42] S. Lei, Y. Hou, F. Qiu, and J. Yan, "Identification of Critical Switches for Integrating Renewable Distributed Generation by Dynamic Network Reconfiguration," *IEEE Transactions on Sustainable Energy*, pp. 1–1, 2017.

[43] T. Adefarati and R. Bansal, "Reliability assessment of distribution system with the integration of renewable distributed generation," *Applied Energy*, vol. 185, pp. 158–171, Jan. 2017.

[44] Z. Abdmouleh, A. Gastli, L. Ben-Brahim, M. Haouari, and N. A. Al-Emadi, "Review of optimization techniques applied for the integration of distributed generation from renewable energy sources," *Renewable Energy*, vol. 113, pp. 266–280, Dec. 2017.

[45] X. Zhang, H. Chen, Y. Xu, W. Li, F. He, H. Guo, and Y. Huang, "Distributed generation with energy storage systems: A case study," *Applied Energy*, May 2017.

[46] A. Singh and S. Parida, "A novel hybrid approach to allocate renewable energy sources in distribution system," *Sustainable Energy Technologies and Assessments*, vol. 10, pp. 1–11, Jun. 2015.

[47] B. Singh and J. Sharma, "A review on distributed generation planning," *Renewable and Sustainable Energy Reviews*, vol. 76, pp. 529–544, Sep. 2017.

[48] A. Keane, L. F. Ochoa, C. L. T. Borges, G. W. Ault, A. D. Alarcon-Rodriguez, R. A. F. Currie, F. Pilo, C. Dent, and G. P. Harrison, "State-of-the-Art Techniques and Challenges Ahead for Distributed Generation Planning and Optimization," *IEEE Transactions on Power Systems*, vol. 28, no. 2, pp. 1493–1502, May 2013.

[49] A. K. Singh and S. K. Parida, "Need of distributed generation for sustainable development in coming future," in *Power Electronics, Drives and Energy Systems (PEDES), 2012 IEEE International Conference On*. IEEE, 2012, pp. 1–6.

[50] L. Bai, T. Jiang, F. Li, H. Chen, and X. Li, "Distributed energy storage planning in soft open point based active distribution networks incorporating network reconfiguration and DG reactive power capability," *Applied Energy*, Jul. 2017.

[51] B. Novoselnik and M. Baotić, "Dynamic Reconfiguration of Electrical Power Distribution Systems with Distributed Generation and Storage." IFAC-PapersOnLine, 2015, pp. 136–141.

[52] S. Kennedy and M. M. Marden, "Reliability of islanded microgrids with stochastic generation and prioritized load," in *PowerTech, 2009 IEEE Bucharest*. IEEE, 2009, pp. 1–7.

[53] G. Gutiérrez-Alcaraz, E. Galván, N. González-Cabrera, and M. Javadi, "Renewable energy resources short-term scheduling and dynamic network reconfiguration for sustainable energy consumption," *Renewable and Sustainable Energy Reviews*, vol. 52, pp. 256–264, Dec. 2015.

[54] K. K. Mehmood, S. U. Khan, S.-J. Lee, Z. M. Haider, M. K. Rafique, and C.-H. Kim, "A real-time optimal coordination scheme for the voltage regulation of a distribution network including an OLTC, capacitor banks, and multiple distributed energy resources," *International Journal of Electrical Power & Energy Systems*, vol. 94, pp. 1–14, Jan. 2018.

[55] A. Zidan and E. F. El-Saadany, "Distribution system reconfiguration for energy loss reduction considering the variability of load and local renewable generation," vol. 59, pp. 698–707, Sep. 2013.

[56] H. Xing, H. Cheng, S. Hong, Y. Zhang, and P. Zeng, "Minimize active power loss with distribution network reconfiguration considering intermittent renewable energy source uncertainties," in *Power System Technology (POWERCON), 2014 International Conference On*. IEEE, 2014, pp. 127–133.

[57] A. Zidan and E. F. El-Saadany, "Network reconfiguration in balanced distribution systems with variable load demand and variable renewable resources generation," in *Power and Energy Society General Meeting, 2012 IEEE*. IEEE, 2012, pp. 1–8.

[58] S. Das, D. Das, and A. Patra, "Reconfiguration of distribution networks with optimal placement of distributed generations in the presence of remote voltage controlled bus," *Renewable and Sustainable Energy Reviews*, vol. 73, pp. 772–781, Jun. 2017.

[59] V. Calderaro, G. Conio, V. Galdi, G. Massa, and A. Piccolo, "Active management of renewable energy sources for maximizing power production," *International Journal of Electrical Power & Energy Systems*, vol. 57, pp. 64–72, May 2014.

[60] D. Zhang, Z. Fu, and L. Zhang, "An improved TS algorithm for loss-minimum reconfiguration in large-scale distribution systems," *Electric Power Systems Research*, vol. 77, no. 5-6, pp. 685–694, Apr. 2007.

[61] C. Lueken, P. M. Carvalho, and J. Apt, "Distribution grid reconfiguration reduces power losses and helps integrate renewables," *Energy Policy*, vol. 48, pp. 260–273, Sep. 2012.

[62] A. S. Bouhouras, C. Iraklis, G. Evmiridis, and D. P. Labridis, "Mitigating distribution network congestion due to high DG penetration," 2014.

[63] M. Lavorato, J. F. Franco, M. J. Rider, and R. Romero, "Imposing Radiality Constraints in Distribution System Optimization Problems," *IEEE Transactions on Power Systems*, vol. 27, no. 1, pp. 172–180, Feb. 2012.

[64] P. Pavani and S. N. Singh, "Reconfiguration of radial distribution networks with distributed generation for reliability improvement and loss minimization," in *Power and Energy Society General Meeting (PES), 2013 IEEE*. IEEE, 2013, pp. 1–5.

[65] A. Rabiee and S. M. Mohseni-Bonab, "Maximizing hosting capacity of renewable energy sources in distribution networks: A multi-objective and scenario-based approach," vol. 120, pp. 417–430, Feb. 2017.

[66] S. F. Santos, D. Z. Fitiwi, M. Shafie-Khah, A. W. Bizuayehu, C. M. P. Cabrita, and J. P. S. Catalao, "New Multistage and Stochastic Mathematical Model for Maximizing RES Hosting Capacity #8212;Part I: Problem Formulation," *IEEE Transactions on Sustainable Energy*, vol. 8, no. 1, pp. 304–319, Jan. 2017.

[67] S. F. Santos, D. Z. Fitiwi, M. Shafie-khah, A. W. Bizuayehu, C. M. P. Cabrita, and J. P. S. Catalão, "New Multi-Stage and Stochastic Mathematical Model for Maximizing RES Hosting Capacity #x2014;Part II: Numerical Results," *IEEE Transactions on Sustainable Energy*, vol. 8, no. 1, pp. 320–330, Jan. 2017.

[68] S. Montoya-Bueno, J. I. Munoz, and J. Contreras, "A Stochastic Investment Model for Renewable Generation in Distribution Systems," *IEEE Transactions on Sustainable Energy*, vol. 6, no. 4, pp. 1466–1474, Oct. 2015.

[69] A. W. Bizuayehu, A. A. Sanchez de la Nieta, J. Contreras, and J. P. S. Catalao, "Impacts of Stochastic Wind Power and Storage Participation on Economic Dispatch in Distribution Systems," *IEEE Transactions on Sustainable Energy*, vol. 7, no. 3, pp. 1336–1345, Jul. 2016.

[70] G. Munoz-Delgado, J. Contreras, and J. M. Arroyo, "Multistage Generation and Network Expansion Planning in Distribution Systems Considering Uncertainty and Reliability," *IEEE Transactions on Power Systems*, vol. 31, no. 5, pp. 3715–3728, Sep. 2016.

[71] Y. Yang, S. Zhang, and Y. Xiao, "Optimal design of distributed energy resource systems based on two-stage stochastic programming," *Applied Thermal Engineering*, vol. 110, pp. 1358–1370, Jan. 2017.

[72] R. Dai and M. Mesbahi, "Optimal power generation and load management for off-grid hybrid power systems with renewable sources via mixed-integer programming," *Energy Conversion and Management*, vol. 73, pp. 234–244, Sep. 2013.

[73] W. S. Ho, S. Macchietto, J. S. Lim, H. Hashim, Z. A. Muis, and W. H. Liu, "Optimal scheduling of energy storage for renewable energy distributed energy generation system," *Renewable and Sustainable Energy Reviews*, vol. 58, pp. 1100–1107, May 2016.

[74] S. Talari, M.-R. Haghifam, and M. Yazdaninejad, "Stochastic-based scheduling of the microgrid operation including wind turbines, photovoltaic cells, energy storages and responsive loads," *IET Generation, Transmission & Distribution*, vol. 9, no. 12, pp. 1498–1509, Sep. 2015.

[75] D. Z. Fitiwi, S. F. Santos, C. M. P. Cabrita, and J. P. S. Catalão, "Stochastic mathematical model for high penetration of renewable energy sources in distribution systems." IEEE, Jun. 2017, pp. 1–6.

[76] H. Alharbi and K. Bhattacharya, "Stochastic Optimal Planning of Battery Energy Storage Systems for Isolated Microgrids," *IEEE Transactions on Sustainable Energy*, pp. 1–1, 2017.

[77] M. Di Somma, G. Graditi, E. Heydarian-Forushani, M. Shafie-khah, and P. Siano, "Stochastic optimal scheduling of distributed energy resources with renewables considering economic and environmental aspects," *Renewable Energy*, Sep. 2017.

[78] A. Karimi, Z. Ranjbar, A. Fereidunian, and H. Lesani, "A stochastic approach to optimal sizing of energy storage systems in a microgrid," in *Smart Grids Conference (SGC), 2016*. IEEE, 2016, pp. 1–8.

[79] A. Kavousi-Fard and T. Niknam, "Multi-objective stochastic Distribution Feeder Reconfiguration from the reliability point of view," vol. 64, pp. 342–354, Jan. 2014.

[80] D. Q. Hung, N. Mithulananthan, and R. Bansal, "Analytical strategies for renewable distributed generation integration considering energy loss minimization," *Applied Energy*, vol. 105, pp. 75–85, May 2013.

[81] D. Z. Fitiwi, L. Olmos, M. Rivier, F. de Cuadra, and I. Pérez-Arriaga, "Finding a representative network losses model for large-scale transmission expansion planning with renewable energy sources," vol. 101, pp. 343–358, Apr. 2016.

[82] E. dos Açores, "Caracterização das redes de transporte e distribuição de energia eléctrica," Tech. Rep., 2016.